

The E2F1-responsive microRNA-449 promotes apoptosis

Dissertation

zur Erlangung des mathematisch-naturwissenschaftlichen

Doktorgrades

"Doctor rerum naturalium"

der Georg-August-Universität Göttingen

vorgelegt von

Muriel Lizé

aus Pontoise, Frankreich

Göttingen, Juli 2010

Anleiter: **Prof. Dr. Matthias Doppelstein**

Referent: **Prof. Dr. Ralf Ficner**

Koreferent: **Prof. Dr. Tomas Pieler**

Tag der mündlichen Prüfung: **23.08.2010**

Index I-III

1. Abstract.....	7
2. Introduction	8
2.1. The DNA damage response	8
2.1.1. DNA damage in cancer & cancer therapy	8
2.1.2. Principal actors of the DNA damage response pathway	8
2.2. The E2F transcription factors	10
2.3. microRNAs	11
2.3.1. Biogenesis and function	11
2.3.2. microRNAs in cancer	13
2.3.3. The miR-34/449 family of microRNAs.....	13
2.4. Airway epithelium and its differentiation.....	15
2.5. Central question.....	18
3. Material.....	19
3.1. Equipment	19
3.2. Consumables	20
3.3. Chemicals	20
3.4. Kits	22
3.5. Buffers and solutions	23
3.6. Nucleic acids	24
3.6.1. Plasmids & vectors.....	25
3.6.2. Synthetic microRNAs & other small RNAs.....	25
3.6.3. Primers.....	25
3.7. Proteins & Peptides	26
3.7.1. Protein marker.....	26
3.7.2. Enzymes	26
3.7.3. Antibodies	27
3.8. Cell culture	28
3.9. Cells	28
3.9.1. Prokaryotic cells	28

3.9.2. Eukaryotic cells	29
3.10. Animals & tissues	29
4. Methods	30
4.1. Cell biological methods	30
4.1.1. Isolation of human primary airway epithelial cells	30
4.1.2. Air-liquid interface cultures & smoke condensate exposition	30
4.1.3. Cell culture & drug treatment of tumour cell lines.....	30
4.1.4. Transfection of eukaryotic cells	31
4.1.5. Clonogenic assays	31
4.1.6. Flow cytometry	31
4.1.7. Dual luciferase assay	32
4.2. Molecular biological methods.....	33
4.2.1. Transformation, cultivation and selection of bacteria	33
4.2.2. DNA preparation.....	33
4.2.3. RNA preparation.....	33
4.2.4. Concentration of nucleic acids	34
4.2.5. DNA sequencing	34
4.2.6. Reverse transcription of mRNA in cDNA.....	34
4.2.7. Semi-quantitative Realtime PCR using SYBR Green.....	34
4.2.8. Reverse transcription of mature microRNAs and semi-quantitative Realtime PCR using Taqman.....	35
4.2.9. microRNA microarray analysis	36
4.3. Protein biochemical methods	36
4.3.1. Protein lysates.....	36
4.3.2. BCA test	36
4.3.3. Immunoblot analysis.....	36
5. Results	37
5.1. E2F1 regulates miRNA expression.....	37
5.2. microRNA-449 is strongly responsive to E2F1 and DNA damage.....	38
5.3. miR-449 expression is coupled to its host gene CDC20B and reduced in cancer	40
5.4. miR-449 induces apoptosis and cell cycle arrest	42
5.5. Target analysis of miR-449a.....	47
5.5.1. Negative feedback on the E2F pathway.....	49

5.5.2.	miR-449 targets the histone deacetylases HDAC1 and SIRT1: a positive feedback on the p53 pathway	52
5.5.3.	miR-449 provokes the accumulation of DNA damage	54
5.5.4.	miR-449 targets vital mitosis checkpoints: Chk1 and BRCA1.....	56
5.6.	miR-449 expression correlates with the development of ciliated cells in lung in vivo	59
5.7.	miR-449 levels sharply increase upon differentiation of airway epithelial cells	62
5.8.	miR-449 levels further increase upon exposure of airway epithelia to tobacco smoke	64
6.	Discussion	66
6.1.	Regulation of the E2F and p53 pathways	66
6.2.	miR-449-mediated p53-independent apoptosis	69
6.2.1.	miR-449 as a regulator of cell cycle progression: cell death by mitotic catastrophe?	69
6.2.2.	miR-449 & DNA damage: a role in DNA repair?	70
6.3.	miR-449 as a regulator of general gene expression.....	71
6.4.	miR-449 in vivo: cell differentiation and development.....	72
6.5.	Outlook	73
7.	Supplementary data.....	75
8.	References.....	93
9.	Acknowledgements	103
10.	Curiculum Vitae.....	104

Figures & Tables

Fig. 2.1: Simplified overview of the DNA damage response	9
Fig. 2.2: microRNAs: from transcription to active form	12
Fig. 2.3: Seed sequence comparison within the miR-34 family	14
Fig. 2.4: Position of the miR-449 cluster within the CDC20B gene.....	15
Fig. 2.5: Selective expression of transcription factors in the respiratory epithelium.....	16
Fig. 2.6: The five stages of the developing lung	17
Fig. 2.7: microRNAs in the p53-E2F1 interdependent regulation of cell proliferation and cell death?	18
Fig. 4.1: pGL3-3'UTR-E2F1 vector	32
Fig. 5.1: Validation of the Saos2 tet-on E2F1 overexpression system	37
Fig. 5.2: E2F1-induced microRNAs identified by microRNA hybridization.....	38
Fig. 5.3: miR-449a is induced by E2F1 overexpression and DNA damage	39
Fig. 5.4: miR-449a levels are reduced in tumour cells, and its expression pattern resembles the expression of CDC20B	41
Fig. 5.5: miR-449 induces apoptosis.....	43
Fig. 5.6: miR-449 suppresses colony formation in a testicular carcinoma cell line	44
Fig. 5.7: Alterations in DNA content by miR-449a and miR-34a.....	45
Fig. 5.8: Induction of caspase activity by miR-449a and miR-34a	45
Fig. 5.9: Knockdown of miR-449 reduces E2F1-mediated apoptosis	46
Fig. 5.10: miR-449 inhibits the E2F pathway	50
Fig. 5.11: miR-449 induces the p53 pathway while inhibiting the E2F pathway	50
Fig. 5.12: no direct binding of miR-449 to the E2F1 3' UTR	51
Fig. 5.13: HDAC1 and SIRT1 mRNA levels are reduced by miR-449	53
Fig. 5.14: miR-449a, as well as its parologue miR-34a, target SIRT1	53
Fig. 5.15: miR-449a and miR-34a target HDAC1	53
Fig. 5.16: miR-449 overexpression leads to gammaH2AX accumulation	54
Fig. 5.17: gammaH2AX accumulation after miR-449 is dependent on caspase activity.....	55
Fig. 5.18: Chk1 is downregulated by miR-449a and miR-34a	56

Fig. 5.19: miR-449a and miR-34a target BRCA1 but not Chk1 mRNA for degradation	57
Fig. 5.20: Chk1 knockdown by siRNA accumulates DNA damage similarly to miR-449a overexpression but in a caspase-independent manner	58
Fig. 5.21: The combined knockdown of the miR-449 targets SIRT1, CHK1 and E2F1 mimics miR-449-mediated apoptosis.....	59
Fig. 5.22: miR-449a is highly abundant in lung tissue, in particular around birth	60
Fig. 5.23: Comparison of the miR-449a and miR-34a levels in various tissues in mouse.....	61
Fig. 5.24: Strong miR-449a induction in differentiating human airway epithelial cells	63
Fig. 5.25: Levels of miR-449a and FoxJ1 mRNA in differentiating airway epithelia	64
Fig. 5.26: Further induction of miR-449a in airway epithelial cells exposed to tobacco smoke	65
Fig. 6.1: Mutual regulation of p53 and E2F1.....	68
Suppl. Fig. S 1: Apoptotic phenotype of Saos2 tet-on E2F1 cells after E2F1 induction	75
Suppl. Fig. S 2: rejected targets	75
Tab. 3.1: Oligonucleotides	25
Tab. 3.2: Primary antibodies	27
Tab. 3.3: Secondary antibodies	27
Tab. 4.1: Home-made 10x qPCR Mix	35
Tab. 4.2: Home-made 2x qPCR-Master Mix	35
Tab. 4.3: Master mix per 1 μ l cDNA from the reaction described in 4.2.6	35
Tab. 4.4: Realtime PCR cycling program	35
Tab. 5.1: potential miR-449 targets	47
Supp. Tab. 1: microRNA micro-array data.....	76

1. Abstract

E2F1 is a positive regulator of cell cycle progression and also a potent inducer of apoptosis, especially when activated by DNA damage. To identify E2F1-inducible microRNAs, I performed array hybridization and found miR-449a and miR-449b (collectively termed miR-449) to be strongly E2F1-responsive. The levels of miRNAs 449a and 449b, as well as their host gene CDC20B, are strongly upregulated by E2F1 overexpression and DNA damage. Strikingly, miR-449 shares seed sequences and target genes with the miR-34 family, which has tumour suppressive properties. MiR-449 is expressed at high levels and very specifically in testes, lung, and trachea, but not in tumour cells. However, the expression of miR-449 can be reactivated in tumour cells lines by HDAC inhibition, suggesting epigenetic silencing in cancer. Furthermore, miR-449 expression is strongly induced during the mucociliary differentiation of pulmonary epithelia. Exposure to tobacco smoke further increases the levels of miR-449 in airways, consistent with its DNA damage responsiveness. Therefore, miR-449 can serve as an exquisitely sensitive and specific biomarker for the differentiation of mucociliary epithelium. Moreover, it may actively promote differentiation through its ability to block cell cycle progression, and provide a first line of defence against genotoxic stress by its proapoptotic functions.

In agreement with a putative tumour-suppressive role, miR-449 as well as miR-34 reduce proliferation, upregulate p53 activity and strongly promote apoptosis through both p53-dependent and -independent mechanisms. Both miRNAs attenuate E2F1 function by reducing the levels of CDK6, CDK2, E2F1 and E2F3, implying a negative feedback mechanism for the E2F pathway. Moreover, miR-449 and miR-34 decrease the expression of the deacetylases SIRT1 and HDAC1, thereby resulting in p53 activation, which in turn leads to p21 induction and stronger cell cycle arrest in p53 wild type cells. Moreover, since histone deacetylases can regulate complete gene expression programmes, the down-regulation of HDAC1 and SIRT1 might dramatically change the expression patterns, and therefore influence cell fate. In fact, HDAC inhibition has been shown to be very effective in cancer therapy. In addition, miR-449 and miR-34 downregulate two important cell cycle checkpoint proteins, Chk1 and BRCA1, and this can lead to cell death through mitotic catastrophe by interfering with normal mitotic checkpoint regulation. Thus, miR-449 can induce apoptosis in tumour cells in a p53-independent manner.

While E2F1-induced miR-449 as well as p53-induced miR-34 promote p53 activity and apoptosis, they negatively regulate E2F1. Hence, the influence of E2F1 and p53 on each other and on cell fate decisions is sustained by the induction of two miRNA species from the same family. Both miR-449 and miR-34 could provide a twofold safety mechanism to avoid excessive E2F1-induced proliferation by leading to cell cycle arrest or apoptosis.

2. Introduction

2.1. The DNA damage response

2.1.1. DNA damage in cancer & cancer therapy

Today, the most common cause for mutations leading to cancer also paradoxically presents the best option for its therapy: DNA damage. This undesirable damage occurs, for instance, in cells exposed to ultraviolet, ionizing radiation or other genotoxic substances (tobacco smoke, asbestos, alkaloids, bromine or mercury containing compounds, etc.), and it potentially leads to tumorigenesis in a multi-step process starting with mutations of key parts of the DNA (Fearon and Vogelstein, 1990; Hanahan and Weinberg, 2000; Vogelstein and Kinzler, 1993). The very same damage is at the same time the most wanted impact of chemotherapeutics on cancer cells since it can lead to cell death. Most chemotherapeutics are designed to attack proliferating cells (Jackson and Bartek, 2009), assuming that cancer cells go through mitosis more frequently than normal cells. Almost all heavy side effects of such therapies can be explained by the fact that, among normal cells, we find highly proliferative tissues, where cells need to replicate continuously: hair follicles (hair loss), gastrointestinal mucosa (diarrhoea, nausea), immune system (immunosuppression & infections), germ cells (sterility) etc. Therefore, it is important to develop therapies targeting cancer cells as specifically as possible. On a long-term basis this can be achieved by clarifying the pathways that differ in cancerous versus normal cells to allow accurate discrimination between benign and malignant cells during cancer therapy.

2.1.2. Principal actors of the DNA damage response pathway

The DNA damage response is very intricate and still not fully understood. It is very tightly regulated and linked to the cell cycle and cell death regulation (Fig. 2.1).

Depending on the damage, the kinases ATM (Ataxia telangiectasia mutated) and ATR (Ataxia telangiectasia and Rad3 related) can activate different checkpoints (CHK1/2, BRCA1), leading to the induction of cell cycle arrest, DNA repair and eventually, if the damage can not be repaired, cell death programmes like apoptosis.

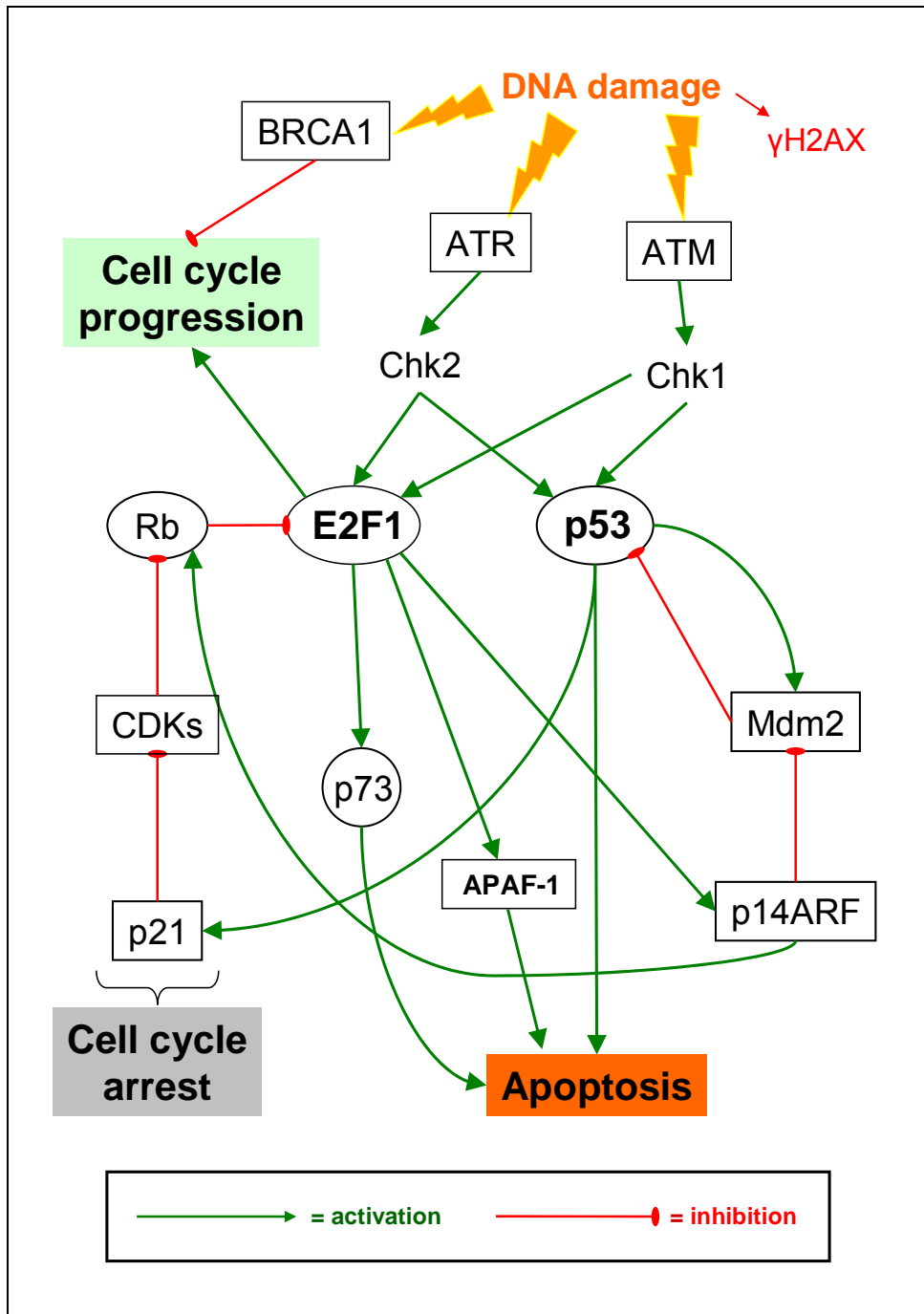


Fig. 2.1: Simplified overview of the DNA damage response

In response to DNA damage, the ATM and ATR kinases are activated and phosphorylate the kinases Chk2 and Chk1, which in turn activate E2F1 and p53. E2F1, which under other circumstances supports cell cycle progression, can then induce cell death by activating the p53 family member p73, or by stabilising the levels of p53 by transactivating the ARF tumour suppressor. In addition, E2F1 can induce apoptosis independently of p53 through direct APAF-1 and caspase induction. After DNA damage, p53 can induce apoptosis or cell cycle arrest, the latter leading to the inhibition of E2F1. Also the BRCA1 protein contributes to cell-cycle arrest and DNA repair by homologous recombination. (Kastan and Bartek, 2004).

Two key players of this pathway are the transcription factors E2F1 and p53. The tumour suppressor p53 is activated by Chk1/2 (checkpoint proteins 1 and 2) and stabilised mostly through post-translational modifications, which leads to the transactivation of its downstream genes. This can either induce cell cycle arrest and repair of the damage, or apoptosis, depending on the form and degree of the inflicted DNA damage. The E2F1 transcription factor is also stabilised and activated after DNA damage, which can lead to apoptosis when surpassing a certain threshold. This will be explained in more details in chapter 2.2.

Two of the possible outcomes of DNA damage are cell cycle arrest or cell death by apoptosis. As pictured in Fig. 2.1, E2F1 and p53 cooperate very tightly in the regulation of both pathways (Sionov and Haupt, 1999).

To make their relationship even more intricate, p53 activity results in negative regulation of E2F1. Most notably, p53 induces the expression of the CDK inhibitor p21, thus leading to the accumulation of hypophosphorylated, active Rb pocket proteins which attenuates E2F activity through its sequestration. Hence, while E2F1 activity enhances p53 activity, p53 synergizes only with the proapoptotic activity of E2F1, while antagonizing E2F1-induced cell cycle progression (Polager and Ginsberg, 2009).

What exactly leads to the induction of apoptosis rather than cell cycle arrest is not quite clear and needs further investigation.

2.2. The E2F transcription factors

The E2F family of transcription factors are DNA binding proteins essential for cell cycle progression, and repressing E2F activity is the key mechanism by which the retinoblastoma (Rb) family of pocket proteins exerts its tumour suppressive function (Qin et al., 1995; Rogoff and Kowalik, 2004). In many tumours, E2F activity is deregulated. Either Rb function is lost, or its phosphorylation status is constitutively changed through cyclin D1 overexpression (that phosphorylates Rb) or loss of p16 (INK4A, CDK inhibitor inhibiting the phosphorylation of Rb). In some other cases, infection with the human papilloma virus leads to the expression of oncoprotein E7 which disrupts Rb–E2F complexes (Sherr and McCormick, 2002).

There are nine different E2F transcription factors. Out of those, E2F1-6 function as heterodimers with members of the DP family (DP1 and DP2) and the DNA-binding specificity depends on the E2F present in the complex. E2F1-3a can, depending on the interaction with Rb, activate or repress the transcription of certain genes. E2F3b-8 are primarily transcriptional repressors (DeGregori and Johnson, 2006; Polager and Ginsberg, 2009).

Cyclin dependent kinases (CDKs) phosphorylate and thereby inactivate pocket proteins (Rb), allowing cell proliferation (Fig. 2.1). This in turn is controlled by CDK inhibitors like the p53-

responsive p21 or the E2F1- and Foxo3a-responsive p27 (Sherr and Roberts, 1999). In addition to cell cycle regulation, E2F proteins are also capable of inducing programmed cell death. This occurs either dependently or independently of p53.

In response to DNA damage, E2F1 is phosphorylated by ATM/ATR (Lin et al., 2001) and Chk2 (Stevens et al., 2003), and therefore stabilised which leads to enhanced transcriptional activity (Bell and Ryan, 2004; Hershko et al., 2006). E2F1-induced p53-dependent apoptosis occurs mainly through direct transactivation of p14ARF/INK4a, which binds to and inactivates the p53 negative regulator Mdm2 (Bates et al., 1998; Haupt et al., 1997; Kubbutat et al., 1997; Pomerantz et al., 1998; Zhang et al., 1998). This in turn leads to p53 accumulation and eventually to p53-mediated apoptosis (Fig. 2.1). Independently of p53, E2F1 strongly induces the expression of TAp73 (Irwin et al., 2000; Lissy et al., 2000; Stiewe and Putzer, 2000), a p53-homologue that shares many activities of p53, including the activation of p14ARF (Bates et al., 1998; Yang and McKeon, 2000). Moreover, similarly to p53, E2F1 transactivates proapoptotic genes like Noxa, Puma and other BH3-only gene products. E2F1 also has other proapoptotic targets, not shared by p53. One of the most prominent ones, APAF-1 (apoptotic protease-activating factor 1), binds and activates procaspase 9, thereby setting off apoptosis (Cain et al., 2002; Furukawa et al., 2002; Moroni et al., 2001; Rodriguez and Lazebnik, 1999; Saleh et al., 1999; Zou et al., 1997). Subsequently, caspase 9 activates the effector procaspases 3, 6 and 7 leading to DNA and protein cleavage, the hallmark of apoptosis (Budihardjo et al., 1999; Franklin and Robertson, 2007). Hence, both E2F1 and p53 are strong inducers of apoptosis, at least in part by transactivating an overlapping but not identical set of target genes (Polager and Ginsberg, 2009).

Consequently, E2F1 has a dual role in cancer. It is primarily considered to be an oncogene (Johnson, 2000; Johnson et al., 1994) because it is found over-expressed in various tumours. However, it was also shown that animals lacking E2F1 develop tumours spontaneously (Yamasaki et al., 1996). In certain contexts, E2F1 works as a tumour-suppressor and induces apoptosis (Johnson, 2000; Shan and Lee, 1994; Tsai et al., 1998; Wu and Levine, 1994) similarly to p53. Since most tumours have lost p53 expression or proper activity, E2F1 is an interesting target for cancer therapy. But the mechanisms regulating the decision between E2F1-induced apoptosis and cell cycle entry are not fully understood and remain a central question in cancer research.

2.3. microRNAs

2.3.1. Biogenesis and function

An important set of genes was only recently discovered: microRNAs. These small, non-coding RNAs represent a novel class of regulators for gene expression and many miRNA-encoding regions are embedded in regular protein-coding genes (Ambros, 2004; Ambros and Lee, 2004; Bartel, 2004). Some microRNAs are ubiquitously distributed, whereas others are expressed in a highly tissue-specific manner (Lagos-Quintana et al., 2002; Landgraf et al., 2007). Rather than encoding proteins, they act as regulators of mRNA stability and/or protein synthesis through specific hybridization of the “seed sequence” (region from base 2 to base 8 of a mature microRNA) with mRNA target sequences, allowing each miRNA species to regulate a characteristic set of mRNAs (Filipowicz et al., 2008; Flynt and Lai, 2008; He and Hannon, 2004). The synthesis of their precursors closely resembles that of mRNAs starting with the transcription of a microRNA precursor called pri-miRNA through the RNA polymerase II (Fig. 2.2). The specific nucleases Drosha and Pasha (DGCR8, “Partner of Drosha”) then recognise and cut the stem-loop structure to produce the pre-miRNA which can be transported to the cytoplasm for further processing through the ribonuclease Dicer.

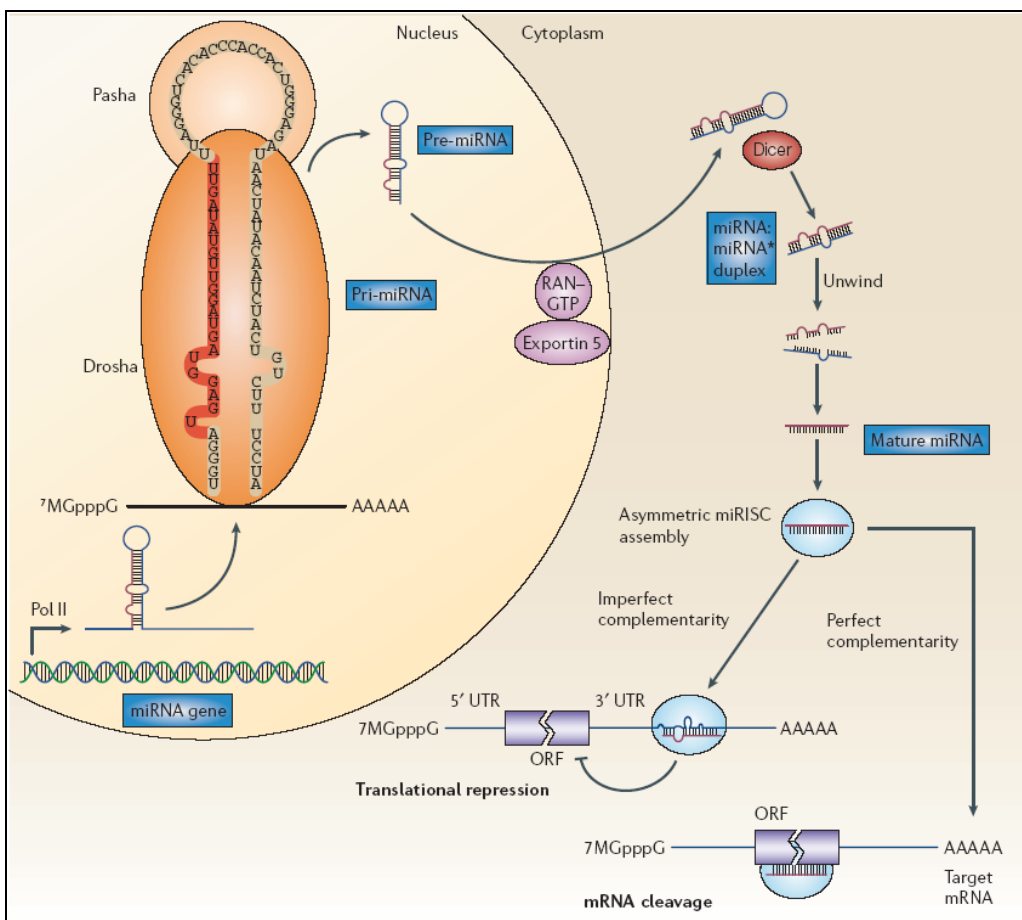


Fig. 2.2: microRNAs: from transcription to active form

Figure adopted from Nature Reviews Cancer April 2006 (Esquela-Kerscher and Slack, 2006).

Mature microRNAs are around 20 bases long and can target mRNAs for degradation (perfect complementarity) or translational repression (imperfect match) (Esquela-Kerscher and Slack, 2006; He and Hannon, 2004; Kim, 2005). Unfortunately, the ability of miRNAs to regulate translation through imperfect binding impedes the accurate prediction of targets. Still, computational predictions are available: miRanda, PicTar, TargetScan and cbio among others.

2.3.2. microRNAs in cancer

Multiple links between miRNA activity and cancer have been established (Croce, 2009; Kumar et al., 2007). Several miRNAs have been described as oncogenes (Cho, 2007; Esquela-Kerscher and Slack, 2006) while others act as tumour suppressors (Friedman et al., 2009a; Lee et al., 2009; Lee and Dutta, 2007; Lin et al., 2009; Shenouda and Alahari, 2009; Welch et al., 2007). In fact, normal cells harbour totally different microRNA profiles than cancer cells (Calin and Croce, 2006). The miRNA profile of tumour cells can even be used to classify them since it reflects their origin and degree of transformation (Lu et al., 2005; Volinia et al., 2006).

Interestingly, p53 was found to induce the expression of some miRNAs. Most notably, the miR-34 family of miRNAs contributes to apoptosis and cell cycle arrest upon induction by p53 (Braun et al., 2008; Chang et al., 2007; Corney et al., 2007; Georges et al., 2008; Georges et al., 2009; He et al., 2007a; Hermeking, 2009a; Raver-Shapira et al., 2007; Tazawa et al., 2007).

Together with the fact that E2F1 can induce programmed cell death, these findings raise the question whether E2F1 may induce miRNAs that contribute to apoptosis. Indeed, E2F1-responsive microRNAs were previously identified, like the miR-17-92 cluster (Novotny et al., 2007; Sylvestre et al., 2007; Woods et al., 2007) and at least partially characterized as to their functions in cancer, but so far mostly with anti-apoptotic functions (Petrocca et al., 2008a; Sylvestre et al., 2007; Yan et al., 2009) or no reported influence on apoptosis.

2.3.3. The miR-34/449 family of microRNAs

The characterisation of the miR-34 family of microRNAs started with the discovery of miR-34a as a p53-responsive gene capable of inducing apoptosis and cell cycle arrest in tumour cell lines (Bommer et al., 2007; Braun et al., 2008; Chang et al., 2007; Corney et al., 2007; Georges et al., 2008; Georges et al., 2009; He et al., 2007a; He et al., 2007b; He et al., 2007c; Hermeking, 2007; Hermeking, 2009a; Hermeking, 2009b; Raver-Shapira et al., 2007; Tarasov et al., 2007; Tazawa et al., 2007). MiR-34a is encoded separately; its homologues

miR-34b and c share a common primary transcript. MiR-34 targets the histone deacetylases SIRT1 (Yamakuchi et al., 2008; Yamakuchi and Lowenstein, 2009) leading to the accumulation of acetylated and therefore highly active p53. Additionally, miR-34 down-regulates several CDKs, cyclins and E2Fs (Lodygin et al., 2008; Sun et al., 2008; Tazawa et al., 2007; Welch et al., 2007), leading to cell cycle arrest and inhibition of the E2F pathway. The down-regulation of the anti-apoptotic protein BCL2 (B-cell CLL/lymphoma 2) could also contribute to miR-34-dependent apoptosis (Chang et al., 2007).

Later on, the miR-449 cluster encoding miR-449a and miR-449b was found to have similar sequence and secondary structure to the miR-34 family, and they were therefore classified as one family of microRNAs. In particular, they share the same seed sequence (Fig. 2.3) suggesting similar targets (Filipowicz et al., 2008). In line with the tumour-suppressive role of miR-34, miR-449 was shown to be significantly down-regulated in prostate cancer (Coppola et al., 2010; Noonan et al., 2009).

	seed sequence
miR-449a	U GGCAGUGU AUUGUUAGCUGGU
miR-449b	A GGCAGUGU AUUGUUAGCUGGC
miR-34a	U GGCAGUGU CUUAGCUGGUUGU
miR-34b*	UA GGCAGUGU CAUUAGCUGAUUG
miR-34c	A GGCAGUGU AGUUAGCUGAUUGC

Fig. 2.3: Seed sequence comparison within the miR-34 family

Sequences of miR-449a and b, aligned with miR-34a, b and c. Shared seed sequence is shown in bold. Data published in Cell Death & Differentiation, March 2010. Source of the sequences: <http://www.mirbase.org/> (Faculty of Life Sciences, University of Manchester, previously hosted and supported by the Wellcome Trust Sanger Institute) (Griffiths-Jones, 2004; Griffiths-Jones, 2006; Griffiths-Jones et al., 2006; Griffiths-Jones et al., 2008)

MicroRNAs of the miR-34 family are highly conserved. MiR-449 was found in apes (rhesus macaque, chimpanzee, orang-utan), mouse, rat, dog, horse, cattle, chicken and frog. In human, the miR-449 cluster is located on chromosome 5 in a highly conserved region of the second intron of the CDC20B gene (Fig. 2.4), a homologue of CDC20 (involved in mitosis exit). Gene products of the CDC family are thought to have roles in cell cycle regulation, but only very little is known about the function of CDC20B. The CDC20B gene is also conserved in apes, dog, cow, horse and chicken which may reflect its importance. Interestingly, CDC20B was recently detected in different screens of lung tissue and airway epithelia,

implicating a role of CDC20B or its host miR-449 in such tissues. E.g. it was upregulated after infection in the trachea of chicken (Wang et al., 2009) and, most notably, its expression was induced more than 180-fold in human mucociliary differentiation (Ross et al., 2007). This idea is supported by the fact that other miR-34 family members were also found to be expressed in the respiratory system and reduced in tumours (Bommer et al., 2007; Chang et al., 2007; Dong et al., 2010; Ji et al., 2009; Landgraf et al., 2007; Welch et al., 2007).

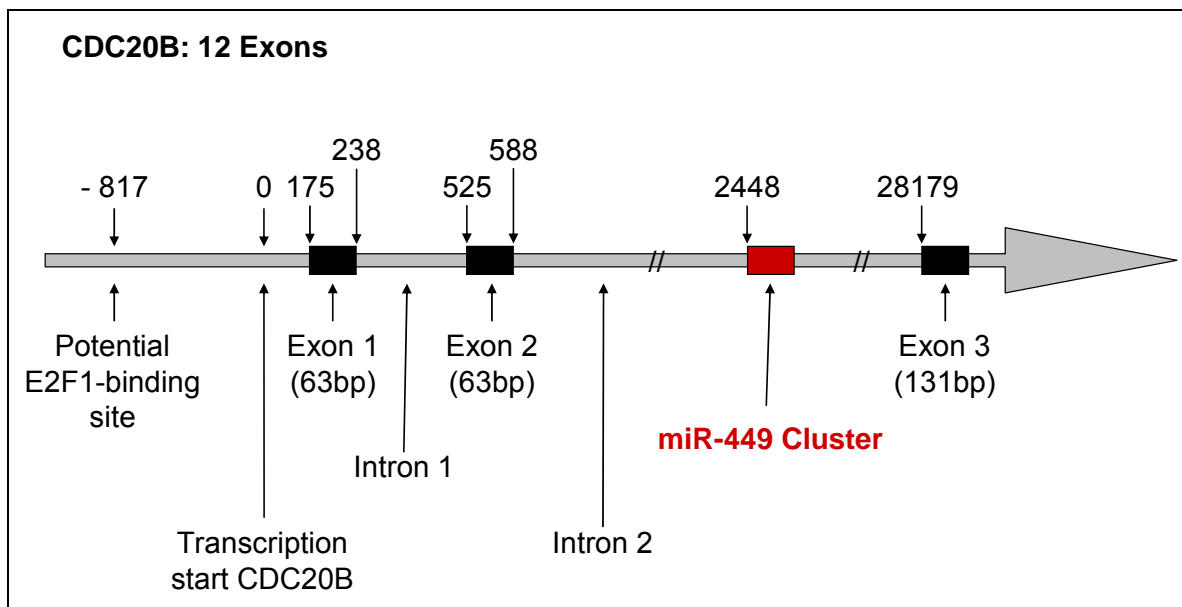


Fig. 2.4: Position of the miR-449 cluster within the CDC20B gene

The genomic region encoding both miR-449a and miR-449b is embedded into an intronic sequence of the mRNA-encoding gene CDC20B, consisting of 12 exons (Lize et al., 2010).

These data strongly suggest that the CDC20B host, miR-449, could be another tumour-suppressive microRNA playing a role in the first line defence of the respiratory tract and in the differentiation of airway epithelium.

2.4. Airway epithelium and its differentiation

Due to their “open” nature, airways are exposed to many risks. The air we breathe transports viruses, bacteria, small particles, smoke, solvents, toxins etc. All of these are potential threats to the respiratory tract and the integrity of the cells it is made of, especially to its “coating”, the bronchial epithelium. To allow proper respiration and host defence, epithelial cells within the respiratory system must differentiate in a highly ordered fashion (Metzger et al., 2008). Particularly, the airway epithelium covering the trachea and bronchia must ensure proper ventilation and gas exchange, prevent the loss of fluid, and contribute to mucociliary

clearance and host defence by avoiding the accumulation of toxic substances from the environment. Thus, it acts as a protective barrier. This epithelium forms a pseudo-stratified layer consisting of basal cells, Goblet cells (mucus secretion), Clara cells (secretion, detoxification and renewal of ciliated cells), and ciliated cells (Fig. 2.5). Defects in mucociliary clearance, the most important mechanism of defence in this tissue, are associated with respiratory disorders like cystic fibrosis or chronic obstructive pulmonary diseases (COPD) (Ross et al., 2007).

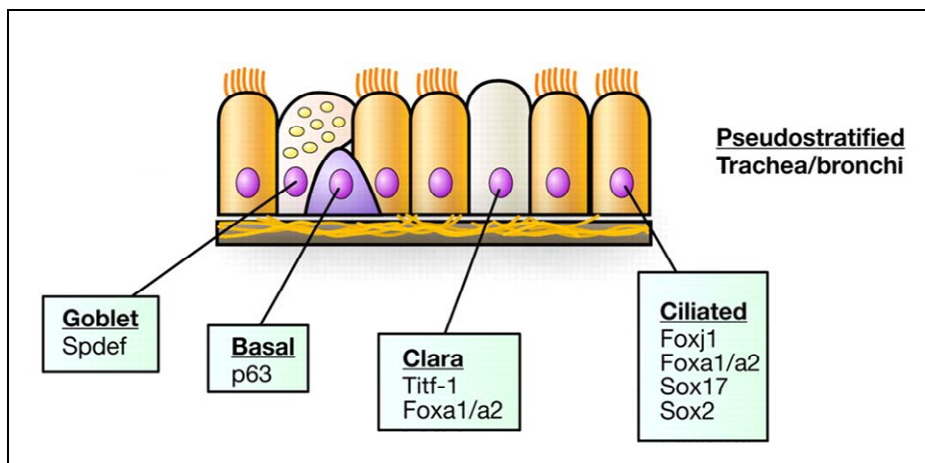


Fig. 2.5: Selective expression of transcription factors in the respiratory epithelium

Large conducting airways (trachea and bronchi) are lined by a pseudo-stratified epithelium consisting primarily of Goblet, basal, Clara (secretory), and ciliated cells. Transcription factors influencing cell type differentiation and gene expression are indicated. Adopted from the review “Transcriptional control of lung morphogenesis” (Maeda et al., 2007)

The process of mucociliary differentiation starts during the pseudo-glandular phases of lung development (around E12 in mouse) and continues until lung maturity (P5-P20) (Fig. 2.6 and Post and Copland, 2002).

Consequently, the differentiation of airway epithelia represents one of the most dramatic changes in cell function that occurs shortly before and after birth, essential for the survival of the organism. The development of the lung involves the activity of several transcription factors in a sequential and cell-specific manner (Fig. 2.5)(Chuang and McMahon, 2003; Maeda et al., 2007). However, our knowledge of the posttranscriptional master regulators behind this process remains incomplete at this stage.

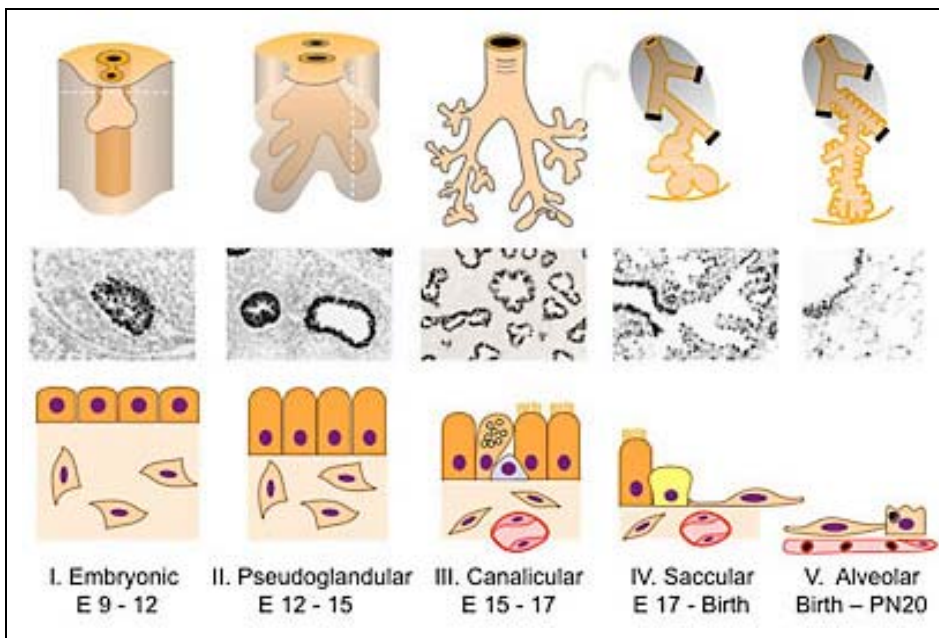


Fig. 2.6: The five stages of the developing lung

The organogenesis of the lung can be divided into five distinct stages: embryonic budding (incl. division of tracheal-oesophageal tube), pseudo-glandular (bronchial branches, acinar tubules and buds; vasculogenesis and innervation), canalicular (pulmonary vascular bed, pulmonary acinus, increasing innervation), saccular (peripheral airspaces, vascularity of the saccules, surfactant synthesis) and alveolar (alveoli, vascular system) phases, shown here for the mouse. Adopted from the homepage of the Whitsett lab, Pulmonary Biology, Cincinnati Children Hospital and (Maeda et al., 2007)

To gain insight into the differentiation process of bronchial epithelia, it has been recapitulated in a cell culture setting. Primary airway epithelial cells (AECs) can be obtained from human donors and maintained in culture. When such a cell monolayer is lifted from a liquid environment to the interface between liquid and air (air-liquid interface, ALI), a mucociliary differentiation program is initiated that reflects the physiological processes occurring in the lung (Bals et al., 2004). By analyzing the associated changes in mRNA levels, a number of differentially regulated genes were previously identified (Ross et al., 2007). Among those, the transcription factor FoxJ1 was suspected to represent one of the regulatory factors that govern downstream genes triggering differentiation (Bals et al., 2004; Brody et al., 2000; Chen et al., 1998; Maeda et al., 2007). Little is known about other master regulators that act at the same stage of differentiation.

Interestingly, mice deficient for E2F1 and Rb die at birth from respiratory failure, which could indicate a role for E2F1/Rb in lung differentiation (Tsai et al., 1998). Additionally, the microRNA processing enzyme Dicer is required for proper pulmonary development (Harris et al., 2006), arguing that microRNAs are essential in this process. Moreover, microRNAs were found to be differentially regulated when lungs develop (Bhaskaran et al., 2009; Dong et al.,

2010; Lu et al., 2008; Wang et al., 2007; Williams et al., 2007; Zhang et al., 2010). Therefore, the evident question arising is whether the miR-34 family, especially the members highly expressed in respiratory tissues, or E2F1-responsive microRNAs play a role in lung development or the differentiation of bronchial epithelium.

2.5. Central question

The transcription factor E2F1 is very often deregulated in cancer and displays paradoxical activities as an oncogene which pushes cell proliferation and as a tumour suppressor that induces apoptosis. Yet, the balance and regulation between those two cell fates are not fully understood. MicroRNAs are a new class of regulatory genes, acting in the regulation of pathways on a new level.

The central purpose of this work was to identify and characterise new E2F1-responsive microRNAs which may play a role in controlling of the E2F1-mediated cellular decision between proliferation and death, and elucidate the physiological relevance of such microRNAs (Fig. 2.7).

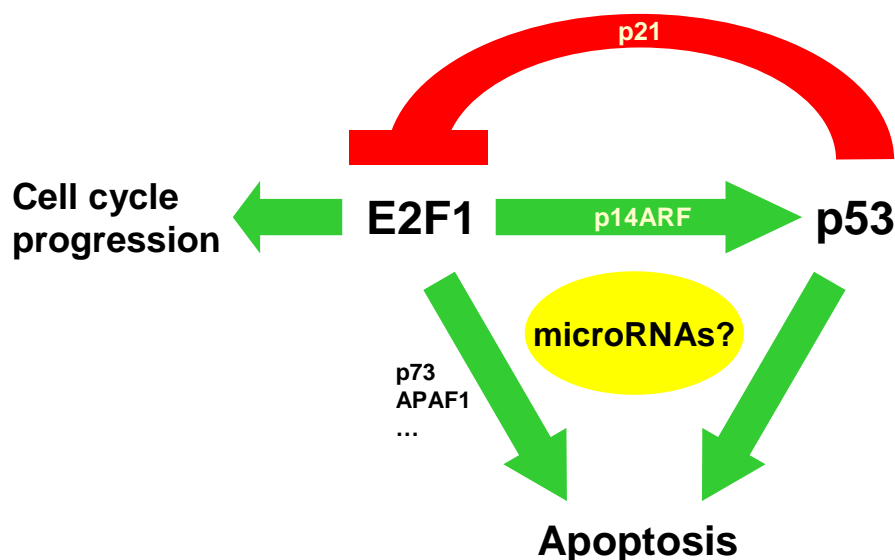


Fig. 2.7: microRNAs in the p53-E2F1 interdependent regulation of cell proliferation and cell death?

E2F1 transactivates not only cell cycle promoting factors, but also p14ARF, leading to p53 stabilisation. p53 in turn transactivates p21, a cyclin-dependent inhibitor, repressing the transcriptional activity of E2F1 and promoting cell cycle arrest. Both E2F1 and p53 are capable of inducing apoptosis through various mechanisms, eventually via the induction of proapoptotic microRNAs.

3. Material

3.1. Equipment

Block Heater "Grant Boekel BBA2"	Grant Instruments
Camera "Power shot A620"	Canon
Developing machine "Optimax X-Ray Film Processor"	
Model 1170-1-000	Protec Medizintechnik
Epithelial ohmmeter EVOM	World Precision Instruments
Foil welding apparatus "Vacupack plus F380 70"	Krups
Freezer -80°C "Hera freeze"	Thermo
Freezer -20° C	Liebherr
Gel documentation system „Gel Doc 2000“	INTAS
Incubator (cell culture) "Hera Cell 150" Thermo Incubator	Memmert
Laminar Flow „HeraSafe®“	Thermo
Low Voltage Power Supplier „Standard Power Pack P25T“	Whatman Biometra
Luminometer "Centro LB960" coupled to software "MikroWin2000"	Berthold Technologies
Magnetic stirrer "MR 3001"	Heidolph Instruments
Microscope „HBO 100“	Karl Zeiss
Microscope "Hund Wetzlar Wilovert LL"	Helmut Hund
Microwave "MW 17705"	Cinex
Mini centrifuge "GMC-060"	LMS Laboratory & Medical Supplies
PCR-Machine "advanced primus 25"	Peqlab Biotechnologie
PCR-Machine „Cycler Biometra ® T personal“	Biometra
pH meter „CG 832“	Schott
Pipettes „Research“ (2.5 µl, 20 µl, 200 µl und 1000 µl)	Eppendorf
Pipet-Aid ® "portable XP"	Drummond
Precision balance	Sartorius
Real-time PCR-machine „DNA Engine (PTC-200) Peltier Thermal Cycler" linked to the detection system „Chromo4™"	
Real-Time PCR Detector"	BioRad Laboratories
Refrigerator 4°C "Profi line"	Liebherr
Refrigerated centrifuge "Megafuge 1.0 R"	Thermo
Refrigerated tabletop centrifuge "5415R"	Eppendorf
Shaker incubator „Minitron“	Infors
Shaker „Promax 2020“	Heidolph Instruments
SDS-PAGE-Chamber „MiniVE“	GE Healthcare
Spectrophotometer „NanoDrop ® ND-100“	Peqlab Biotechnologie
Tabletop centrifuge „5415D“	Eppendorf

Thermomixer "comfort"	Eppendorf
Vacuum system „Vacusafe Comfort“	IBS Integra Biosciences
Vortex-Mixer „Vortex Genie 2“	Scientific Industries
Water bath WB14	Memmert
Water bath TW20	Julabo Labortechnik
Western transfer chamber (wet blot) „MiniVE Blotter“	GE Healthcare
Western transfer chamber (semi-dry blot)	Harnischmacher, Labor- und Kunststofftechnik
Rocker „Rocky“	Schütt Labortechnik
X-ray cassette 13x18cm	Rego X-Ray
Counting chamber Neubauer Improved	Brand

3.2. Consumables

9,6 cm ² -well / 3,9 cm ² -well – cell culture plates	Greiner
Adefodur developer concentrate	Adefochemie
Adefodur fixer concentrate	Adefochemie
Chamber slides system "LabTek®" (4 chambers)	NUNC
Filtertips „Biosphere®“ (20µl, 200µl und 1000µl)	Sarstedt
Whatman paper „GB002“	Schleicher & Schuell
Gloves „Safe Skin PFE“	Kimberly Clark
Cryotubes (1.8ml)	NUNC
Nitrocellulose protran transfer membrane BA83	Schleicher & Schuell
Optical film sealing kit (96-well-plates)	BioRad Laboratories
Pasteur pipettes 150 mm and 230 mm WU Mainz	
PCR multiplate 96-well unskirted PCR plates (white)	BioRad Laboratories
PCR reaction tubes (200 µl)	Sarstedt
PVDF membrane	Schleicher & Schuell
Reaction tubes (1,5 ml/2 ml)	Sarstedt
X-ray films (blue) RX 13x18 100BI	Fuji, Ernst Christiansen
Screw tube 15ml, 120x17mm, sterile	Sarstedt
Screw tube 50ml, 114x28mm, sterile	Sarstedt
Heat sealing plastic film (transparent)	Krups
Cell culture dishes	Greiner
Cell scraper (16cm/25cm)	Sarstedt
Transwell six-well culture plates	Corning Life Science

3.3. Chemicals

β-mercaptoethanol	Roth
-------------------	------

2-propanol	Roth
Acetic acid	Roth
Ammonium persulphate (APS)	Roth
Ammonium sulphate ((NH4)2PO4)	Roth
Bromophenol blue	Sigma-Aldrich
Bovine serum albumin (BSA)	Roth
Calcium chloride (CaCl)	Roth
Camptothecin (CPT)	Sigma-Aldrich
Chloroform	Roth
Coelenterazine	Promega
Complete, EDTA-free	Roche
Coomassie Brilliant Blue	Sigma-Aldrich
D-Luciferin	ICN
DAPI (4,6 Diamidino-2-Phenyindole)	Sigma-Aldrich
Deoxycholate (DOC)	AppliChem
Dimethylsulfoxid (DMSO)	AppliChem
Disodium-hydrogen-phosphate (Na ₂ HPO ₄)	Merck
dNTP-Mix, 20mM	BioBudget
DTT (1,4-Dithiothreitol)	Roth
EDTA (ethylenediaminetetraacetate)	Jena Bioscience
Ethanol 99,9%	Merck
Fluorescein reference standard	Invitrogen
Formaldehyde	Roth
Glycerine	Roth
Glycine p.A.	Roth
Glycogen, 20mg/ml	Fermentas
H ₂ O, RNase-Free	Ambion
HCl acid	Roth
HEPES	Roth
Iodoacetamid	AppliChem
Isoamyl alcohol	Roth
Magnesium chloride (MgCl)	Merck
Manganese chloride (MnCl)	Roth
Methanol	Roth
NaOH pellets	Roth
Nuclease-free water	Promega
Nutlin-3a	Sigma-Aldrich
pH solution 10.01	Roth
pH solution 4.01	Roth
pH solution 7.01	Roth
Ponceau S	Roth
Potassium acetate (CH ₃ COOK)	Sigma-Aldrich

Potassium chloride (KCl)	Roth
Potassium dihydrogen phosphate (KH ₂ PO ₄)	Roth
Protease inhibitor mix "Complete"	Roche Diagnostics
Rotiphorese Gel 30 (30% acrylamide–solution)	Roth
SDS (sodium lauryl sulphate, Natriumdodecylsulfate)	Roth
Skimmed milk powder Naturaflor	Töpfer
Sodium azide 0.1 M solution	Sigma-Aldrich
Sodium acetate	Roth
Sodium carbonate	Roth
Sodium chloride (NaCl)	Roth
Sodium deoxycholate	Applichem
Sodium dihydrogen phosphate	Roth
Sodium hydrogen carbonate	Roth
Sucrose	Serva
SYBR Green I	Stratagene
TEMED (N,N,N',N'-tetramethylendiamine)	Roth
Trasylol	AppliChem
Trehalose	USB Corporation
Trichostatin A (TSA)	Bayer Vital
Tris	Roth
Triton x-100	Roth
TRIzol ® Reagent	Invitrogen
Tween 20	AppliChem
Urea	Roth

3.4. Kits

BCA™ Protein Assay kit	Pierce
Developer „Adevodur”	OMNILAB
Dual-Luciferase® Reporter Assay System	Promega
E.Z.N.A. Plasmid Miniprep Kit II	Peqlab
Fixer „Adevodur”	OMNILAB
Lipofectamine™ 2000 transfection reagent	Invitrogen
Sequencing mix and buffer “ABI Prism Big Dye Terminator v3.1 cycle sequencing kit RR100”	Applied Biosystems
SuperSignal West Dura extended duration	Pierce
SuperSignal West Femto maximum sensitivity	Pierce
Taq buffer (NH ₄) ₂ SO ₄ and 25 mM MgCl ₂	Fermentas
PureYield™ Plasmid Midiprep System	Promega
RNeasy® Mini Kit	Qiagen

3.5. Buffers and solutions

Coelenterazine solution (1500x stock):	3mM in Ethanol	
Coomassie staining solution:	0.25% coomassie brilliant blue 50% methanol 10% acetic acid	
D-Luciferin solution (4x stock):	5mg D-Luciferin 18ml Glycylglycine [25mM] (pH 8.0) store at -80°C in the dark	
EB buffer:	10 mM Tris (pH 8.5)	
Firefly Buffer (in dark bottle):	25mM Glycylglycine 15mM K ₂ HPO ₄ 4mM EGTA pH 8.0	
Laemmli buffer (6x):	0.35 M tris pH 6.8 30% glycerin (v/v) 10% SDS (w/v) 9.3% Dithiothreitol (DTT) (w/v) 0.02% bromphenol blue (w/v)	
PBS (Phosphate Buffered Saline)(10x):	236.9 mM NaCl 2.7 mM KCl 8.1 mM Na ₂ HPO ₄ 1.1 mM MgCl ₂ 1.5 mM KH ₂ PO ₄ 1.2 mM CaCl ₂	
PBS ^{deficient} :	composition like PBS, but without MgCl ₂ und CaCl ₂ .	
PBST:	composition like PBS with 0.1% Tween20.	
Ponceau S solution:	0.5 g ponceau S 1 ml glacial acetic acid ad 100 ml ddH ₂ O	
Renilla Buffer (pH 5.1; in dark bottle):	1.1M NaCl 2.2mM Na ₂ EDTA	

	0.22 M	K ₂ HPO ₄
RIPA buffer:		
	0.1%	triton X-100 (v/v)
	0.1%	desoxycholate (v/v)
	0.1%	SDS (w/v)
	2 mM	Tris/HCl, pH 8.5
	9 mM	NaCl
	1 mM	EDTA
	1.4%	trasylol (100000 KIE)
	18.5%	Iodacetamide
SDS running buffer (10x):		
	151 g	Tris
	720 g	glycine
	50 g	SDS
	ad 5 L	ddH ₂ O
Stripping buffer:		
	50 ml	1M Tris pH 6.8
	400 ml	10% SDS
	10 ml	β-mercaptoethanol
	ad 1 L	ddH ₂ O
TBS (Tris Buffered Saline) (10 x) pH 7.6:	24,2 g	Tris
	80 g	NaCl
	ad 1 L	ddH ₂ O.
TBST:		
	100 ml	10 x TBS
	0.1%	Tween20
	ad 1 L	ddH ₂ O
Transfer buffer for wet blot:		
	100 ml	Western Salts (10x)
	150 ml	Methanol
	850 ml	ddH ₂ O
Western salts (10x):		
	60.55 g	Tris
	288 g	glycine
	0.02%	SDS
	ddH ₂ O ad 2 L,	pH = 8.3

3.6. Nucleic acids

3.6.1. Plasmids & vectors

- miR-Vec library: microRNA expression plasmids with Blasticidin resistance for selection in eukaryotic cells, generous gift of R. Agami (Voorhoeve et al., 2006).
- pcDNA3-empty (Invitrogen): used as a control. Mammalian expression vector with CMV promoter and Ampicillin and Neomycin resistance cassettes.
- pcDNA3-E2F1: Mammalian expression vector pcDNA3 (Invitrogen) for E2F1.
- pGL3-Basic Vector (Promega): Firefly luciferase reporter vector (empty) with Ampicillin resistance.
- pGL3-3'UTR-E2F1: Luciferase reporter vector (pGL3-Basic, Promega) containing the 3'UTR of E2F1 (Fig. 4.1).
- pRL-tk (Promega): Renilla luciferase vector (control reporter) with Ampicillin resistance.

3.6.2. Synthetic microRNAs & other small RNAs

Pre-miRs (miR-449a, miR-34a, NC#1, NC#2, miR-302*)	Ambion
LNAs (Locked Nucleic Acids) to miR-449a, miR-449b and scramble	Exiqon
Negative control siRNA #1	Ambion
Silencer select siRNA CDK6 (s51)	Ambion
Silencer validated siRNA CHEK1 (108)	Ambion
Custom siRNA to E2F1 (sense: GAAGUCCAAGAACCAUCUU, antisense: GAUGUGGUUCUUGGACUUCUU)	Ambion
MISSION siRNA universal negative control #1	Sigma
Pre-designed siRNA to SIRT1 (4113770, 4113771)	Sigma

3.6.3. Primers

All primers were synthesized by Metabion and resuspended in nuclease-free water to a final concentration of 100µM.

Tab. 3.1: Oligonucleotides

human primers	sequence
36B4 forward	GATTGGCTACCCAACTGTTG
36B4 reverse	CAGGGGCAGCAGGCCACAAA

BCL2 for	GTTGGTTTATTGAAACCTG
BCL2 rev	TTCTTATAGTCCCCACCATT
BCL6 for	CAGATTGTACAGGTGGCCC
BCL6 rev	AGATTCTGAGAAGGGGCTGG
BRCA1 for	GCGCCCTCACAAATAAT
BRCA1 rev	CTTGACCATTCTGCTCCGTT
CDC20b for	AACTTGCAGAAGAGGCTGTC
CDC20b rev	TCTTCTCAGGCAGGTGTCTT
CDK2 for	GTGGTACCGAGCTCCTGAAA
CDK2 rev	GGAGAGGGTGAGATTAGGGC
CDK6 for	AGACCCAAGAACAGCAGTGTGG
CDK6 rev	AAGGAGCAAGAGCATTAGC
Chk1 for	TGTTGGATGAAAGGGATAAC
Chk1 rev	AAACATCAACTGGTTCTGC
E2F-1 forward	CGGTGTCGTCGACCTGAAC
E2F-1 reverse	AGGACGTTGGTATGTATAGATG
FoxJ1 for	GCCCAGGACCAGAACATCGCT
FoxJ1 rev	GGAAGACGCAGCAATGAAACAC
GAPDH forward	TGAAGGTCGGAGTCACGGATTTGGT
GAPDH reverse	GCAGAGATGATGACCCTTGGCTC
HDAC1 forward	ACCATGCAAAGAACGTCCGAG
HDAC1 reverse	GGCTGAAAATGGCCTCATA
p21 forward	TAGGCCGTTGAATGAGAGG
p21 reverse	AAGTGGGGAGGAGGAAGTAG
SIRT1 forward	GAGATAACCTCTGTTGGTG
SIRT1 reverse	CGGCAATAATCTTAAGAAT
murine primers	
mmu CDKn1a(p21Cip1) fwd	GTGGCCTTGTGCGCTGTCTT
mmu CDKn1a(p21Cip1) rev	GCGCTTGGAGTGATAGAAATCTG
mmu E2F1 fwd	AACTGGGCAGCTGAGGTGC
mmu E2F1 rev	CAAGCCGCTTACCAATCCC
mmuTAp73 fwd 382-402	AGCAGAATGAGCGGCAGCGTT
mmuTAp73 rev 544-523	TGTTGGACTCCTCGCTGCCTGA

3.7. Proteins & Peptides

3.7.1. Protein marker

PageRuler™ Prestained Protein Ladder Fermentas

3.7.2. Enzymes

M-MuLV reverse transcriptase

New England Biolabs GmbH

Protease 14

Sigma

RNase Inhibitor
Taq Polymerase, hot start [5 units/ μ l]

New England Biolabs GmbH
Axon Labortechnik

3.7.3. Antibodies

Tab. 3.2: Primary antibodies

Antigen	species	clone	Dilution/ Concentration	Company
Acetyl-p53 (Lys382)	Rabbit, polyclonal		1:1000	Cell Signaling
Beta-actin	Mouse, monoclonal	AC-15	1:20000 (0.08 μ g/ml)	Abcam
CDK6	Mouse, monoclonal	DCS83	1:500	Cell Signaling
Chk1	Mouse, monoclonal	2G1D5	1:1000	Cell Signaling
Cleaved caspase-3 (Asp175)	Rabbit, monoclonal	5A1	1:400	Cell Signaling
E2F1	Mouse, monoclonal	KH95	1:400 (0.5 μ g/ml)	Santa Cruz
E2F3	Rabbit, monoclonal	N-20	1:1000	Santa Cruz
GammaH2AX (phospho-histone H2A.X) (Ser139)	Mouse, monoclonal	JBW301	1:5000	Upstate
HDAC1	Rabbit, polyclonal		1:500	Cell Signaling
Hsc70	Mouse, monoclonal	B-6	1:50000	Santa Cruz
Noxa	Mouse, monoclonal	114C307	1:400 (1.25 μ g/ml)	Abcam
p21WAF1 (Ab-1)	Mouse, monoclonal	EA10	1:1000	Calbiochem
p27	Mouse, monoclonal	F-8	1:1000	Santa Cruz
p53	Mouse, monoclonal	DO-1	1:1000 (0.2 μ g/ml)	Santa Cruz
Parp-1 (Ab-2)	Mouse, monoclonal		1:500	Calbiochem
Phospho-Chk1(Ser317)	Rabbit, polyclonal		1:500	Cell Signaling
Phospho-Chk2 (Thr68)	Rabbit, polyclonal		1:800 (0.11 μ g/ml)	Cell Signaling
Phospho-p38(Thr180/Tyr182)	Rabbit, polyclonal		1:500	Cell Signaling
Phospho-p53 (Ser15)	Mouse, monoclonal	16G8	1:800 (0.125 μ g/ml)	Cell Signaling
SIRT1	Mouse, monoclonal	B-7	1:500	Santa Cruz

Tab. 3.3: Secondary antibodies

Name	Dilution/Concentration	Company
Peroxidase-conjugated affiniPure F(ab') ₂ Fragment, donkey anti-mouse IgG (H+L)	1:10000 (0.08 μ g/ml)	Jackson ImmunoResearch
Peroxidase-conjugated affiniPure F(ab') ₂ Fragment, donkey anti-rabbit IgG (H+L)	1:10000 (0.08 μ g/ml)	Jackson ImmunoResearch

3.8. Cell culture

Bacteria:

Agar	Sigma-Aldrich
Ampicillin [ad 200 µg/ml]	Sigma-Aldrich
Kanamycin [ad 25 µg/ml]	Sigma-Aldrich
Tryptone	Roth
Yeast extract	Sigma-Aldrich
2YT medium: 1.6% tryptone (w/v), 1% yeast extract (w/v) and 0.5% NaCl (w/v) in water.	
LB medium: 1% tryptone (w/v), 1% yeast extract (w/v) und 0.5% NaCl (w/v) in water.	
LB agar plates: 15% Agar (w/v) in LB medium.	

Mammalian cells:

Airway epithelial cell growth medium	Promocell
Blasticidine S HCL	Sigma-Aldrich
Ciprofloxacin (Ciprobay®200)	Bayer Vital
Dulbecco`s Modified Eagle Medium (DMEM)	GibcoBRL/Invitrogen
Fetal calf serum, FCS	GibcoBRL/Invitrogen
L-Glutamine	GibcoBRL/Invitrogen
McCoys 5A	GibcoBRL/Invitrogen
Penicillin / Streptomycin	GibcoBRL/Invitrogen
Tetracycline	Roth
Trypsin/EDTA	GibcoBRL/Invitrogen
Ultroser G serum substitute	Pall Life Science

Media were completed with 10 µg/ml Ciprofloxacin, 50 U/ml Penicillin, 50 µg/ml Streptomycin, 2 µg/ml Tetracycline, 10% FCS and 200 µM L-Glutamine.

The differentiation medium for the AECS (DMEM/HamF12, 1:1) was supplemented with 2% Ultroser G serum substitute.

3.9. Cells

3.9.1. Prokaryotic cells

Electrocompetent cells *Escherichia coli* DH 10 B „Electromax“, Invitrogen

3.9.2. Eukaryotic cells

Tumour cell lines

- H1299 cells, from human lung adenocarcinoma, p53 deleted (from A. Levine)
- U2OS cells, from human osteosarcoma, wild-type p53, p14^{ARF} silenced (ATCC)
- HCT116 wt and -/- p53 cells, from human colon carcinoma with and without p53 (obtained from B. Vogelstein (Bunz et al., 1998))
- Saos2 cells, from human osteosarcoma, p53 and Rb deleted (ATCC)
- Saos2 tet-on E2F1 cells, from human osteosarcoma, p53 and Rb deleted, with tet-inducible E2F1 (from K. Vousden (Phillips et al., 1999))
- GH cells, from human testicular teratocarcinoma, p53 wt but inactivated (from R. Loewer)
- 833KE cells, from human testicular teratocarcinoma, p53 wt but inactivated (from R. Loewer)
- T98G cells, from glioblastoma multiforme, p16 and p53 deleted (ATCC)

Primary cells

- Aero-epithelial cells (Elaut et al.), human primary bronchial epithelial cells (HBEC) obtained from human donors during large airways resection (see method section 4.1.1 for detailed procedure).

3.10. Animals & tissues

Male C57BL/6 mice (B6N, n=3 per group) were used for adult tissue analysis. At the age of 5 (n=3), 10 (n=4) or 11 weeks (n=3), male B6N mice were killed by cervical dislocation and organs were isolated. Younger animals (P1, P3, P9 and P14) were killed by decapitation, sex was not determined. For embryonic stages, pregnant female B6N mice were killed at day 16.5 post coitum. Uteri containing the embryos were isolated and dissected in ice cold PBS. Embryonic lung tissue was isolated in cold PBS under a stereomicroscope. Animals were handled in accordance with the German Animal Protection Law and with the permission of the Bezirksregierung Braunschweig.

4. Methods

4.1. Cell biological methods

4.1.1. Isolation of human primary airway epithelial cells

Human primary bronchial epithelial cells (HBEC) were isolated from large airways resected during surgery and cultivated as submersed or air liquid interface (ALI) cultures as described previously (Bals et al., 2004). Donors underwent lung transplantation due to pulmonary fibrosis. The protocol was approved by the ethics committee of the University of Marburg and informed consent was obtained from the patients. Briefly large airways were digested enzymatically with protease 14. The cells were expanded in airway epithelial cell growth medium supplemented with growth factors and preserved in liquid nitrogen.

4.1.2. Air-liquid interface cultures & smoke condensate exposition

HBECs were seeded in cell culture plates and grown until they reached 70-80 % confluence. For the establishment of ALIs $2.5\text{-}3 \times 10^5$ cells/well were seeded in transwell six-well culture plates in airway epithelial cell growth medium supplemented with growth factors and 1% of a mixture of Penicillin and Streptomycin. The cells were incubated for 3 days in a standard cell culture incubator. The apical medium was removed and the basolateral medium replaced by differentiation medium (DMEM/HamF12, 1:1) containing 2% Ultroser G serum substitute. The cells were regarded as fully differentiated after reaching a transepithelial resistance greater than 1000 Ohms/cm² as measured by an epithelial ohmmeter. Tissue cultures were exposed to volatile cigarette smoke (CS) as described previously (Beisswenger et al., 2004). Briefly, tissue cultures were exposed to CS for 15 min (= 3 cigarettes). After the exposure, the medium of the cultures was replaced immediately. Control cultures were incubated in the exposure chamber for the same time period without burning a cigarette.

4.1.3. Cell culture & drug treatment of tumour cell lines

HCT116 cells with and without p53 were grown in McCoy's 5A, H1299, U2OS, GH and 833KE and Saos-2 cells without or with tet-inducible E2F1 were cultivated in Dulbecco's Modified Eagle's medium, each supplemented with 10% foetal bovine serum. Camptothecin (CPT; solved in DMSO), a topoisomerase I inhibitor known to induce double-strand breaks

(DSBs), was used at 2.9 μ M. The Mdm2-inhibitor Nutlin-3a (in DMSO) was used at 8 μ M to accumulate p53. The caspase inhibitor Z-VAD (in DMSO) was used at 50 μ M. Doxycycline (solved in water) was used for the induction of the tet-on system at 2 μ g/ml. Trichostatin A (TSA), an antifungal antibiotic, selectively inhibits class I and II histone deacetylases, but not Sirtuins (class III HDACs). TSA was used at a final concentration of 250 nM.

4.1.4. Transfection of eukaryotic cells

Transient transfection of cells with pre-microRNAs:

Cells were reverse-transfected with synthetic pre-micro-RNAs (Ambion/Applied Biosystems). microRNA was diluted in 250 μ l medium without serum to get 10 nM end concentration. 4 μ l Lipofectamine2000 (Invitrogen) was incubated with 250 μ l medium for 5 min. The combination of both mixtures was incubated for 20 min at room temperature and added to a suspension of freshly trypsinized cell, followed by seeding in 6-well dishes.

Transient transfection of cells with siRNAs:

siRNAs were reverse transfected using the same protocol as for pre-microRNAs at 30nM.

Transient transfection of cells with plasmid-DNA:

Cells were seeded in 6-well plates one day prior to transfection and forward transfected using the standard operating procedure for Lipofectamine2000 (8 μ l Lipofectamine2000 and 2,4 μ g DNA per well).

Stably transfected cells:

Stable transfection was achieved by selection of the transfected cells using Geneticin [500 μ g/ml] or Blasticidin [10 μ g/ml] depending on the resistance cassette of the transfected construct.

4.1.5. Clonogenic assays

Cells were transfected in 6-well plates with miR-vectors, a generous gift of R. Agami (Voorhoeve et al., 2006). Cultures were maintained for 2 to 3 weeks with Blasticidin [10 μ g/ml] selection of the transfectants, followed by fixation with 70% methanol at 4°C and staining with crystal violet.

4.1.6. Flow cytometry

Analysis of cell cycle distribution using propidium iodide (PI) staining of the DNA content

Attached cells combined with floating cells were harvested and fixed in 70% ethanol at 4°C. The cells were then resuspended and incubated for 30 minutes in PBS containing 1 mg/ml RNase A, and stained with 15 µg/ml PI (end concentration), a fluorescent DNA intercalating agent. Samples were analyzed by the Guava/Millipore Easycyte Plus System using the Guava ExpressPro or ModFit Software.

4.1.7. Dual luciferase assay

Method adapted from “Noncommercial Dual Luciferase Enzyme Assay System for Reporter Gene Analysis”, Analytical Chemistry 2000 (Dyer et al., 2000)

To find out if microRNAs could regulate E2F1 through binding to its 3'UTR we used the construct pictured in Fig. 4.1. If a microRNA binds to the 3'UTR and targets the mRNA for degradation or translational repression, luciferase activity should be decreased.

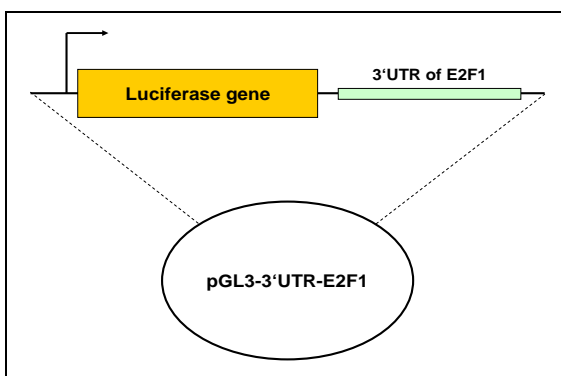


Fig. 4.1: pGL3-3'UTR-E2F1 vector

H1299 cells (20,000 per 96-well) were reverse transfected with pGL3-3'UTR-E2F1 (30ng), pRL-tk (50ng) and each miR-Vec (160ng) containing a microRNA or the hTR control using lipofectamine2000 and incubated for 24h at 37°C. The cells were then shaked for 15 min at room temperature in 65µl Passive Lysis Buffer (Promega) per well. After short centrifugation, 40µl of the supernatant was transferred into a 96-well Optiwell plate. The following working reaction buffers were made fresh as follows.

Per 10 ml Firefly Buffer (stock), addition of: 200 µl of 1M MgSO₄ (~15mM final concentration), 500 µl of 100mM ATP pH 7.0 (~4mM final concentration), 15 µl of 1M DTT (~1.25mM final concentration), 120 µl of 10mM CoA (0.1mM final concentration), 1 ml Luciferin (~80µM final concentration). Per 10 ml Renilla Buffer (stock), addition of: 500 µl of 10 mg/ml BSA

(~0.5mg/ml final concentration), 12 µl of 1.3M NaN₃ (~1.5mM final concentration), 2.5 µl of 6mM Coelenterazine (~1.5µM final concentration).

Luminometer (Berthold Technologies) was set to dispense 100 µl of working Firefly Buffer with a 2 second delay and a 10 second integration. This was followed by injection of 100 µl of working Renilla Buffer with a 2 second delay and a 10 second integration.

4.2. Molecular biological methods

4.2.1. Transformation, cultivation and selection of bacteria

50 µl of chemical competent E. coli DH10B were mixed with 100 ng DNA [0.5-1 µl DNA] and incubated on ice for 30 min (can vary depending on plasmid size!). Cells were subsequently incubated for 10 min at 37°C and cooled down on ice for 10 min. After addition of 50 µl LB or 2YT medium, cells were plated on agar containing Ampicillin [200 µg/ml] or Kanamycin [25 µg/ml] (Sigma-Aldrich) depending on the resistance cassette of the plasmid and incubated overnight at 37°C.

4.2.2. DNA preparation

Midi preparation of DNA was performed using the PureYield™ Plasmid Midiprep System kit from Promega as recommended by the manufacturer.

4.2.3. RNA preparation

Cell culture

For microRNA-analysis, total RNA was isolated using the mirVana RNA Isolation kit (Ambion). For mRNA analysis, total RNA was isolated either with TRIzol (Invitrogen) or with the RNeasy Mini Kit from Qiagen when it was necessary to discard the transfected pre-micro-RNAs from the preparation prior to reverse transcription.

Murine tissues

Mice or embryos were sacrificed and organs were isolated. The tissue was homogenized in 1 ml of TRIzol (Invitrogen) and frozen in liquid nitrogen. After thawing, the lysate was chloroform-extracted and ethanol-precipitated. The pellet was dissolved in pre-heated (95°C) miRVana elution buffer (Ambion).

4.2.4. Concentration of nucleic acids

The concentration and purity of the isolated nucleic acids was measured using standard spectrophotometric quantification by the NanodropTM ND-1000.

4.2.5. DNA sequencing

Plasmid (200-400ng) or PCR product (10-30ng) was mixed to 8 pmol of the sequencing primer, sequence mix (1.5 µl or 1µl respectively) and sequence buffer (1.5 µl or 1µl respectively). Water was added to 10µl prior to sequence PCR (10sec at 96°C, 15 sec at 55°C and 4 min at 60°C for 25 cycles). Each sample was incubated 5 min with 1µl 125mM EDTA, 1µl 3M NaAc and 50µl 100% EtOH and then centrifuged at 12,000 rpm for 15 min. Supernatant was washed with 70µl of 70% EtOH, repelleted and dried. The sequencing was carried out in 30µl HPLC water by the sequencing facility in our institute using the ABI 3100 Automated Capillary DNA Sequencer (Applied Biosystems).

4.2.6. Reverse transcription of mRNA in cDNA

To detect mRNA expression, the isolated RNA was reverse transcribed using the following procedure. 1 µg of total RNA in 10 µl DEPC water was mixed with 2 µl of a primer solution (containing 15 µM random nonamers and 50 µM dT23VN primers) and 4 µl of a dNTP mix [2.5 mM], and heated for 5 min at 70°C. Then, 4µl of the following master mix was added to each sample: 2 µl 10X Reaction Buffer, 0.25 µl RNase Inhibitor (10 U), 0.125 µl M-MuLV Reverse Transcriptase (25 U) and 1.625 µl DEPC water. The samples were incubated at 42°C for 1 h for reverse transcription and at 95°C for 5 min for enzyme inactivation. The reaction was diluted to 50 µl by adding 30 µl water.

4.2.7. Semi-quantitative Realtime PCR using SYBR Green

For Realtime PCR applications, following home-made master mix was prepared as a 10x qPCR mix prior to use (Tab. 4.1). After sterilisation using a 0.2 µm filter, further ingredients were added to the 10x qPCR Mix to produce the 2x qPCR-Master Mix (Tab. 4.2). The 2x qPCR Mix was then aliquoted and snap frozen. The final reaction was mixed as shown in Tab. 4.3. The qPCR program is shown in Tab. 4.4. The list of the RT-PCR primer sets can be found in Tab. 3.1. The standard curve method was used for the relative quantification of gene expression.

Tab. 4.1: Home-made 10x qPCR Mix

component	stock conc.	for 50 ml	final conc.
Tris-HCl (pH 8.8)	1.5 M	25 ml	750 mM
(NH ₄) ₂ SO ₄	1 M	10 ml	200 mM
Tween-20	10%	500 µl	0.10%
H ₂ O		14.5 ml	

Tab. 4.2: Home-made 2x qPCR-Master Mix

component	stock conc.	µl for 1 sample	µl for 3000 samples	final conc.
10 x qPCR Mix (Tab. 4.1)	10 x	2.5	7500	1 x
MgCl ₂	25 mM	3	9000	3 mM
Trehalose (in 10mM Tris pH 8.0)	1 M	7.5	22500	
Triton X-100	10%	0.625	1875	0.25%
Sybr Green	1:100	0.0313	93.9	1:80000
dNTPs	20 mM	0.25	750	0.2 mM
Taq-polymerase	5 U/µl	0.1	300	20 U/ml
Total		14	42000	

Tab. 4.3: Master mix per 1µl cDNA from the reaction described in 4.2.6

	for 1 sample	
	Final concentration	Volume in µl
2x qPCR Master Mix (Tab. 4.2)	1x	10
H ₂ O		8.2
Primer forward (10 µM)	250 nM	0.4
Primer reverse (10 µM)	250 nM	0.4
Total		19

Tab. 4.4: Realtime PCR cycling program

Time	Temperature	Comments
00:02:00	95°C	Hot start
00:00:15	95°C	
00:00:20	60°C	melting + annealing + elongation x 39 times
00:00:25	65°C	
		melting curve from 60° to 95°C, read every 1°C, hold 00:00:01

4.2.8. Reverse transcription of mature microRNAs and semi-quantitative Realtime PCR using Taqman

Stem-loop qRT-PCR for mature microRNAs was done using the TaqMan MicroRNA assays (Applied Biosystems) as recommended by the manufacturer. microRNA expression levels

were normalized to RNU6b or to U6 snRNA (non-coding small nuclear RNA component of the U6 small nuclear ribonucleoprotein, part of the spliceosome).

4.2.9. microRNA microarray analysis

Saos2 cells with an integrated, inducible (“tet-on”) E2F1 expression construct (Phillips et al., 1999) were treated or not with doxycycline at a concentration of 2 µg/ml for 24 hours. RNA samples enriched for small RNA molecules were isolated by using the miRVana RNA Isolation kit (Ambion/Applied Biosystems). Array hybridization was carried out using the Exiqon system of arrayed locked nucleic acids (LNAs) as recommended by the manufacturer.

4.3. Protein biochemical methods

4.3.1. Protein lysates

Adherent and floating cells were combined and pelleted at 4°C and 500g. Pellet was dissolved in a lysis buffer made of RIPA, 2x laemmli and 2.7M urea and cooked at 95°C and 1400 rpm for 5 minutes.

4.3.2. BCA test

The protein concentration of the 1:300 diluted samples (prepared as in 4.3.1) was determined using the BCATM Protein Assay Kit from Pierce as recommended by the manufacturer and the BCA test mode of the Nanodrop.

4.3.3. Immunoblot analysis

After SDS-polyacrylamide gel electrophoresis and wet transfer to nitrocellulose, the membranes were blocked and incubated with antibodies in PBS containing 5% non-fat milk powder or 5% bovine albumin fraction V when the milk-phosphoprotein casein would interfere with proper staining (mostly because of its numerous phosphorylated sites). Primary antibodies used for detection are listed in Tab. 3.2. Detection was performed by HPR-conjugated antibodies (Tab. 3.3) and chemoluminescence.

5. Results

5.1. E2F1 regulates miRNA expression

In order to identify E2F1-responsive microRNAs, we employed Saos2 cells with tetracycline/doxycycline-inducible E2F1 (Phillips et al., 1999), controlled for E2F1 and E2F1 target gene expression (Fig. 5.1), and isolated total RNA before and after doxycycline treatment. Upon E2F1 induction, this cell line was shown to undergo p53-independent apoptosis (Phillips et al., 1999 and Suppl. Fig. S 1).

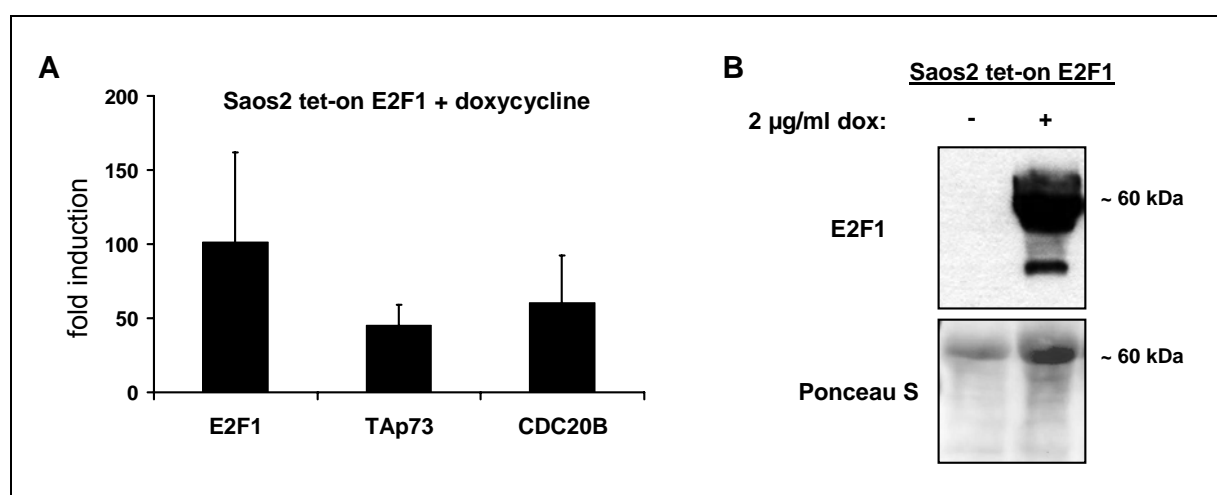


Fig. 5.1: Validation of the Saos2 tet-on E2F1 overexpression system

A, Induction of E2F1-responsive genes. Saos2 cells with an integrated, tet-on expression cassette for E2F1 were treated with doxycycline, followed by RT-PCR analysis of E2F1, TApx73, and CDC20B mRNA levels. Data published in Cell Death & Differentiation, March 2010.

B, E2F1 accumulation in Saos2 tet-on E2F1 cells after doxycycline treatment. Cells were treated as in A and analysed by western blot as described in 4.3.1.

Subsequent fluorescence labelling and array hybridization identified a number of E2F1-responsive microRNAs, some of which have been described as such earlier (Fig. 5.2 and Supp. Tab. 1), e. g. members of the miR-17-92 or 106b-25 clusters (Petrocca et al., 2008b; Pickering et al., 2009; Sylvestre et al., 2007). The strongest response, however, was observed with a pair of closely related microRNAs, miR-449a and miR-449b, recently reported as E2F1-inducible by another group (Yang et al., 2009), and collectively referred to as miR-449 from here on.

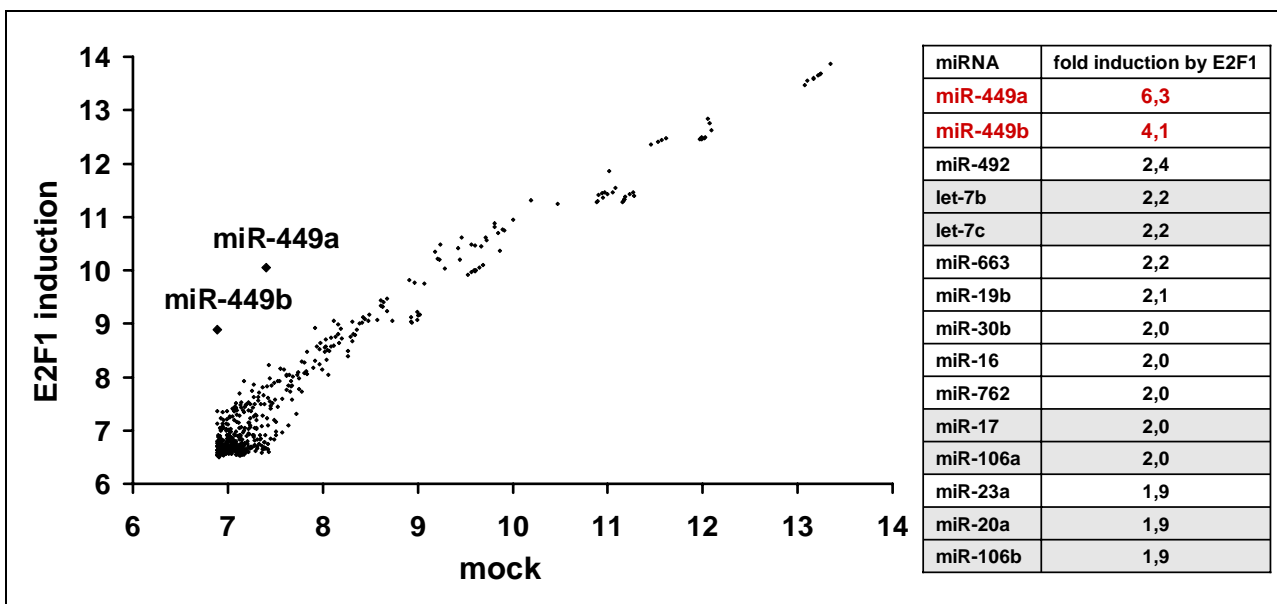


Fig. 5.2: E2F1-induced microRNAs identified by microRNA hybridization

Saos-2 cells with an integrated, tet-inducible expression cassette to synthesize E2F1 (Phillips et al., 1999) were treated with doxycycline or mock-treated. Twenty-four hours after infection, the cells were harvested. MicroRNAs from each sample were fluorescence-labelled and hybridized to a microRNA microarray. The fluorescence intensity corresponding to each microRNA with or without E2F1 overexpression is shown plotted against each other. The microRNAs most strongly upregulated by E2F1 are shown in the table (relative increase in miRNA levels upon E2F1 expression). Tinged with grey are the microRNAs already described as E2F1-responsive (Petrocca et al., 2008b; Pickering et al., 2009; Sylvestre et al., 2007). For a complete set of data, see Supp. Tab. 1. Data published in Cell Death & Differentiation, March 2010.

These microRNAs show strong similarities to the other miR-34 family members miR-34a-c, especially within their 5' portion (Fig. 2.3) that is generally believed to act as a "seed sequence" that determines the specificity of target mRNAs (Filipowicz et al., 2008). Since miR-449a levels exceeded those of miR-449b in all systems analyzed so far (Fig. 5.2 and Landgraf et al., 2007), the further analysis focussed on miR-449a.

5.2. microRNA-449 is strongly responsive to E2F1 and DNA damage

The enhanced expression of miR-449a in response to E2F1 was first confirmed by RT-PCR in doxycycline-treated Saos2-cells with tet-on E2F1, whereas doxycycline did not enhance miR-449-levels in the parental Saos2 cells (Fig. 5.3A). Moreover, a transiently transfected expression plasmid for E2F1 induced miR-449a in H1299 and U2OS cells, ensuring E2F1-responsiveness as a more general property of miR-449a.

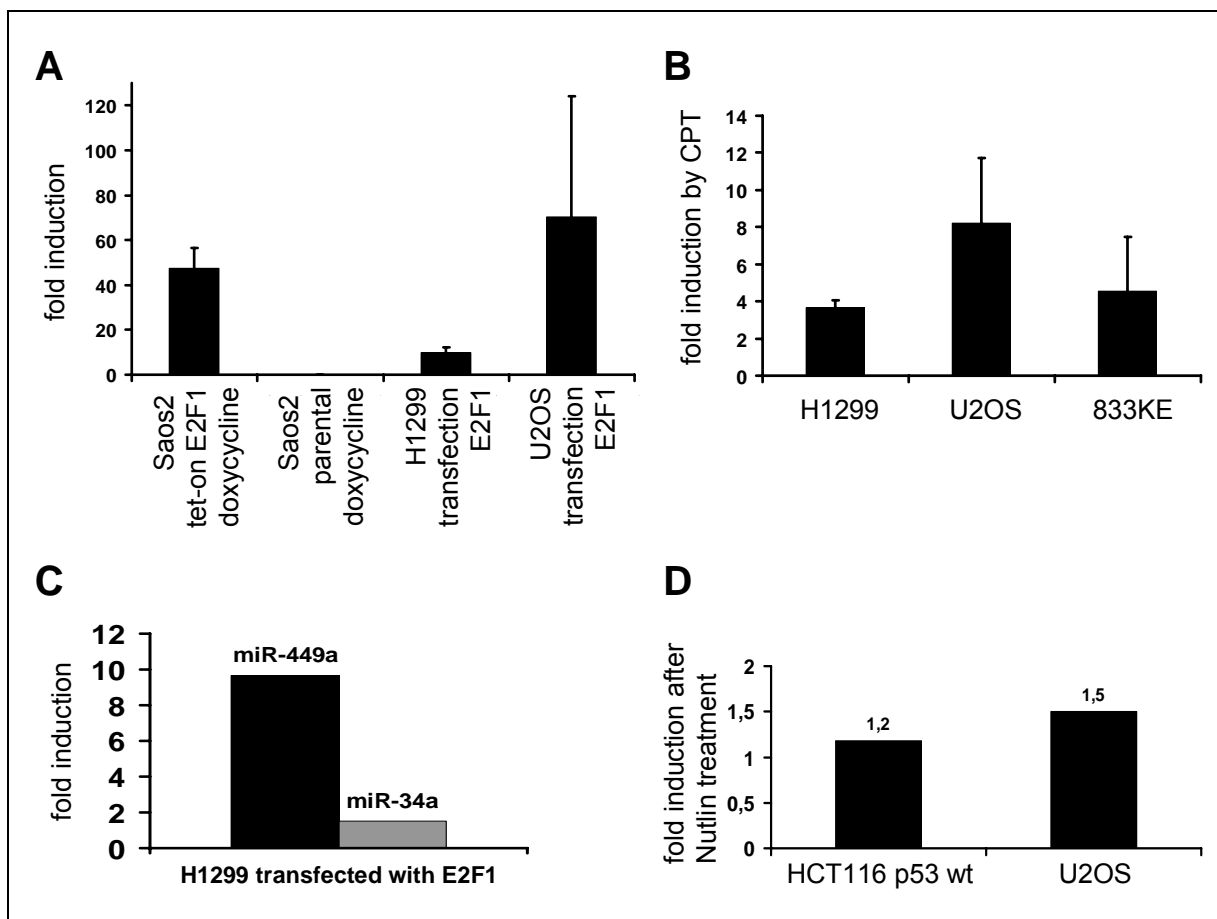


Fig. 5.3: miR-449a is induced by E2F1 overexpression and DNA damage

A, miR-449a induction by E2F1 over-expression. RNA was extracted from Saos2-tet-E2F1 cells with or without earlier doxycycline treatment, or from H1299 or U2OS cells transfected with empty vector or an E2F1 expression plasmid. The levels of miR-449a were determined by RT-PCR analysis and normalized relative to a constitutively expressed small RNA, RNU6b. The ratio of miR-449a levels with versus without E2F1 overexpression was calculated from three independent experiments along with the standard error in each case.

B, miR-449a induction by DNA damage. Cells of the indicated lines (H1299, lung adenocarcinoma, p53 deleted, U2OS, osteosarcoma, p53 wild type; 833KE, testicular cancer and p53 mutant) were treated with Camptothecin (CPT) followed by RT-PCR analysis of miR-449a levels as in A.

C, Failure of E2F1 to induce miR-34a. H1299 cells were transfected to over-express E2F1, or with empty vector plasmid. MicroRNA levels were determined by RT-PCR as in A.

D, Failure of p53 to induce miR-449. HCT116 p53 wt or U2OS cells (both containing wild type p53) were treated with the pharmacological Mdm2 inhibitor Nutlin-3a to induce p53 activity, followed by RT-PCR analysis of miR-449a levels. The samples were obtained and analyzed exactly as in a previous report (Braun et al., 2008), where miR-34a was induced more than 3-fold.

Finally, DNA damage by Camptothecin (CPT), a known trigger of E2F1 activity (Polager and Ginsberg, 2009), enhanced miR-449a expression regardless of the p53 status (Fig. 5.3B). In contrast, E2F1 induced miR-34a far less efficiently than miR-449a (Fig. 5.3C). Conversely, p53 activation by the pharmacological Mdm2-antagonist Nutlin-3a (Vassilev et al., 2004), although capable of inducing miR-34a (Braun et al., 2008), failed to increase the levels of miR-449a (Fig. 5.3D).

Consistent with these data, as I will show later, exposure of epithelial cells to cigarette smoke led to equal induction of E2F1 and miR-449a (Fig. 5.26).

Thus, miR-449 is E2F1- and, probably as a consequence, DNA damage-responsive.

5.3. miR-449 expression is coupled to its host gene CDC20B and reduced in cancer

Next, we sought to determine the pattern of miR-449 expression in various tissues and tumour cells. The genomic region encoding both miR-449a and miR-449b is embedded into an intronic sequence of the mRNA-encoding gene CDC20B, a parologue of CDC20 (Fig. 2.4). RT-PCR analysis revealed that CDC20B was induced by E2F1 as well (Fig. 5.1A).

In human, high levels of miR-449 were found in lung, trachea and testes, and still considerable amounts in cervix and oesophagus. The expression pattern of CDC20B largely reflected the levels of miR-449 in human tissues (Fig. 5.4A). miR-449 thus seems to be regulated through activation of its host gene, as confirmed by another group through chromatin immunoprecipitation showing E2F1 binding to the CDC20B/miR-449 core promoter region (Yang et al., 2009).

High levels of miR-449a in testes, lung, and trachea were again found in murine tissues (Fig. 5.4B). In contrast to pulmonary and testicular tissues, all tumour-derived cell lines under study, including testicular cancer cells (GH and 833KE) and a lung adenocarcinoma cell line (H1299), contained far lower amounts of miR-449 (Fig. 5.4C), at least compatible with the idea that miR-449 may display tumour-suppressive activities.

Other evidences supporting the idea of miR-449 down-regulation in cancer are found in the literature. MiR-449 levels were lower in prostate tumours compared to matched controls, and its overexpression in prostate tumour cells led to growth arrest and apoptosis (Noonan et al. 2009; Weichert et al. 2008).

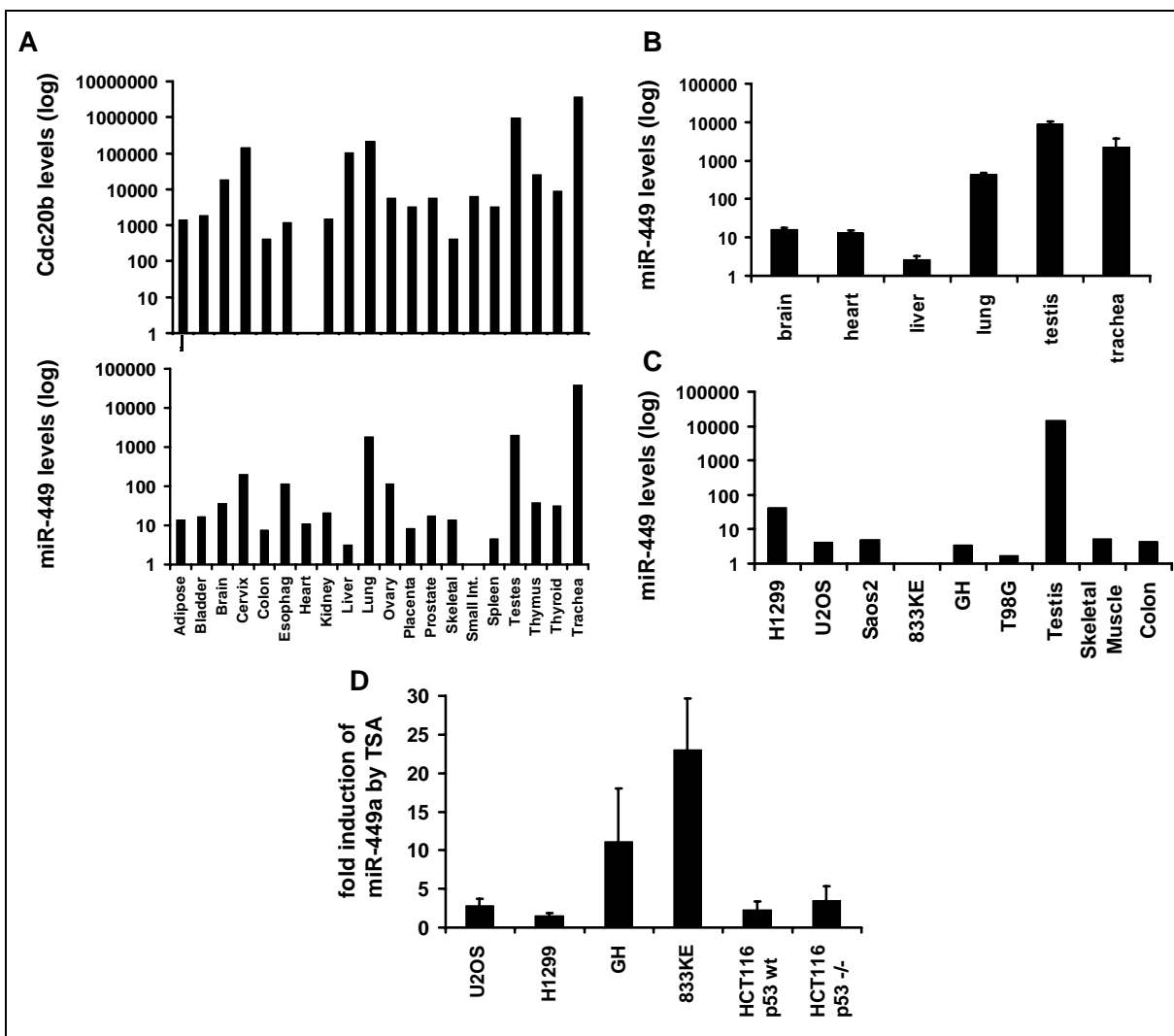


Fig. 5.4: miR-449a levels are reduced in tumour cells, and its expression pattern resembles the expression of CDC20B

A, Parallel expression of CDC20B and miR-449a in a variety of human tissues (RNA panel, Ambion), as quantified by RT-PCR.

B, miR-449a expression levels in murine tissues.

C, miR-449a levels in human cancer-derived cell lines (H1299, lung adenocarcinoma; U2OS and Saos2, osteosarcoma; GH and 833KE, testicular carcinoma; T98G, glioblastoma), as compared with human tissues.

D, Increase of miR-449a levels in testicular cancer cells upon HDAC inhibition. Cells of the indicated lines (U2OS, osteosarcoma; H1299, lung adenocarcinoma; GH and 833KE, testicular carcinoma; HCT116, colon carcinoma) were treated with the histone deacetylase (HDAC) inhibitor Trichostatin A (TSA), followed by miR-449a quantitation through RT-PCR. The ratio of miR-449a levels with or without TSA was calculated and is displayed along with the standard error from three independent experiments.

Data published in Cell Death & Differentiation, March 2010.

Cells undergo severe epigenetic changes during tumorigenesis, mostly through modulation of the methylation and acetylation states of promoter regions, thereby leading to the silencing of tumour suppressive genes and enhanced transcription of oncogenes (Ellis et al., 2009; Espino et al., 2005; Kalebic, 2003). To test whether the down-regulation of miR-449 in cancer cells could be due to epigenetic silencing, we treated the cells with Trichostatin A, a pharmacological inhibitor of histone deacetylases (HDACs). HDACs are thought to deacetylate histones to make the chromatin more compact thereby clogging the access to certain promoters and silencing genes. Their inhibition strongly increased miR-449 levels in cell lines from testicular cancer, albeit less efficiently in other cell lines (Fig. 5.4D). This argues that epigenetic silencing may lead to miR-449 down-regulation in the corresponding tumour cells. However, histone deacetylation seems not to be the only mechanism by which miR-449 is silenced in cancer, as Yang et al. (2009) found miR-449 expression to be repressed by histone H3 Lys27 trimethylation in breast tumour cells.

The down-regulation of miR-449 in tumour cell lines compared to normal tissue indicates a potential tumour-suppressive role for miR-449. This, and its similarity to miR-34, raised the question whether miR-449 could be involved in growth arrest or cell death.

5.4. miR-449 induces apoptosis and cell cycle arrest

Since E2F1 is a potent inducer of apoptosis (Suppl. Fig. S 1), especially in the context of DNA damage, I wanted to investigate whether miR-449 could contribute to the induction of E2F1-mediated apoptosis. Interestingly, miR-34, the p53-responsive homologue of miR-449, was already shown to exhibit proapoptotic activity. Hence, we tested whether miR-449 may act in parallel to miR-34 in growth suppression and apoptosis.

Firstly, we investigated the ability of miR-449 to affect colony formation and survival in clonogenic assays. Therefore, we transfected plasmids encoding each microRNA into HCT116 cells with or without p53, followed by antibiotic selection of stable transfectants. Both miR-34a and miR-449 suppressed clonogenic survival in this system, in a partially p53-independent fashion (Fig. 5.5 A and B). This colony suppression was especially strong in the testicular carcinoma cells from the GH line, where miR-449 expression led to total colony suppression (Fig. 5.6). This might reflect the importance of the loss of miR-449 in cancer arising from testicular tissue, since even though the highest levels of endogenous miR-449 were found in testis, miR-449 was barely detectable in testicular carcinoma (Fig. 5.4C).

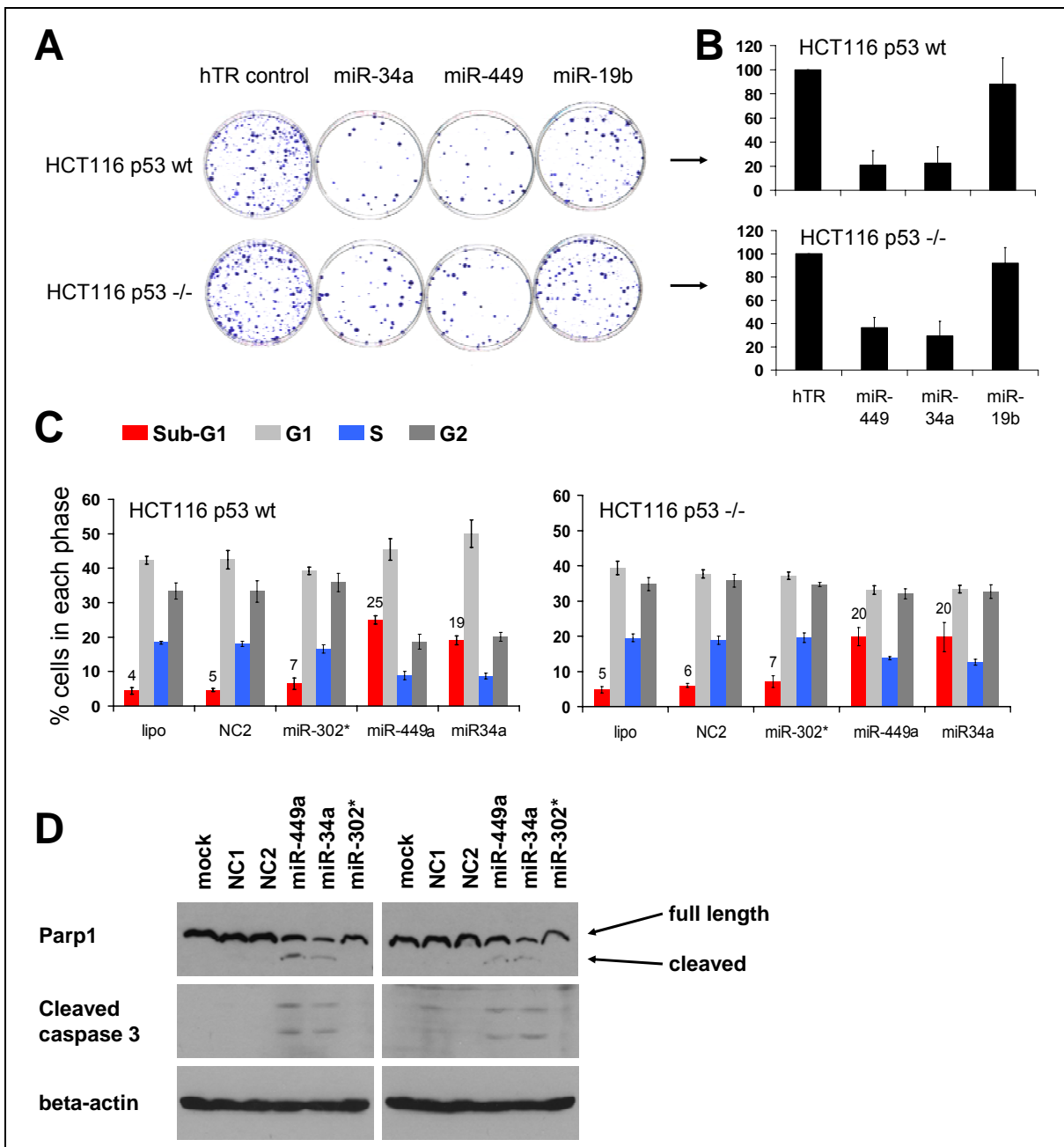


Fig. 5.5: miR-449 induces apoptosis

A, Reduced clonogenic survival on continuous expression of miR-449 and miR-34a. HCT116 wt or p53 -/- cells were transfected with expression plasmids for miR-449a/b, miR-34a, or controls, followed by selection of stably transfected cells. Colonies were fixed and stained with crystal violet two weeks after transfection.

B, Quantification of the assays shown in A, performed by digitally determining the area covered by crystal violet-stained cells. The results of five independent experiments are summarized along with the standard error in each case.

C, Induction of a sub-G1 shoulder and decreased S-Phase fraction by miR-449a and miR-34a. HCT116 cells with or without p53 were transiently transfected with synthetic miR-449a, miR-34a or control miRNAs. At 48h post transfection, the cells were fixed, stained with propidium iodide and subjected to flow cytometry. The percentage of (presumably apoptotic) cells in the sub-G1 fraction was

calculated in each case based on the distribution of staining intensities (exemplified in Fig. 5.7). Results from three independent experiments are shown along with the standard error.

D, Induction of caspase activity by miR-449a and miR-34a. HCT116 cells were treated as in b, followed by immunoblot analysis of poly-ADP ribose polymerase (PARP) (the lower band is characteristic of a caspase-derived cleavage fragment) and cleaved caspase 3.

Data published in Cell Death & Differentiation, March 2010.

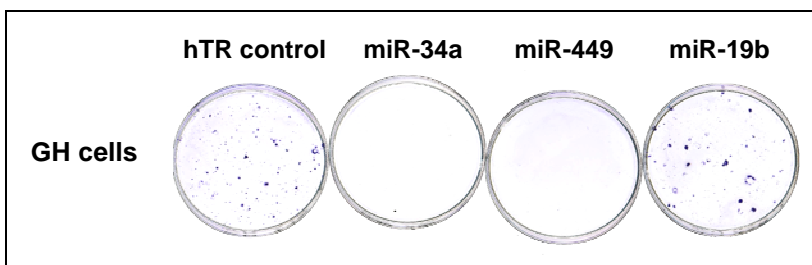


Fig. 5.6: miR-449 suppresses colony formation in a testicular carcinoma cell line

Suppressed clonogenic survival on continuous expression of miR-449 and miR-34a. GH cells were transfected with expression plasmids for miR-449a/b, miR-34a, or with control plasmids, followed by Blasticidin selection of stably transfected cells, as in 5.5 A. Two weeks after transfection, colonies were fixed and stained with crystal violet.

To further elucidate the mechanisms behind this suppressive effect, we analyzed the DNA content of transiently miRNA-transfected cells by flow cytometry to determine cell cycle distribution of the cells. MiR-34a and miR-449a each led to the accumulation of cells in a sub-G1 shoulder (Fig. 5.5C and Fig. 5.7), arguing that both microRNAs induce apoptosis.

To confirm that the observed Sub-G1 fraction, indicative of cell death, was due to apoptosis, we decided to test the cells for caspase activity. Under the same conditions, cleaved poly-ADP-ribose polymerase (PARP) and cleaved caspase 3 were detected by immunoblot analysis in different cell lines, independently of their p53 status (Fig. 5.5D and Fig. 5.8), further supporting this notion. Thus, miR-449 induces apoptosis, at least partially through p53-independent mechanisms.

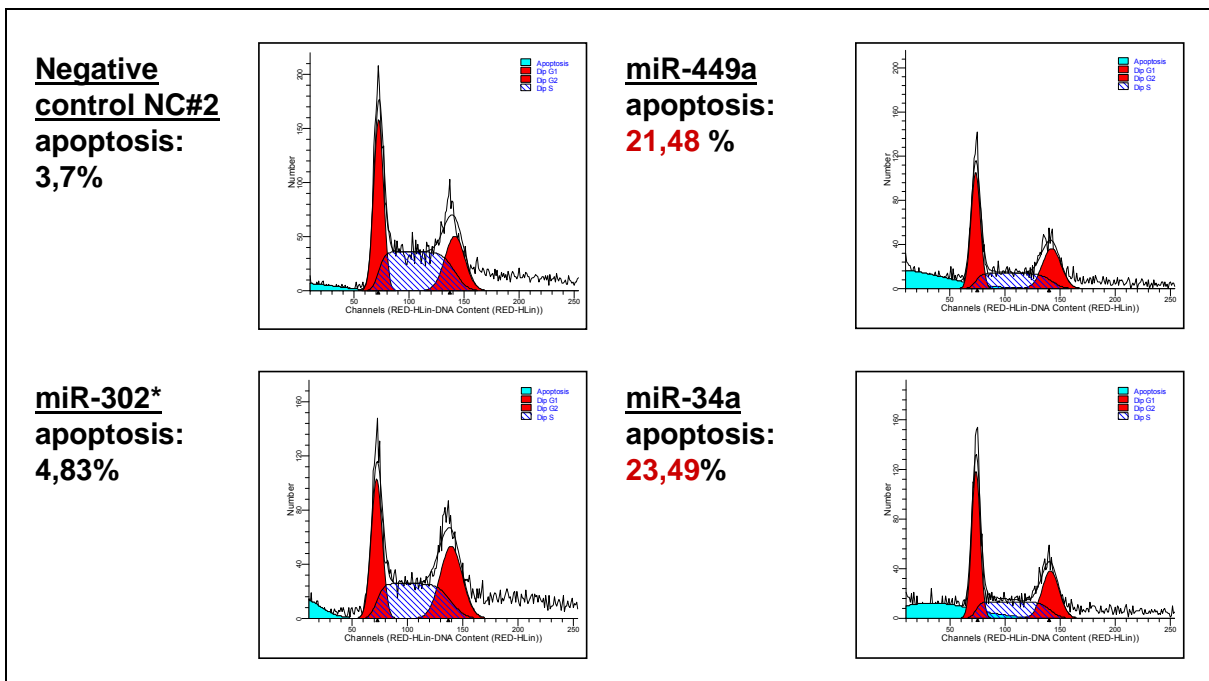


Fig. 5.7: Alterations in DNA content by miR-449a and miR-34a

HCT116 cells (wt p53) were transfected with the indicated microRNAs, NC#2 and miR-302* being negative controls, followed by propidium iodide staining and flow cytometry (cf. legend to Fig. 5.5C). The number of cells in each window of staining intensity is shown by histograms. The fraction of Sub-G1 cells (green overlay) was determined by ModFit analysis. Similar effects were found in p53-deficient HCT116. Data published in Cell Death & Differentiation, March 2010.

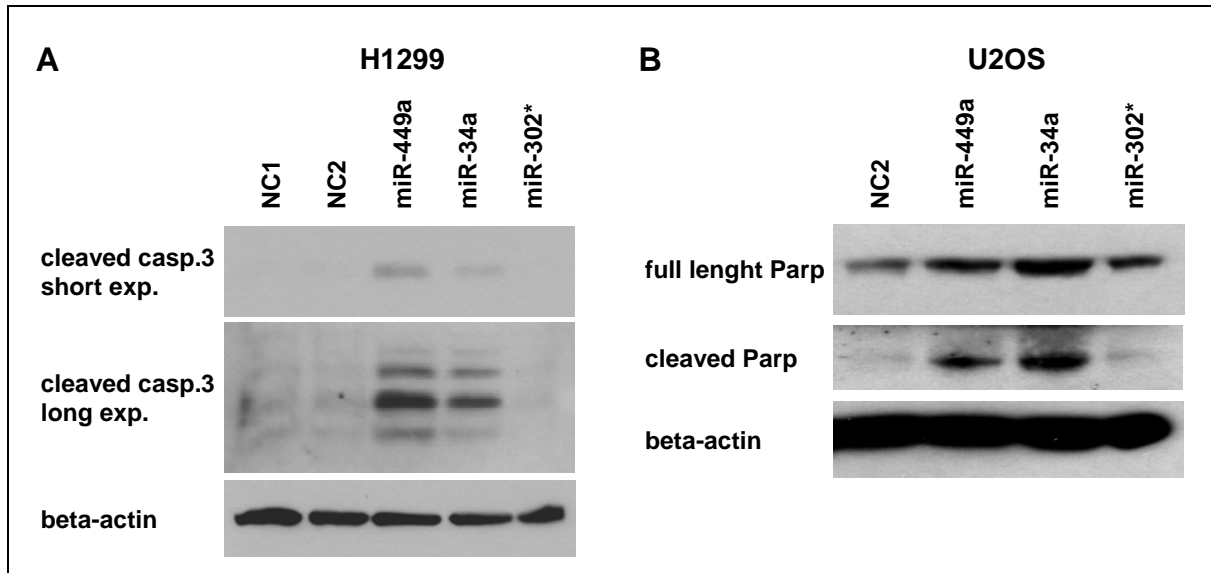


Fig. 5.8: Induction of caspase activity by miR-449a and miR-34a

H1299 (p53 deleted) (A) or U2OS (p53 wild-type) (B) cells were transfected with the indicated microRNAs, followed by immunoblot analysis of cleaved caspase 3 and poly-ADP ribose polymerase (PARP) (the lower band being characteristic of a caspase-derived cleavage fragment) respectively.

Next, I wanted to investigate whether miR-449 antagonisation would alleviate E2F1-mediated, p53-independent apoptosis. Since no tumour cell line harbouring high miR-449 levels was available, I decided to use again Saos2 tet-on E2F1 cells. After induction with doxycycline, they express miR-449 levels that are reasonably high, even though still lower compared to normal tissue. Interestingly, E2F1 overexpression led to apoptotic appearance of the cells in preliminary tests (Suppl. Fig. S 1). In fact, we could observe PARP1 and caspase 3 cleavage after E2F1 induction (Fig. 5.9), and knockdown of miR-449 using the LNA (locked nucleic acid) technology (Naguibneva et al., 2006) slightly reduced caspase activity. Moreover, gammaH2AX accumulation, probably due to DNA cleavage following apoptosis, was also partially reduced by miR-449 antagonisation. Thus, miR-449 is one of the effectors of E2F1-mediated, p53-independent apoptosis.

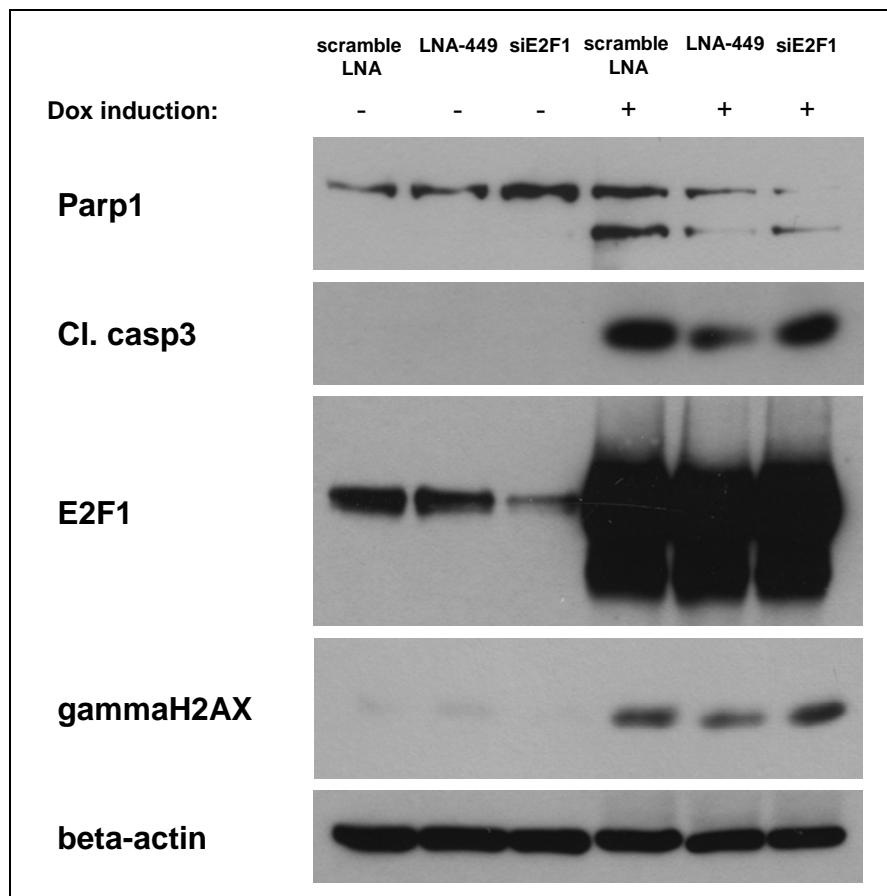


Fig. 5.9: Knockdown of miR-449 reduces E2F1-mediated apoptosis

Saos2 tet-on E2F1 cells (p53 $^{-/-}$) were transfected with LNA against miR-449 or scramble control or with a siRNA against E2F1 and treated with doxycycline or mock. 24h post transfection cells were harvested for immunoblot analysis. E2F1 staining served as a control for correct induction and as an indicator of transfection efficiency (where siRNA against E2F1 was used). Note that E2F1 overexpression alone was able to induce DNA damage as shown by gammaH2AX accumulation.

5.5. Target analysis of miR-449a

To identify possible mechanisms behind miR-449-induced cell death, we analysed putative target genes for miR-449a. Due to the very short microRNA seed sequence and to the ability of microRNAs to bind to their targets by imperfect complementarity, it is very difficult to predict microRNA targets accurately. Fortunately, prediction softwares can give good hints about probable targets. Using the databases and microRNA targets prediction softwares TargetScan, Miranda and cbio, and taking into account the shared seed sequence with miR-34, we looked for the most likely targets of miR-449 (Tab. 5.1).

Tab. 5.1: potential miR-449 targets

Potential targets analysis using the hits from Miranda (John et al., 2004), TargetScan (Friedman et al., 2009b) and cbio (Vert et al., 2006), as well as published data for the miR-34 family. The targets analysed in the course of this work are highlighted in grey.

gene	miranda	sites	species	targetscan	sites	cbio	publications
ACBD3				hsa-miR-449	1	1	
ACCN1	miR-449a	16	3	hsa-miR-449	1	1	
AKT1	miR-449a+b	16	3			1	
ANK2				hsa-miR-449	1		
ANK3	miR-449a+b	13	1	hsa-miR-449	2		
BCAN	miR-449a+b	20	5			1	
BCAS3	miR-449a+b	20	5			1	
BCL2				hsa-miR-34c	1	2	described as miR-34a target (Ji et al., 2008)
BNC2				hsa-miR-449	3		
BTBD11	miR-449a+b	18	3	hsa-miR-449	2	1	
C11orf17	miR-449a	22	5			1	
C8orf13				hsa-miR-449	4	2	
CALCR				hsa-miR-449	2	1	
CCND1				hsa-miR-449	1		described as miR-34a target (Sun et al., 2008)
CCNE2	miR-449a+b	12	7	hsa-miR-449	1		
CD151	miR-449a+b	27	6				
CD47				hsa-miR-449	3		
CDC25A							confirmed miR-449 target (Yang et al., 2009)
CDK6				hsa-miR-449	3	2	described as miR-34 and miR-449 target (Sun et al., 2008; Yang et al., 2009)
CNTNAP2				hsa-miR-449	1	2	
COL12A1				hsa-miR-449	1	1	
CRSP8	miR-449a+b	20	1			1	
DBC1	miR-449a+b	17	7	hsa-miR-449	1	1	
DHRS13	miR-449a+b	28	4				
DKFZP686E2158				hsa-miR-449	1		
DLL1	miR-449a	20	8	hsa-miR-449	3		Potential miR-34 and miR-449 target (Hoesel et al., 2010)
E2F1							
E2F3					1	1	
E2F5	miR-449a+b	24	9			1	described as miR-449 target (Redshaw et al., 2009)
EML5	miR-449a+b	12	7	hsa-miR-449	1		
ESRRA	miR-449a+b	25	6	hsa-miR-34a	1		
FAM123B	miR-449b			hsa-miR-449	4		

FAM76A	miR-449a	18	5	hsa-miR-449	3	1	
FGD6	miR-449a+b	22	4	hsa-miR-449	1		
FOXG1B	miR-449a+b	20	7	hsa-miR-34a	1		
FUT8	miR-449a+b	21	9	hsa-miR-449	1	1	
GALNT7				hsa-miR-449	2	2	
GMFB				hsa-miR-449	1		
GPR22				hsa-miR-449	1	1	
GRM7				hsa-miR-449	1		
HDAC1							described as miR-449 target (Noonan et al., 2009)
HDMX							described as miR-34a target (Markey and Berberich, 2008)
HMGA2							described as miR-34a target (Ji et al., 2008)
HTR2C				hsa-miR-449	1		
IKBKG	miR-449a+b	25	4				
IL16	miR-449a+b	10	1			1	
JAKMIP1	miR-449a+b	10	5	hsa-miR-449	1	1	
KLF4				hsa-miR-449	1	1	
LEF1	miR-449a	15	4		1		
LOXL3	miR-449a+b	21	6	hsa-miR-34c	2	2	
LYST	miR-449b			hsa-miR-449	2		
LZTS2	miR-449a+b	21	6	hsa-miR-34a	1		
MARCH5				hsa-miR-449	1		
MGAT4A				hsa-miR-449	2		
MLLT3				hsa-miR-449	1	1	
Notch1				hsa-miR-449	2		described as miR-34 target (Ji et al., 2008)
NUMBL	miR-449a	24	6	hsa-miR-449	2	2	
ORC6L	miR-449a+b	24	5				
PEA15				hsa-miR-449	1	1	
PGM1	miR-449a+b	23	7	hsa-miR-449	1		
PKP4	miR-449a+b	13	9	hsa-miR-449	1		
PLCG1				hsa-miR-449	1	2	
PNOC	miR-449a+b	21	5	hsa-miR-34a	1	2	
PPP2R3A				hsa-miR-449	2	1	
PREB	miR-449a+b	25	6				
RASGEF1C	miR-449a+b	25	4				
RIMS2	miR-449a+b	7	1			1	
RNF111	miR-449a+b	11	13			1	
SATB2				hsa-miR-449	2	1	
SEMA4C	miR-449a	25	9	hsa-miR-34c	2	2	
SEMA4F				hsa-miR-449	3	1	
SHANK3				hsa-miR-449	2	1	
SIRT1				hsa-miR-34a	2	1	described as miR-34a target (Yamakuchi et al., 2008)
SIRT6	miR-449a+b	26	5				
SIT1	miR-449a+b	25	4				
SLCO3A1	miR-449a+b	17	6	hsa-miR-449	1	1	
SUPT6H	miR-449a+b	25	5			1	
SYT1				hsa-miR-449	3	2	
TBL1XR1				hsa-miR-449	1		
TMCC3				hsa-miR-449	2		
TMEM109	miR-449a+b	14	5	hsa-miR-34a	1		
TMEM22	miR-449a+b	9	8			1	
VAMP2				hsa-miR-449	3		
VPS4A	miR-449a+b	22	6			1	
XYLT1	miR-449a+b	14	5	hsa-miR-449	4	1	
ZDHHC17				hsa-miR-449	1		
ZNF207	miR-449a+b	19	10	34a	1	1	
ZNF644				hsa-miR-449	1		

From these predictions, many different protein-coding genes could be regulated by miR-449. Complex patterns of gene regulation have previously been reported for miR-34 (Chang et al., 2007; Corney et al., 2007; He et al., 2007a; Hermeking, 2009a; Raver-Shapira et al., 2007; Tazawa et al., 2007). However, it is reasonable to assume that a few profoundly regulated target mRNAs may still serve as key targets to mediate the biological functions of miR-34a and miR-449a.

In order to find targets potentially explaining the observed phenotypes after miR-449 overexpression, mainly growth arrest and apoptosis, therefore I decided to further investigate putative targets with roles in the regulation of cell cycle or cell death.

The first candidates were the antiapoptotic genes BCL2 and BCL6, whose knockdown could lead to apoptosis. Therefore, we checked their expression by quantitative RT-PCR (Suppl. Fig. S 2) and, for BCL2, also by western blot analysis (data not shown). Unfortunately, miR-449 did not affect them. Surprisingly, we could not see any down-regulation of BCL2, which was previously shown to be a direct target of miR-34 (Ji et al., 2008), even after overexpression of miR-34a (Suppl. Fig. S 2D). This could be due to the different experimental settings and the tissue provenance of the cells used.

Additionally, there was no direct negative regulation of miR-449a on its host gene CDC20B (Suppl. Fig. S 2B) at least on the mRNA level, but strong effects were found on the E2F and p53 pathways, as discussed in section 5.5.1.

5.5.1. Negative feedback on the E2F pathway

I was particularly interested in the underlying mechanisms of miR-449-mediated cell cycle arrest and apoptosis. Therefore, my attention was turned to the E2F1 pathway. I first tested the effects of miR-449a and miR-34a on CDK6, a predicted target gene (Tab. 5.1) with a role in cell cycle regulation. CDKs are known to activate the E2F pathways through the inhibition of pocket proteins (e.g. Rb). CDK6 as well as CDK2 mRNAs were strongly down-regulated after miR-449 overexpression (Fig. 5.10 A and B).

A strong down-regulation of CDK6 was further confirmed on the protein level (Fig. 5.11A). Moreover, E2F1 and E2F3 themselves were found to be down-regulated by miR-449a and miR-34a in p53-deficient cells (Fig. 5.11B). However, at least for E2F1, this down-regulation seems to be indirect since miR-449a, unlike other microRNAs, was unable to bind to the 3'UTR of E2F1 and inhibit translation in reporter assays (Fig. 5.12).

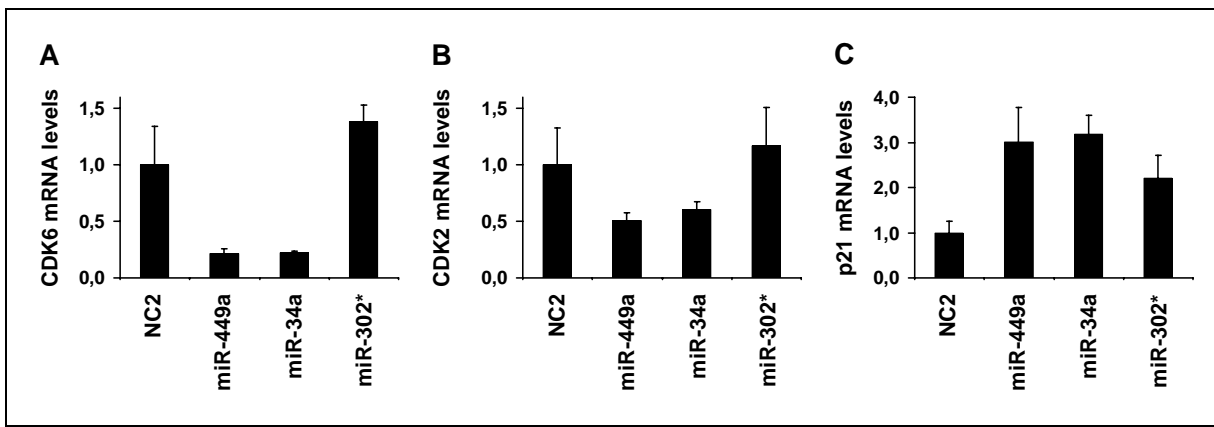


Fig. 5.10: miR-449 inhibits the E2F pathway

H1299 cells transfected with the indicated microRNAs or controls (NC2 and miR-302*) were analysed by RT-PCR to determine the mRNA levels of the cyclin-dependent kinases CDK6 (A) and CDK2 (B), and the cyclin-dependent kinase inhibitor p21 (C). Displayed are the mean results of 3 independent experiments with error bars normalised to 18S rRNA levels in each sample.

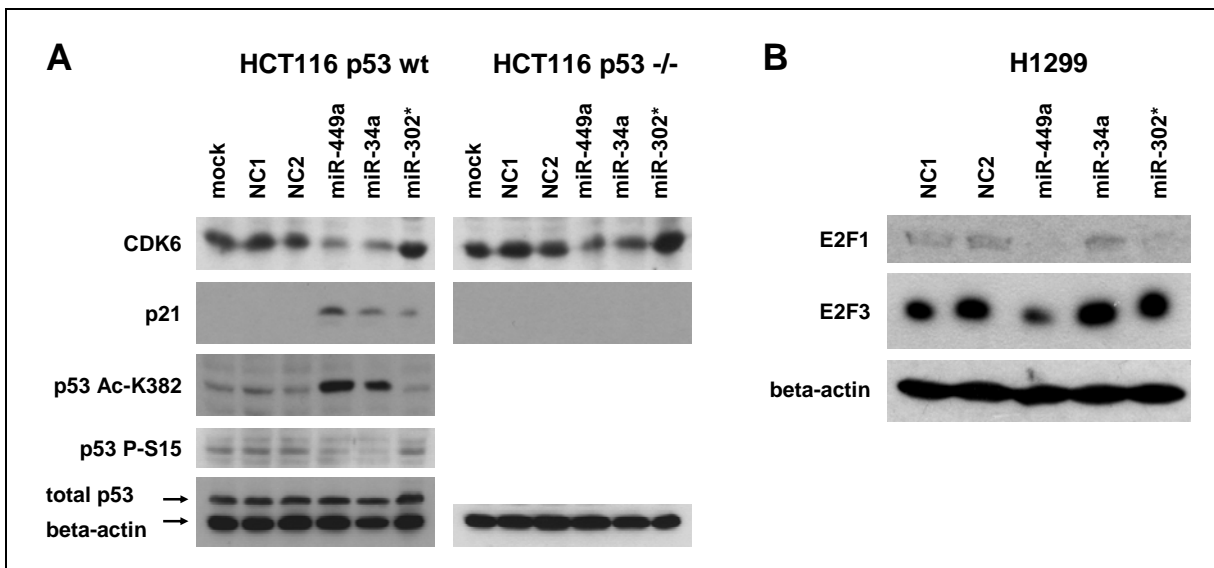


Fig. 5.11: miR-449 induces the p53 pathway while inhibiting the E2F pathway

A, HCT116 p53 wild type (wt) or HCT116 p53^{-/-} cells were transfected with the indicated microRNAs for 48h, followed by immunoblot analysis to detect the indicated gene products and modifications with specific antibodies. p53 staining was only performed in HCT116 p53 wt cells (but lack of p53 was confirmed in HCT116 p53^{-/-} cells in additional experiments, data not shown)(Lize et al., 2010).

B, Same analysis as in A using H1299 cells (p53^{-/-}).

The negative feedback of miR-449 on the E2F pathway is further reinforced by the fact that p21 - a CDK inhibitor also contributing in the p53-mediated inhibition of E2F1 transcriptional activity - was shown to be strongly induced after miR-449 over-expression, probably due to

the accumulation of the highly active acetylated form of p53 (Fig. 5.11A). However, other factors may be involved in the miR-449-mediated induction of p21, since it could be observed in p53-deficient cells (Fig. 5.10C).

Consistent with the negative regulation of the E2F pathway, the E2F1 proapoptotic targets TAp73, Noxa and APAF1 were not induced and therefore probably not involved in miR-449-mediated apoptosis (data not shown).

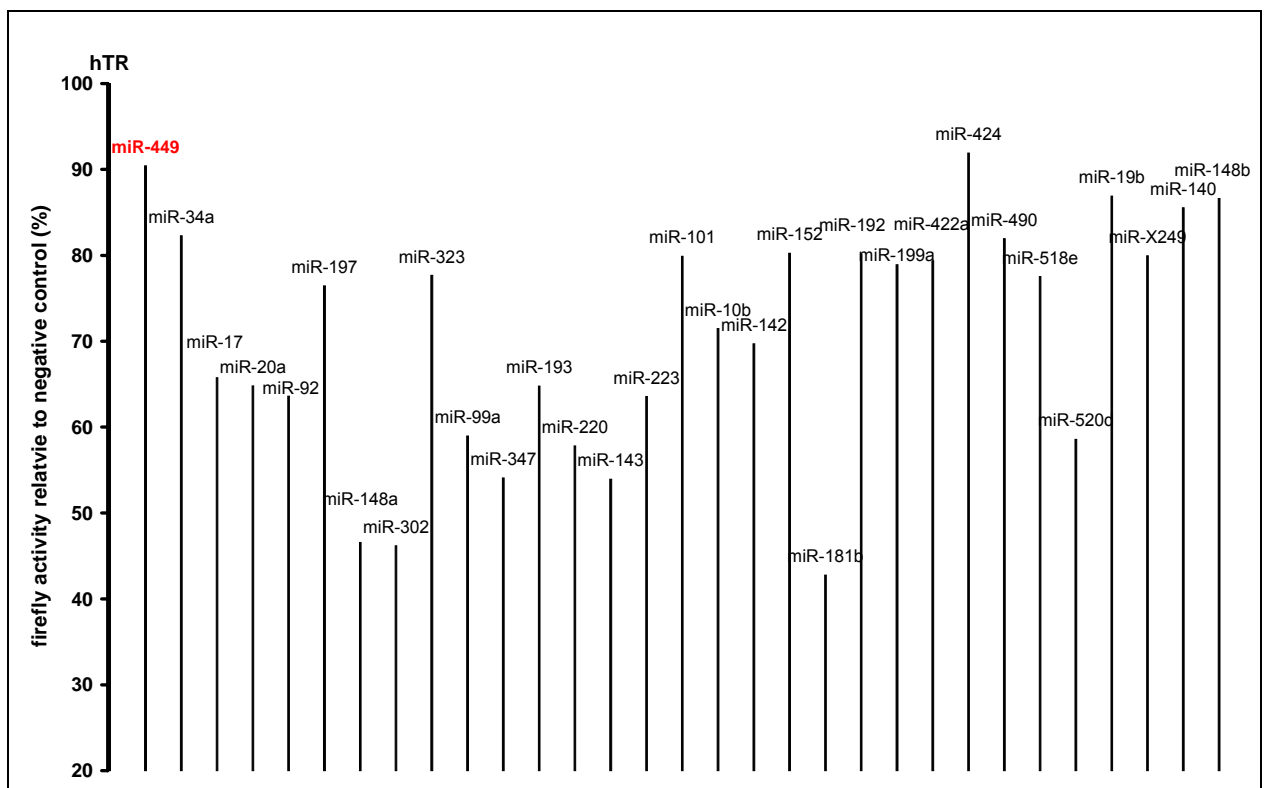


Fig. 5.12: no direct binding of miR-449 to the E2F1 3' UTR

H1299 cells were co-transfected with the pGL3-3'UTR-E2F1 Firefly vector (Renilla as internal standard) and plasmids containing the indicated microRNAs (miR-Vec library, kind gift of R. Agami) for 24h, followed by analysis of luciferase activity. Displayed are the mean results of 3 independent experiments, each performed in technical triplicates.

This argues that miR-449a provides a negative feedback loop that attenuates E2F1 activity in situations where cell death can be avoided. A reduction of CDK6 and CDK2 is in line with the observed decrease of cells in S phase (Fig. 5.5C and Fig. 5.7), presumably due to the hypophosphorylation and consecutive activation of Rb family pocket proteins. MiR-449 may thus prevent the accumulation of cells with excessive E2F1 activity in two ways: providing a direct negative feedback on E2F1 activity, and eliminating cells with uncontrollable E2F1.

5.5.2. miR-449 targets the histone deacetylases HDAC1 and SIRT1: a positive feedback on the p53 pathway

Due to the activation of p53 in response to miR-449 (Fig. 5.11A), it was tempting to speculate whether general regulators of gene transcription could be involved. Histone deacetylases are important regulators of gene expression which are thought to regulate entire pathways through major changes in the “transcriptome” (Dannenberg et al., 2005; Gialitakis et al., 2006; Reid et al., 2005). Histone deacetylases prevent the transcription of certain genes through the removal of acetyl groups from histones, thereby enhancing chromatin condensation (Coppola et al., 2010). They are often upregulated in cancer (Weichert et al. 2008) and HDAC inhibitors show a very effective tumour-suppressive activity in some animal models (Qian et al. 2007; Wedel et al. 2008). Recently, HDAC1 was reported as a target of miR-449 (Noonan et al., 2009). SIRT1 belongs to another class of histone deacetylases, the Sirtuins (class III), and was also predicted as a target of the miR-34 family (Tab. 5.1) and reported for miR-34a (Yamakuchi et al., 2008).

Accordingly, both miR-449a and miR-34a were capable of down-regulating the histone deacetylases HDAC1 and SIRT1 at the mRNA (Fig. 5.13) and protein levels (Fig. 5.14 and Fig. 5.15), independently of the p53 status of the cells. However, the negative regulation could of SIRT1 mRNA (Fig. 5.13A) was much weaker than suggested by the strong decrease in protein levels, suggesting translational repression rather than mRNA destabilisation as the main mechanism in this case.

Since SIRT1 is known to directly affect the acetylation of p53 (Langley et al., 2002; Luo et al., 2001; Solomon et al., 2006; Vaziri et al., 2001; Yamakuchi et al., 2008), this observation is in line with the previously shown accumulation of acetylated p53 and its target p21 (Fig. 5.11A), despite unchanged levels of global p53 and phosphorylated p53. The down-regulation of SIRT1 by miR-449 therefore provides a positive feedback on the p53 pathway, thereby potentially inducing cell cycle arrest or apoptosis in p53 wild-type cells. Unfortunately, this does not explain the induction of apoptosis in p53-deleted cells.

However, whereas HDAC inhibition was able to induce some apoptosis in p53-deficient cells, probably in part due to the resulting enhanced miR-449 expression in most tumour cell lines (Fig. 5.4D), SIRT1 inhibition alone did not phenocopy miR-449-mediated apoptosis in p53-deficient cells, suggesting the collaboration of several miR-449 targets for the proper induction of programmed cell death.

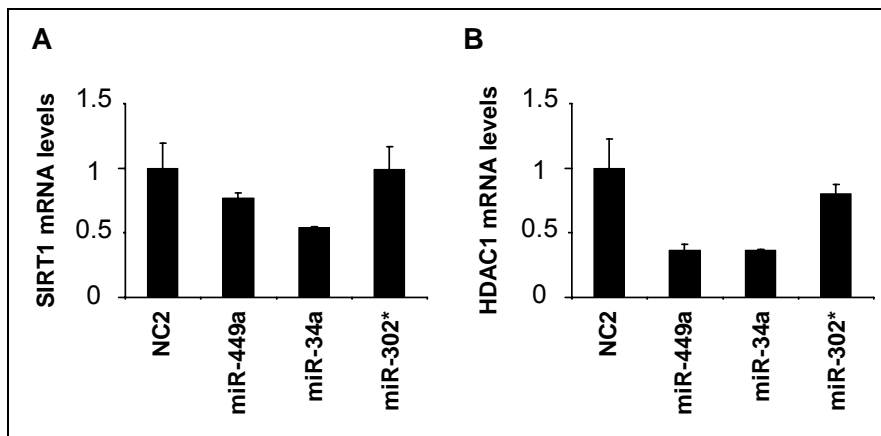


Fig. 5.13: HDAC1 and SIRT1 mRNA levels are reduced by miR-449

H1299 cells were transfected with the indicated microRNAs, 48h post transfection the RNA was analysed by RT-PCR using specific primers for the histone deacetylases SIRT1 (A) and HDAC1 (B).

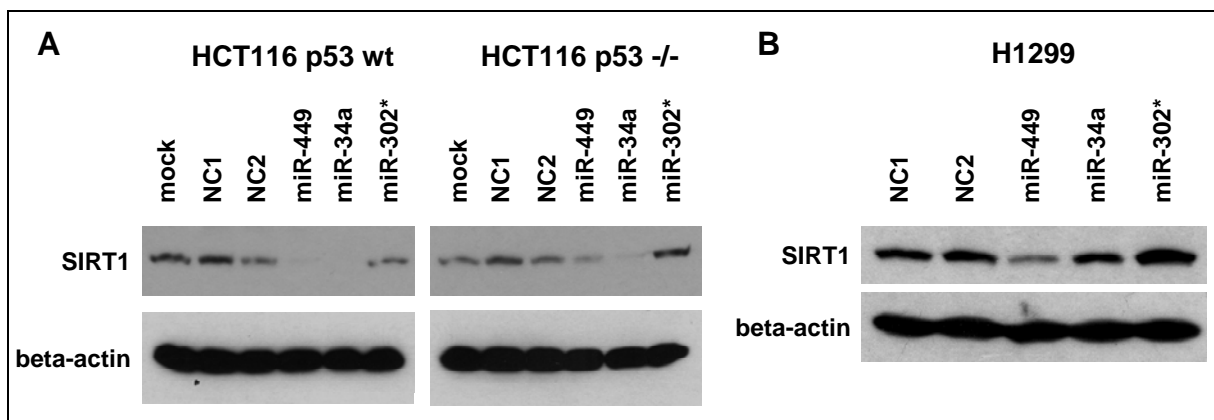


Fig. 5.14: miR-449a, as well as its parologue miR-34a, target SIRT1

A, HCT116 p53 wt or HCT116 p53-/- cells were transfected with the indicated microRNAs for 48h, followed by immunoblot analysis of SIRT1 and beta-actin as a loading control (Lizé et al., 2010).

B, H1299 cells (p53 -/-) were transfected with the indicated microRNAs for 48h, followed by immunoblot analysis of SIRT1 and beta-actin as a loading control.

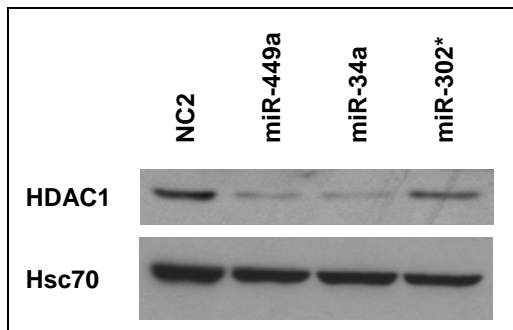


Fig. 5.15: miR-449a and miR-34a target HDAC1

Analysis of HDAC1 protein levels in H1299 as described for SIRT1 in Fig. 5.14 B. Hsc70 is a loading control. Experiment performed by Ines Rudolf under my supervision.

5.5.3. miR-449 provokes the accumulation of DNA damage

Surprisingly, phosphorylated Histone 2AX (a marker of DNA damage, Fig. 2.1) was detected at increased levels following E2F1 induction (Fig. 5.9) and miR-449 overexpression (Fig. 5.16), arguing that miR-449a and miR-34a are perhaps capable of increasing the susceptibility of cells to DNA damage. Additionally, miR-449 seemed to slightly enhance the accumulation of DNA damage after chemotherapeutic treatment (Fig. 5.16B). Interestingly, E2F1-mediated phospho-H2AX (gammaH2AX) accumulation was slightly alleviated by concurrent knockdown of miR-449a (Fig. 5.9).

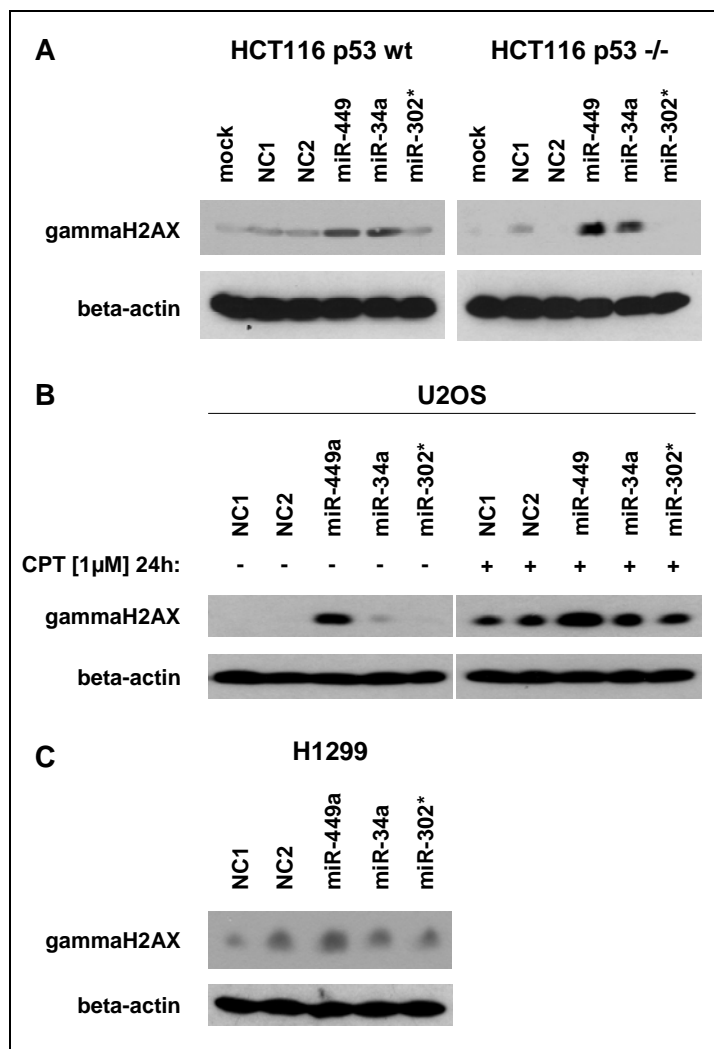


Fig. 5.16: miR-449 overexpression leads to gammaH2AX accumulation

A, Lysates of HCT116 p53 wt or p53-/- cells transfected with the indicated microRNAs for 48h were analysed by immunoblot for gammaH2AX and beta-actin levels (Lizé et al., 2010).

B, U2OS cells (p53 wild type) were transfected for 72h and treated with the DNA damaging agent Camptothecin (CPT) or mock for 24h, followed by the same analysis.

C, H1299 cells were transfected with the indicated microRNAs for 72h, followed by the same analysis. Note that the increase in gammaH2AX upon miR-449a transfection was less pronounced in these cells than in HCT116 or U2OS cells.

Although not fully explained at present, the miR-449 mediated accumulation of the DNA damage marker gammaH2AX would be in line with the known ability of E2F1 to induce a DNA damage response, and with similar responses to oncogenic stress during early cancerogenesis (Bartkova et al., 2005). Additionally, it was shown that HDAC1 inhibition was sufficient to accumulate DNA damage (Kim et al., 2008).

This effect, however, seems to be dependent on caspase activity, since it could be repressed by caspase inhibition with Z-VAD (Fig. 5.17).

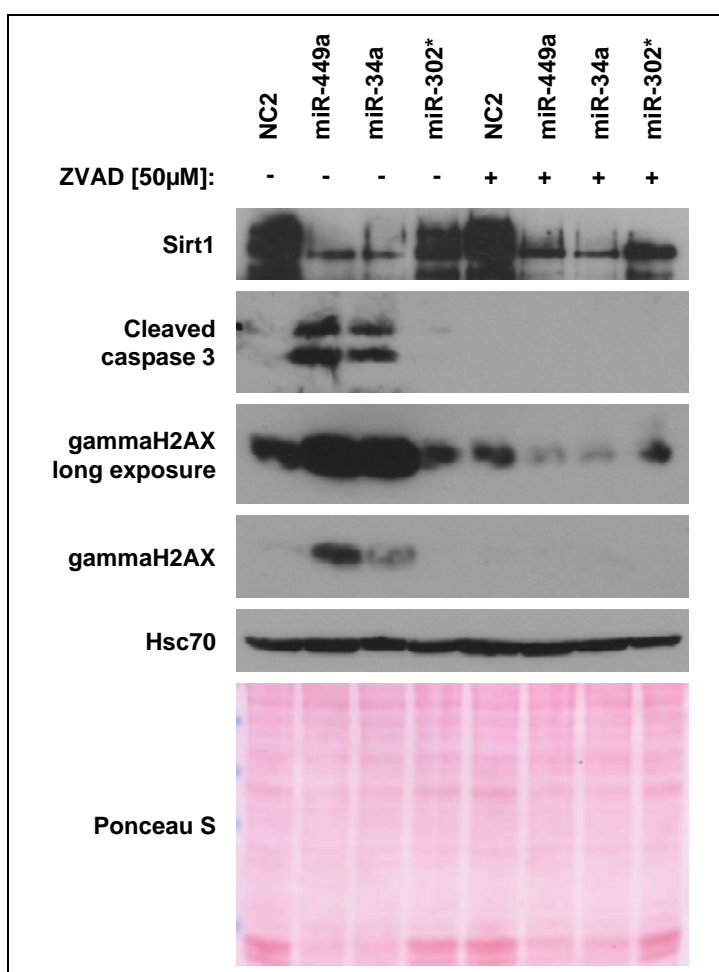


Fig. 5.17: gammaH2AX accumulation after miR-449 is dependent on caspase activity

H1299 cells were simultaneously transfected with the indicated microRNAs and treated with the caspase inhibitor ZVAD or mock for 72h, followed by immunoblot analysis using specific antibodies. The blot was stained with Hsc70 and Ponceau S as loading and transfer controls. Staining of cleaved caspase 3 and SIRT1 were used as control of the transfection efficiency.

5.5.4. miR-449 targets vital mitosis checkpoints: Chk1 and BRCA1

It was recently reported that the knockdown of the checkpoint protein Chk1 could lead to an enhanced accumulation of DNA damage and apoptosis by caspase activation (Pan et al., 2009; Romagnoli et al., 2009; Wang et al., 2004), a phenotype similar to the one observed after miR-449 overexpression. Hence, I next tested whether miR-449 would affect Chk1 activity or levels and therefore promote apoptosis and DNA damage accumulation.

Both miR-449a and miR-34a were able to down-regulate not only the active, phosphorylated form of Chk1, but also its overall levels (Fig. 5.18). Since the mRNA levels of Chk1 remained largely unchanged (Fig. 5.19A), miR-449 might act through translational repression in this case (Fig. 2.2). Additionally, BRCA1 (breast cancer 1), another checkpoint protein, was affected at least at the mRNA level (Fig. 5.19B).

Since both Chk1 and BRCA1 have been implicated in the DNA repair pathway of homologous recombination (Helleday, 2010), their knockdown by miR-449 could contribute to the observed enhanced susceptibility to DNA damage and, as a consequence, to apoptosis.

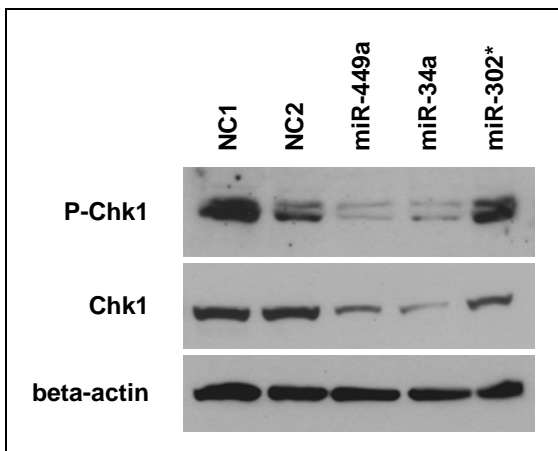


Fig. 5.18: Chk1 is downregulated by miR-449a and miR-34a

H1299 cells (*p53* *-/-*) were transfected with the indicated microRNAs for 48h, followed by immunoblot analysis of Chk1 and phospho-Chk1 (Ser317; P-Chk1) and beta-actin as a loading control.

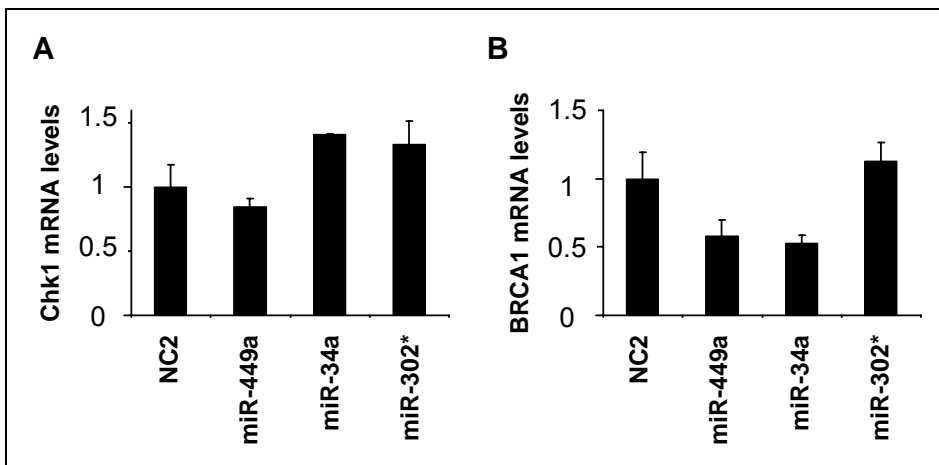


Fig. 5.19: miR-449a and miR-34a target BRCA1 but not Chk1 mRNA for degradation

H1299 cells were transfected with the indicated microRNAs, 48h post transfection the RNA was analysed by quantitative RT-PCR using specific primers for the mRNA of CHK1 (A) and BRCA1 (B).

However, although the siRNA-mediated knockdown of Chk1 in the same cell line accomplished similar gammaH2AX accumulation as miR-449 (Fig. 5.20), it failed to induce apoptosis equally (data not shown). In addition, the siRNA-mediated gammaH2AX accumulation was independent of caspase activity (as shown in Fig. 5.20 after ZVAD treatment) quite in contrary to the miR-449-mediated gammaH2AX accumulation (Fig. 5.17). Surprisingly, the knockdown of Chk1 reduced the E2F1 levels, maybe due to a decreased stability of the protein since Chk1-mediated phosphorylation of E2F1 is known to stabilise it (Fig. 2.1). The knockdown of E2F1 reduced Chk1 levels as expected, since Chk1 is E2F1-responsive (Verlinden et al., 2007).

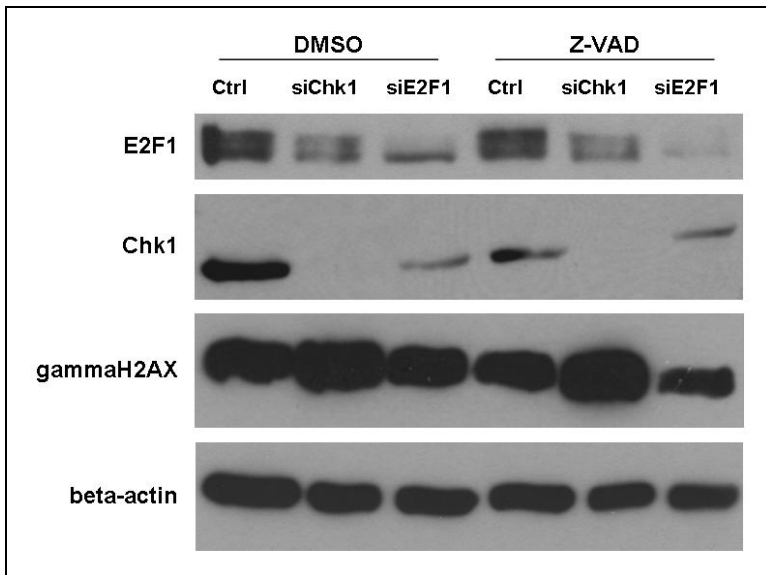


Fig. 5.20: Chk1 knockdown by siRNA accumulates DNA damage similarly to miR-449a overexpression but in a caspase-independent manner

H1299 cells were simultaneously transfected with the indicated siRNAs and treated with the caspase inhibitor ZVAD or mock for 48h, followed by immunoblot analysis using specific antibodies. Beta-actin served as loading control. Experiment performed by Miriam Weiss under my supervision.

Since the individual inhibition of the miR-449 targets CDK6, SIRT1, E2F1 or Chk1 failed to fully phenocopy miR-449-mediated, p53-independent apoptosis, I decided to combine the knockdown of more than one target at a time. As shown in Fig. 5.21, the cumulated knockdowns of SIRT1 with Chk1 or E2F1 were most efficient in inducing caspase cleavage while reduction of CDK6 seemed to have a rather protective effect, as expected for cell cycle arrest.

According to these preliminary results, the hypothesis of a cumulative effect of several miR-449 targets to achieve full effect is currently under investigation. However, it is in agreement with the hypothesis that microRNAs act through several targets to regulate complete pathways and cell fate decisions.

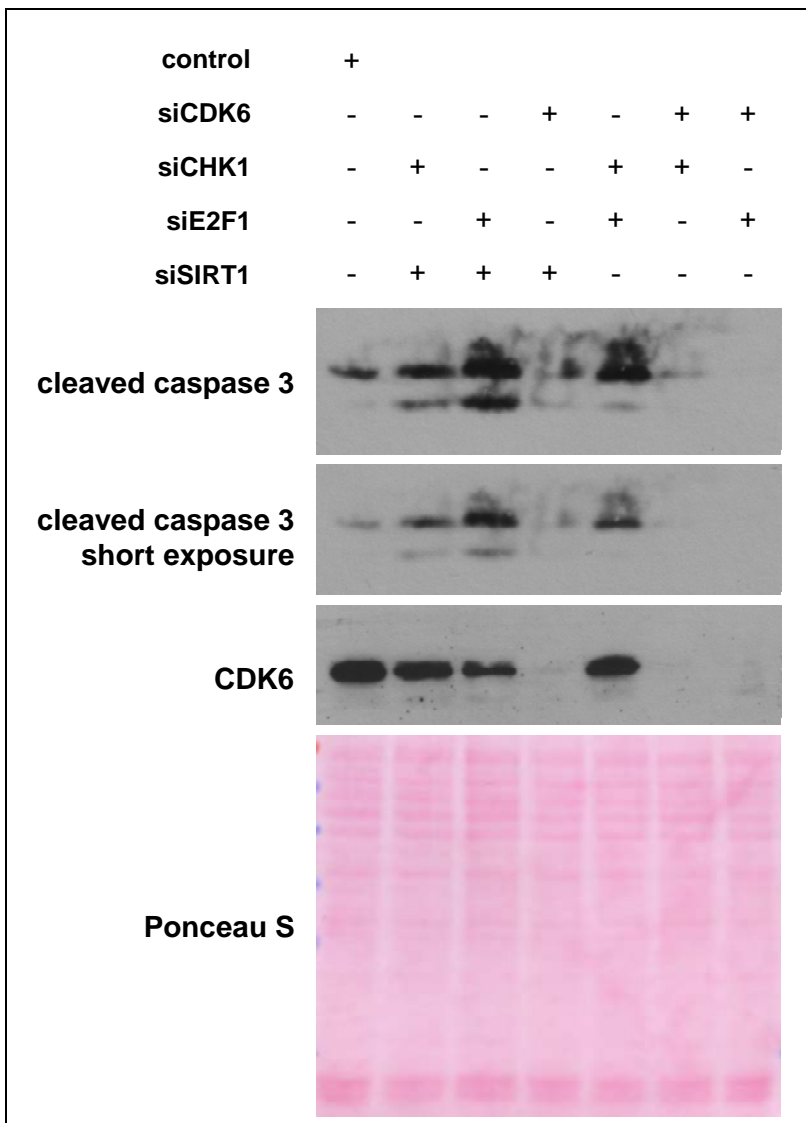


Fig. 5.21: The combined knockdown of the miR-449 targets SIRT1, CHK1 and E2F1 mimics miR-449-mediated apoptosis

H1299 cells were transfected with a combination of the indicated 2 siRNAs in each lane. Control transfection was achieved by combining 2 different scramble siRNAs. 48h post transfection the cells were harvested and analysed by immunoblot using a specific antibody against the cleaved form of caspase 3 to assess apoptosis. CDK6 was stained as a control of transfection efficiency. Ponceau S staining shows an equal protein amount in each lane.

5.6. miR-449 expression correlates with the development of ciliated cells in lung *in vivo*

To gain insight into the expression patterns, and therefore putative role of miR-449a and miR-34a *in vivo*, we assessed the levels of both microRNA species in murine tissues by quantitative RT-PCR. Whereas miR-34a showed a broader distribution, miR-449a was largely restricted to testes and lung (Fig. 5.22A), in accordance with my first findings in

human and mouse (Fig. 5.4 A and B). In these tissues, miR-449a levels appear to exceed those of miR-34a (Fig. 5.23).

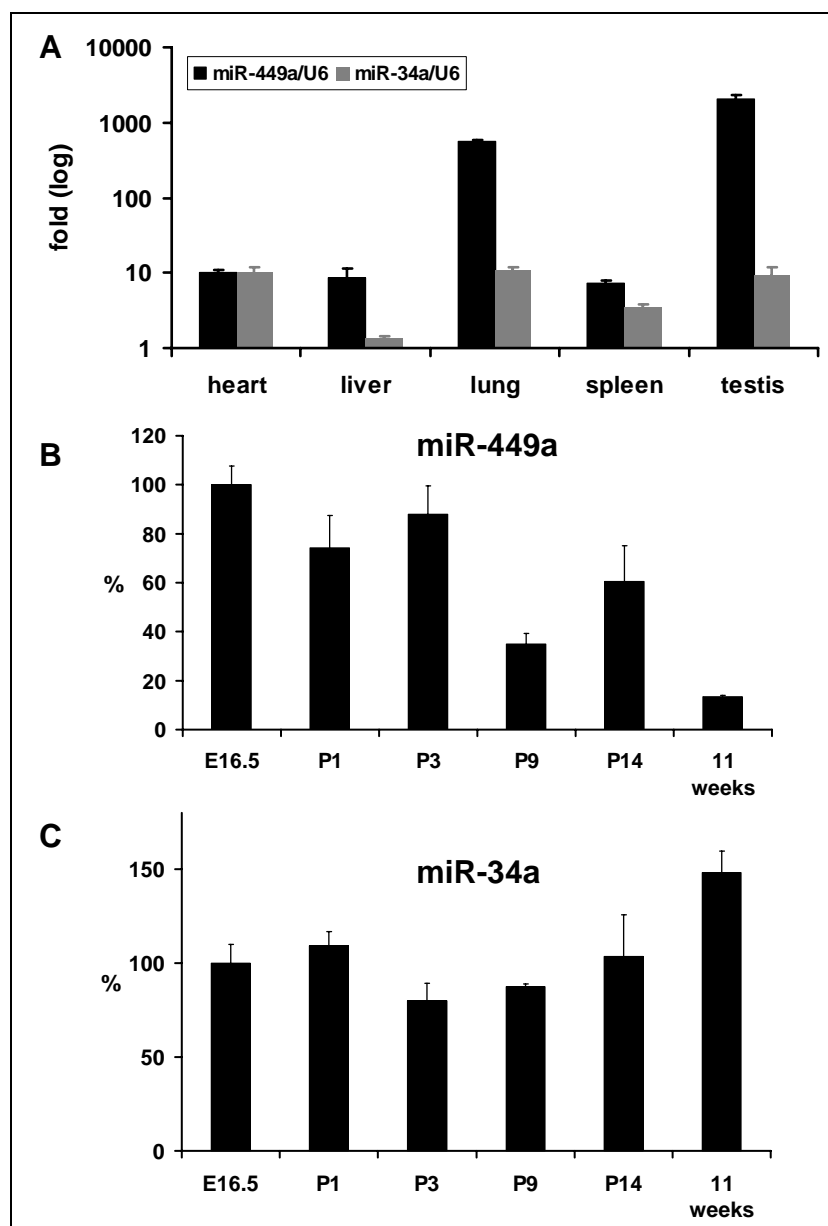


Fig. 5.22: miR-449a is highly abundant in lung tissue, in particular around birth

RNA was extracted from the indicated tissues obtained from C57BL/6 mice, followed by quantitative RT-PCR to determine the levels of microRNAs miR-34a and miR-449a.

A, Tissues were obtained from adult mice, 11 weeks of age.

B/C, Lung tissue was prepared from mouse embryos at stage E16.5 (shortly before birth), day 1, 3, 9 and 14 after birth, and 11 weeks after birth, followed by quantification of miR-449a (B) and miR-34a (C).

From the manuscript Lizé et al., submitted for peer review in June 2010.

To assess the temporal pattern of miR-449a expression in the lung, RNA was extracted from murine pulmonary tissue shortly before and after birth. MiR-449a was highly expressed in the lungs of mouse embryos at stage E16 (i. e. 3 days before term) and then steadily decreased (Fig. 5.22B). In contrast, the levels of miR-34a remained largely unchanged (Fig. 5.22C). Thus, miR-449a is specifically expressed in pulmonary tissue, but mostly during the time around birth.

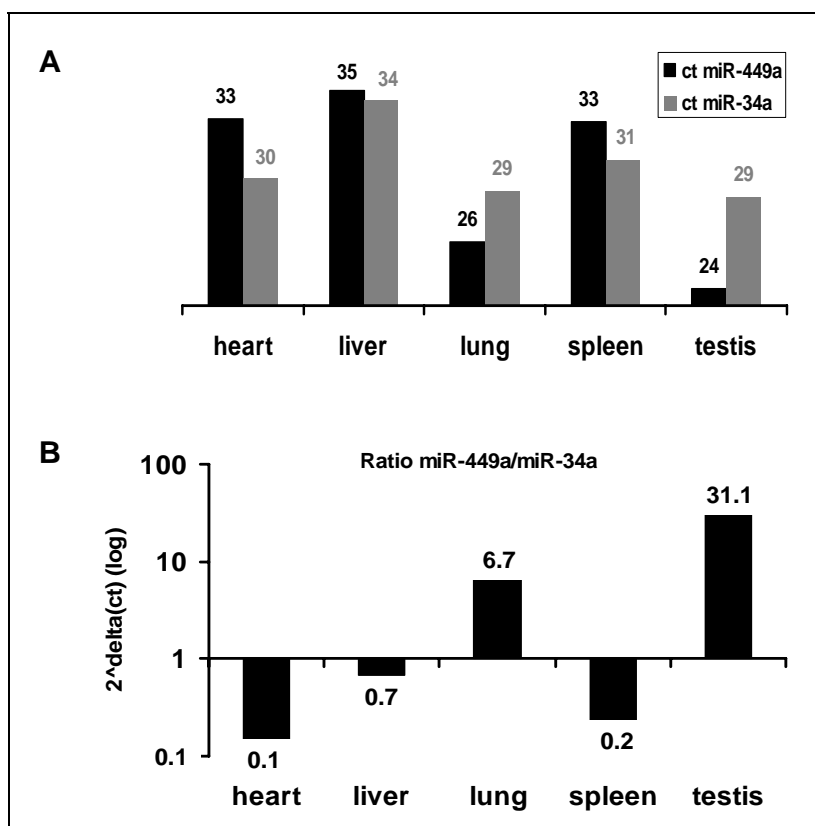


Fig. 5.23: Comparison of the miR-449a and miR-34a levels in various tissues in mouse

A, The results of RT-PCR (cf. Fig. 5.22) are shown as ct values (i. e. the number of PCR cycles required to obtain a pre-defined amount of the corresponding PCR product). Note that a low ct value corresponds to a high amount of template. Assuming similar efficiencies of PCR amplification, it is concluded that miR-449 levels are higher than miR-34a levels in lung and testes, but not in other tissues under study.

B, The ratio of miR-449a and miR-34a levels was calculated, approximating the amplification factor by 2. It is thereby estimated that the levels of miR-449 exceed those of miR-34a by a factor of 6.7 in lung tissue and by 31.1 in testicular tissue. Note that this comparison is limited by the efficiency of PCR amplification and therefore only represents an estimation.

From the manuscript Lizé et al., submitted for peer review in June 2010.

Since mucociliary epithelia are a major component of the respiratory tract, it can be speculated that they represent the site of high miR-449a levels. Interestingly, the highest

levels of miR-449 (found shortly before and after birth) correlate with the time span where mucociliary differentiation takes place (Fig. 2.6) to ensure proper breathing at birth.

5.7. miR-449 levels sharply increase upon differentiation of airway epithelial cells

To test whether mucociliary epithelium was the site of high miR-449 expression, we employed a system to recapitulate aero-epithelial cell differentiation *in vitro*. Human AECs were lifted to the liquid air interface and thereby induced to fully differentiate as described previously (Bals et al., 2004). At several time points, RNA was extracted to quantify microRNA levels. Before airlift, miR-449a was barely detectable by RT-PCR. Strikingly, however, miR-449a levels sharply increased 100-fold within 7 days, and more than 1000-fold within the following week in AECs from different donors (Fig. 5.24A and Fig. 5.25).

In parallel, the host gene CDC20B (containing the miR-449a encoding region within an intron) was upregulated (Fig. 5.24B), as reported previously (Ross et al., 2007), although not as dramatically as miR-449a. A similar pattern was found for a previously described putative master regulator of AEC differentiation (as introduced in Fig. 2.5), FoxJ1 (Fig. 5.24B and Fig. 5.25). Simultaneously, the generation of a seal with high electrical resistance was observed, indicating the generation of a differentiated cell monolayer (Fig. 5.24C).

In contrast to miR-449a, the levels of miR-34a remained largely unchanged (Fig. 5.24A). Curiously, the levels of E2F1 mRNA also remained unaffected (Fig. 5.24B), in contrast to the mutual regulation of E2F1 and miR-449a previously described for cells of different origin that undergo DNA damage (Fig. 5.3B).

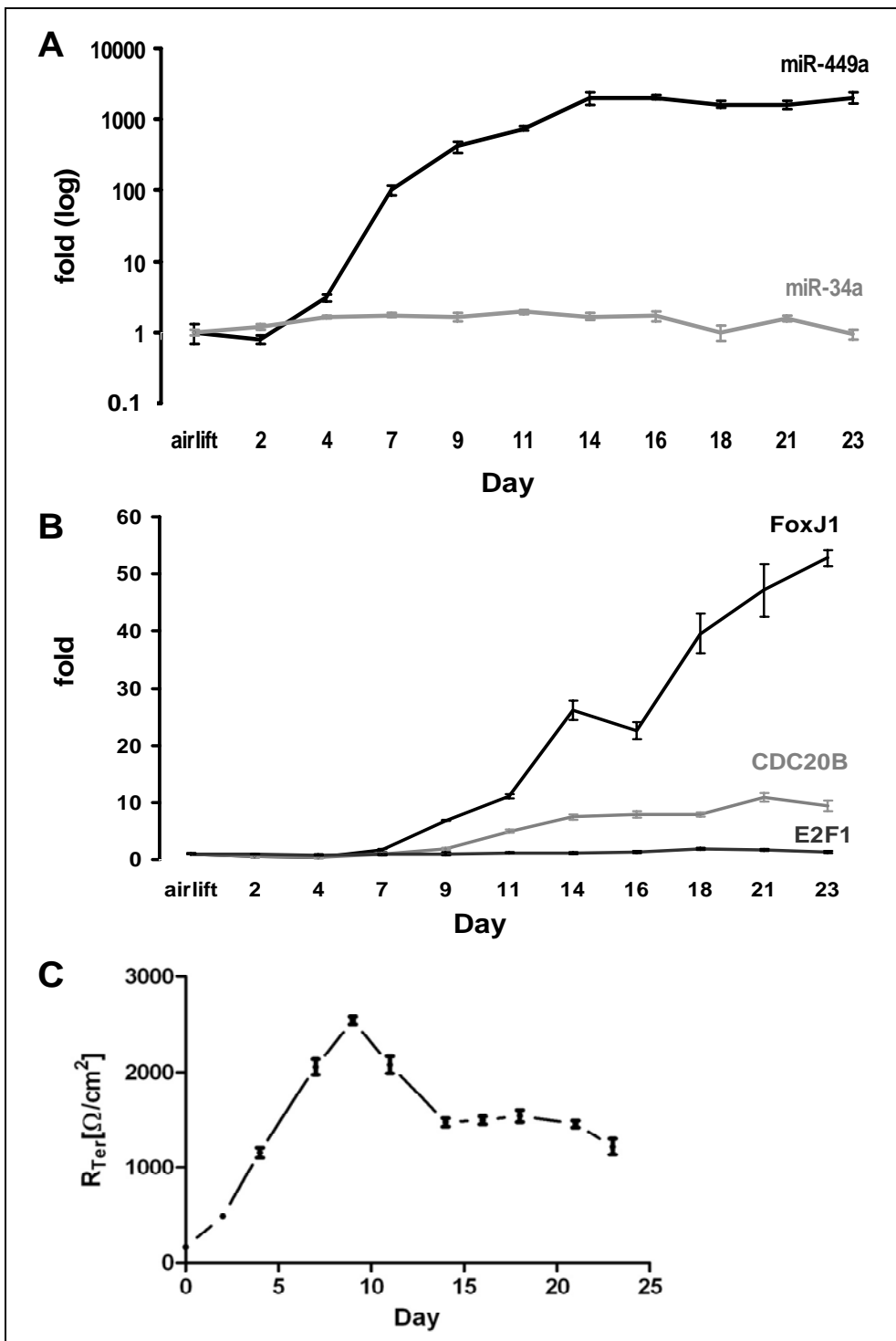


Fig. 5.24: Strong miR-449a induction in differentiating human airway epithelial cells

Airway epithelial cells (AECs) were cultivated for 3 days in liquid media and lifted to the interface between the media and the air. At the indicated time points (days after airlift), samples of the cells were harvested to prepare RNA, followed by RT-PCR to quantitate specific RNA species.

A, The levels of microRNAs 34a and 449a were quantified.

B, The abundance of the indicated mRNA species was assessed

C, The electrical resistance of the cell monolayer was measured to ensure full differentiation.

From the manuscript Lizé et al., submitted for peer review in June 2010.

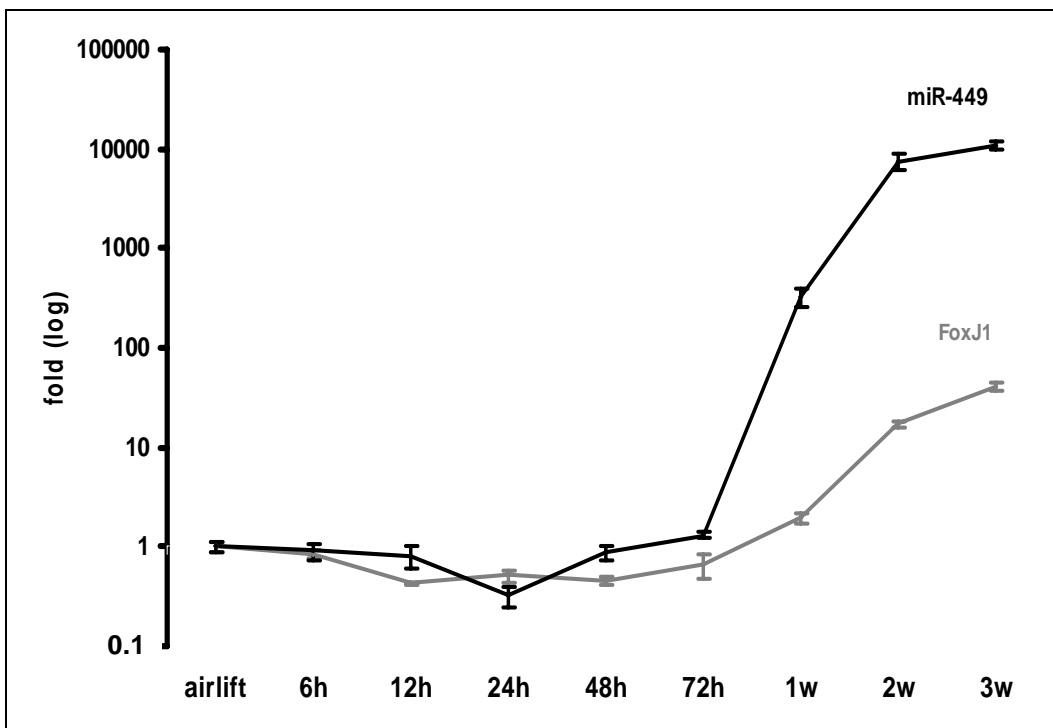


Fig. 5.25: Levels of miR-449a and FoxJ1 mRNA in differentiating airway epithelia

AECs were obtained from a different individual than in Fig. 5.24, followed by airlift and RNA preparation at the indicated time points. RNA levels were analyzed as described in the legend to Fig. 5.24. h = hours, d = days, w = weeks. From the manuscript Lizé et al., submitted for peer review in June 2010.

In conclusion, miR-449a represents a highly specific marker for differentiated AECs, perhaps acting as a master regulator of the AEC-specific gene expression program. To my knowledge, and in comparison to other differentially regulated genes, the increase in miR-449a represents the strongest change in gene expression levels that occurs upon AEC differentiation.

5.8. miR-449 levels further increase upon exposure of airway epithelia to tobacco smoke

During the first characterisation of miR-449a, its up-regulation in response to DNA damage was shown (Fig. 5.3B), and similar findings were reported for miR-34a (Hermeking, 2007). To assess this in the context of airway epithelia, I exposed a differentiated AEC monolayer to tobacco smoke, as previously described by my collaborators (Beisswenger et al., 2004).

This procedure increased the levels of miR-449a even further (Fig. 5.26A). This increase was also found for the mRNA encoding E2F1 (Fig. 5.26B), possibly explaining the up-regulation of miR-449a.

Similarly, miR-34a levels were increased under such circumstances (Fig. 5.26A), perhaps as a result of the known p53-responsiveness of miR-34a (Hermeking, 2007).

This is in contrast to a number of other microRNA species that were previously found downregulated by tobacco smoke exposure (Schembri et al., 2009).

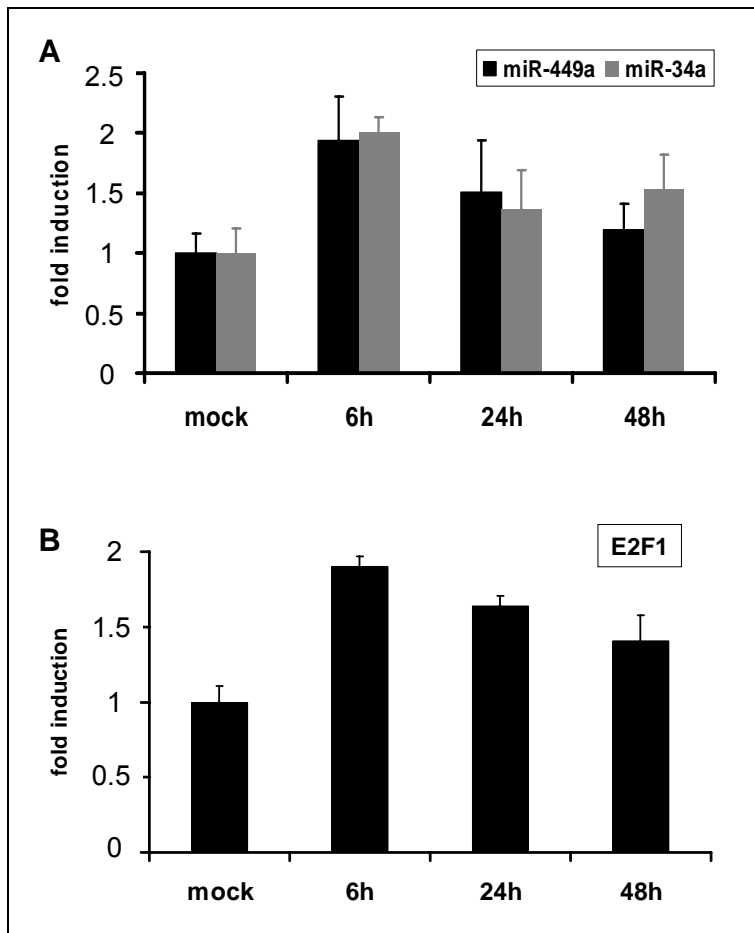


Fig. 5.26: Further induction of miR-449a in airway epithelial cells exposed to tobacco smoke

A fully differentiated monolayer of AECs (more exactly the very same AECs as obtained in Fig. 5.25), were exposed to cigarette smoke for 15 min (= 3 cigarettes) or mock-treated at 21 days after airlift, followed by RT-PCR quantification of microRNA-449a and -34a levels (A) and E2F1 mRNA (B). From the manuscript Lizé et al., submitted for peer review in June 2010.

Thus, miR-449a is further regulated by genotoxic stress, as it occurs in response to exposure of AECs to tobacco smoke. Unlike the differentiation-associated up-regulation of miR-449a, the induction of miR-449a by genotoxicity may be a result of the DNA damage dependent activation of E2F1.

6. Discussion

E2F1 has a paradoxical role in cancer, sometimes acting as an oncogene (Johnson, 2000; Johnson et al., 1994), sometimes as a tumour-suppressor (Johnson, 2000; Shan and Lee, 1994; Tsai et al., 1998; Wu and Levine, 1994; Yamasaki et al., 1996). This reflects the ability of E2F1 to promote cell proliferation or cell death by apoptosis depending on the cellular context. However, the regulation of the life or death decision made by E2F1 is still poorly understood.

The results reported in this thesis describe miR-449 as a new E2F1-responsive microRNA from the miR-34 family. The activity of this microRNA recapitulates many properties of E2F1-p53 interdependence in the regulation of cell proliferation and cell death. Indeed, in response to DNA damage, miR-449 can promote apoptosis and p53 activity (like E2F1) while repressing E2F1 activity (like p53).

MiR-449, as well as its poorly described host gene CDC20B, is expressed at high levels in a tissue-specific manner, mainly in differentiated pulmonary tissue or tissue from the reproduction tracts. In line with its tumour-suppressive function, miR-499 is strongly downregulated in cancer, most probably through epigenetic inactivation.

In tumour cell lines, the reactivation of miR-449 expression by drug treatment or its reintroduction both lead to growth arrest and apoptosis, and might therefore have therapeutic relevance in cancer arising from pulmonary or reproductive tissues like lung or testis.

6.1. Regulation of the E2F and p53 pathways

The results presented here demonstrate that miR-449 provides a negative feedback to E2F1 and a positive feedback to p53 activity, reinforcing the E2F1-p53 interdependence summarized in the model presented in Fig. 6.1A.

Both p53 and E2F1 are activated in response to DNA damage, and they subsequently induce proapoptotic genes. However, the mutual regulation of E2F1 and p53 is asymmetric. E2F1 induces the expression of p14arf, thereby stabilising p53, and of TAp73, leading to enhanced induction of p53 target genes. On the other hand, p53 transactivates the gene encoding p21, a CDK inhibitor that negatively regulates E2F1.

MiR-449 recapitulates this asymmetric, mutual regulation. The negative regulation of the E2F pathway by miR-449 occurs through several, different mechanisms pointing to the importance of this effect. First, miR-449 targets CDK2 and CDK6, two cyclin-dependent kinases responsible for the phosphorylation of pocket proteins (e.g. Rb). As a result,

hypophosphorylated Rb can bind to and inactivate E2F. Interestingly, miR-449 not only inhibits E2F activity but also affects E2F1 and E2F3 protein levels. Since miR-449 does not directly bind to the 3'UTR of E2F1, this suggests that it regulates E2F1 stability. Furthermore, another miR-449 target, SIRT1, has been linked to cell cycle regulation through E2F inhibition. SIRT1 is known to deacetylate Rb (Wong and Weber, 2007). A knock-down of SIRT1 as a result of miR-449 expression leads to the accumulation of acetylated, active Rb (through the obstruction of inhibitory phosphorylation sites), thereby inactivating E2F and promoting growth arrest. In p53 wild type cells, the negative regulation of E2F1 by miR-449 is further supported by the upregulation of the p53-responsive CDK inhibitor p21 (Fig. 6.1A). This is probably due to the down-regulation of SIRT1, which allows the accumulation of a highly active, acetylated form of p53 (Yamakuchi et al., 2008). This p53 activation may result in the induction of p53-dependent apoptosis, as described earlier consequently to SIRT1 down-regulation (Sun et al., 2007). However, the knockdown of SIRT1 alone did not fully phenocopy the proapoptotic effects of miR-34 or miR-449 under the conditions used in my study, although it did suppress clonogenic survival in preliminary tests. Nevertheless, this does not exclude a contribution of SIRT1 down-regulation to the observed cell death when combined with broader gene regulation.

Thus, the activities of the miR-34 family reported here are in analogy to the classical model of E2F-p53 mutual regulation (Fig. 6.1A). Firstly, miR-34 and miR-449 are each capable of promoting apoptosis, presumably by antagonizing an overlapping set of pro-survival genes. On top of this, both microRNAs activate p53 while attenuating E2F1 (Fig. 6.1B), thereby repressing cell proliferation. This strongly argues that microRNAs of the 34/449 family fortify both the proapoptotic activities of p53 and E2F1, but also the asymmetric mutual regulation of these two factors.

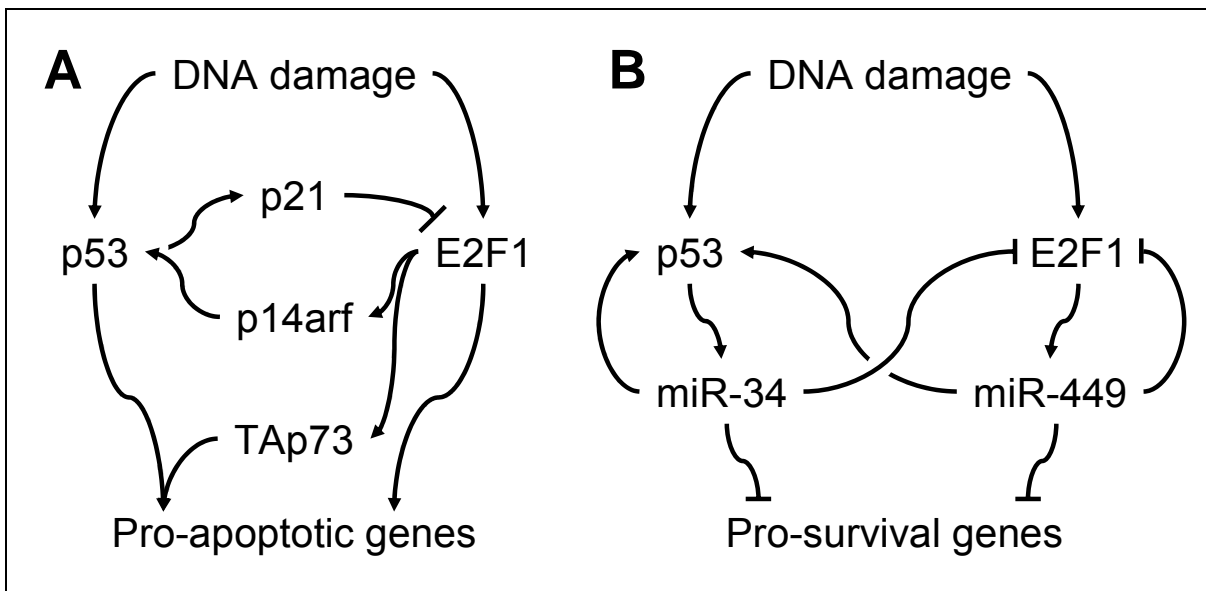


Fig. 6.1: Mutual regulation of p53 and E2F1

A, Mutual regulation through protein-coding target genes. DNA damage activates p53 and E2F1, and both induce an overlapping set of proapoptotic target genes. Although E2F1 further enhances p53 activity through p14arf and TAp73, p53 inhibits E2F1 through the CDK inhibitor p21.

B, This asymmetric mutual regulation is recapitulated and presumably fortified by microRNAs. On DNA damage, p53 induces miR-34 and E2F1 increases the levels of miR449 family members. Both microRNAs induce apoptosis by antagonizing the expression of prosurvival genes. In addition to this, both microRNAs support p53 activity (for example, through enhanced acetylation), but negatively regulate E2F1 (for example, by down-regulating CDK6). Arrowheads symbolize activation and bars inhibition.

Lizé et al., Cell Death & Differentiation, March 2010.

However, since both miRNAs were shown to induce cell death in p53 deficient cells, they must also trigger proapoptotic mechanisms independently of p53. Extensive studies on miR-34 target genes have revealed a multitude of potential genes as being miR-34-regulated (Chang et al., 2007; He et al., 2007a). It therefore can be assumed that miR-449 has a similarly broad spectrum of target mRNAs, largely excluding a moncausal model to explain its proapoptotic effects. In fact, the combined knockdown of two miR-449 targets, namely SIRT1 and E2F1, in contrast to individual inhibition, was able to activate caspase cleavage in p53-deficient cells.

As the majority of tumour cells have lost proper p53 activity, the mechanisms behind miR-449-induced p53-independent apoptosis could be of high therapeutic relevance.

6.2. miR-449-mediated p53-independent apoptosis

Most tumour cell lines have lost proper p53-activity, thereby overcoming the induction of apoptosis in response to DNA damage. The reexpression of miR-449 however was able to induce apoptosis independently of the p53 status of the cell, which might be of high therapeutic value. During this work, several pathways potentially involved in the miR-449-mediated p53-independent apoptosis were investigated.

In contrast to the results of other studies (Ji et al., 2008), the down-regulation of antiapoptotic proteins from the BCL-family, namely BCL2 and BCL6, could not be confirmed as the mechanism by which miR-449 induces apoptosis, at least not in the cell lines used in our lab.

Moreover, the E2F1-responsive p53-homologue TAp73 is not relevant for the observed phenotype since it wasn't induced after miR-449 expression. This probably reflects the inhibition of E2F1 activity. In line with this, another proapoptotic, E2F1-responsive gene APAF1 was not induced by miR-449, excluding APAF1 accumulation as the mechanism behind miR-449-mediated p53-independent apoptosis (although caspase mediated APAF1 cleavage was observed in response to miR-449, data not shown).

In the following paragraphs, several potential mechanisms for miR-449-mediated p53-independent apoptosis are discussed.

6.2.1. miR-449 as a regulator of cell cycle progression: cell death by mitotic catastrophe?

On top of the negative regulation of cell proliferation by inhibition of the E2F pathway, miR-449 seems to also affect mitosis regulation.

The first hint was given by the fact that miR-449a and miR-449b are both encoded in an intron of the CDC20B gene. While little is known about the function of this gene, its parologue CDC20 is an essential component of the cellular machinery that enables the anaphase promoting complex to destruct its targets in a timely fashion, allowing progression through mitosis (Yu, 2007). Moreover, several mitosis-promoting genes, e. g. Polo-like kinase and others, have previously been identified as E2F1-targets, implying E2F1 in mitotic progression (Ren et al., 2002). It is tempting to speculate that E2F1 regulates mitosis through CDC20B/miR-449 induction, and uncontrolled E2F1-activity is avoided by miR-449 negative feedback.

In fact, miR-449 modulates the histone deacetylase HDAC1, which has been shown to be required for the correct formation of chromatin after DNA replication (Milutinovic et al., 2002). MiR-449 might therefore disturb proper mitosis exit through the down-regulation of HDAC1.

Consistently, HDAC inhibition can lead to G2/M arrest (Milutinovic et al., 2002). As an interesting, additional link, BRCA1 (breast cancer 1), another miR-449 target, was shown to interact with both Rb and HDAC1 (Yarden and Brody, 1999).

Among its targets, miR-449 also down-regulates two major cell cycle checkpoint proteins, Chk1 (checkpoint kinase 1) and BRCA1, both shown to be deregulated in cancer (Enders, 2008; Yarden et al., 2002), and both closely related to mitotic catastrophe (Huang et al., 2005). Most notably, Chk1 contributes to many cell cycle checkpoints (G1/S, intra-S, G2/M and mitotic spindle checkpoint) including the mitotic exit DNA damage checkpoint (Dai and Grant, 2010; Huang et al., 2005). Chk1 depletion is therefore expected to prevent proper, damage-free cell cycle progression and to promote the G1 entry of damaged mitotic cells (Lee et al., 2010). This causes cell death by mitotic catastrophe (Canman, 2001; Fishler et al., 2010). In fact, Chk1 inhibition or deletion killed mammary tumour cells in a recent study (Fishler et al., 2010). Interestingly, cell death following Chk1 depletion is usually accompanied by caspase-3 activation and accumulation of double-stranded DNA breaks (Xiao et al., 2005) as observed after miR-449 overexpression. Furthermore, the inhibition of BRCA1 similarly induces cell cycle arrest and mitotic catastrophe (Tominaga et al., 2007). Thus, miR-449 might induce p53-independent apoptosis by promoting mitotic catastrophe through the inhibition of key regulators of cell cycle progression and mitosis exit, namely HDAC1, BRCA1 and Chk1.

That way, in normal, differentiated cells, miR-449 would preferably inhibit cell cycle entry and promote growth arrest through the inhibition of the E2F pathway. In tumour cells, however, uncontrolled proliferation could overcome this arrest signal and, together with enhanced genetic instability, push miR-449 regulation toward the induction of cell death by mitotic catastrophe.

6.2.2. miR-449 & DNA damage: a role in DNA repair?

In this work, several links between miR-449 and DNA damage were found. First, miR-449 is induced by DNA damage, probably as a consequence of its E2F1 responsiveness. Additionally, besides apoptosis, one of the phenotypes observed after miR-449- as well as E2F1-overexpression in tumour cells was the accumulation of a DNA damage marker, gammaH2AX, arguing that miR-449 may sensitise cells to intrinsic DNA damage.

Tumour cells constantly undergo replicative stress (Bartkova et al., 2006; Di Micco et al., 2006), therefore they need efficient DNA repair for survival. During cancer development, tumour cells acquire genetic instability, through mutation, deletion or inhibition of several tumour-suppressor genes e.g. p53 and BRCA1. These genes contribute to the protection of genome integrity not only through the induction of apoptosis in DNA repair defective cells

(e.g. p53) but also through direct involvement in DNA repair (e.g. BRCA1). Even though tumour cells with defects in the homologous recombination machinery are still viable, this is mostly due to the maintenance of “backup” mechanisms (Helleday, 2010; Helleday et al., 2008). Targeting the last functional parts of this machinery might kill cancer cells effectively, as lately shown for HDAC (Adimoolam et al., 2007) and PARP inhibitors (Bryant et al., 2005; Farmer et al., 2005; Fong et al., 2009; Helleday et al., 2005).

Interestingly, miR-449 targets several proteins with a role in DNA repair. For instance, HDAC1 (Adimoolam et al., 2007), BRCA1 (O'Donovan and Livingston, 2010), SIRT1 (Helleday, 2010; Uhl et al., 2010) and Chk1 (Stracker et al., 2009) have been shown to play a role in homologous recombination (Helleday, 2010). In cancer cells, even in p53-defective cells, the inhibition of homologous recombination could become fatal because of the excessive accumulation of DNA damage.

Unfortunately, even though miR-449 can be linked to mitotic catastrophe and tumour cell death as a consequence of DNA repair impairment, the exact mechanisms behind miR-449-mediated, p53-independent cell death are still unclear and need further investigation.

6.3. miR-449 as a regulator of general gene expression

Certainly, the downregulation of the histone deacetylases SIRT1 and HDAC1 by miR-449 shown here not only affects DNA repair, but also general gene expression, through epigenetic modulation (i.e. acetylation of histones) and regulation of the activity of transcription factors (through acetylation levels of e.g. p53, Sp1).

Interestingly, HDACs, in contrast to microRNAs from the miR-34 family, are overexpressed in various cancers (Halkidou et al., 2004; Patra et al., 2001; Weichert et al., 2008a; Weichert et al., 2008b; Wilson et al., 2006; Zhang et al., 2005). This mostly correlates with poor prognosis (Weichert, 2009). HDAC inhibitors have been shown to efficiently kill tumour cells, and accordingly, HDAC inhibitors are currently in clinical trials (Carew et al., 2008; Moradei et al., 2008; Shankar and Srivastava, 2008). Interestingly, also another histone deacetylase is targeted by miR-449. SIRT1 was shown to be highly expressed in cancer, and its knockdown was able to induce apoptosis independently of p53 (Stunkel et al., 2007), accompanied by caspase activation (Alcendor et al., 2004). The specific inhibition of SIRT1 has also been shown to sensitise tumour cells to chemotherapeutics (Wang et al., 2008).

However, the mechanism leading to HDAC overexpression in cancer is not yet clear. Mir-449 is generally reduced in tumour cells, mainly through epigenetic silencing (Noonan et al., 2009). Cells might be selected for miR-449 silencing since they may otherwise undergo cell cycle arrest or apoptosis. The fact that E2F1 is frequently overactive in cancer may further

increase the need for miR-449 silencing. Therefore, the loss of miR-449 observed in cancer may contribute to HDAC1 enhanced expression, thereby eventually contributing to carcinogenesis through “cell reprogramming” (Trosko, 2009). Intriguingly, miR-449 itself is induced by HDAC inhibition. Thus, miR-449 induction may even contribute to cell death upon HDAC inhibitor treatment.

Hence, HDACs keep miR-449 low in tumour cells while miR-449 keeps HDACs low in non-cancerous cells. This mutual regulation might provide a “switch” for general gene expression, such as often observed in tumorigenesis or differentiation.

6.4. miR-449 *in vivo*: cell differentiation and development

MiR-449 is strongly induced during the mucociliary differentiation of airway epithelium, and its expression in the murine lung is highest around birth, when this process is needed the most.

To my knowledge, this is the first description of a microRNA that displays strong specificity for mucociliary differentiation, although several microRNAs, including miR-449a, were reported to be expressed in lung tissue depending on the developmental stage (Dong et al., 2010; Lu et al., 2008). MiR-449a undergoes the strongest induction of gene expression that was so far observed during AEC differentiation. This observation raises the possibility that miR-449, perhaps in addition to FoxJ1, serves as a master regulator to ensure the proper differentiation of this vital cell population.

Previous studies have used microarray hybridization to identify changes in mRNA levels that occur in the course of AEC differentiation. Strikingly, one of the most differentially expressed genes found in this study was the miR-449 host gene, CDC20B (Ross et al., 2007). The mRNA of CDC20B and miR-449 are usually coregulated. Therefore, it is probable that at least some of the regulatory mechanisms that govern miR-449 up-regulation upon AEC differentiation apply to its host gene CDC20B as well. However, it is remarkable that the upregulation of miR-449a was even stronger than that of CDC20B. Differences in PCR efficiency cannot be fully ruled out since microRNAs and mRNAs were measured using different methods. However, it is tempting to speculate that AEC differentiation is associated with increased efficiency of miR-449a processing from its precursor RNA, explaining the additional increase. Interestingly, some of the miR-449 targets described in my thesis were found to be downregulated during AEC differentiation, most notably Chk1 and CDKs (Ross et al., 2007). It is therefore very probable that miR-449a not only marks differentiated AECs but also serves as an active regulator of this differentiation process. MiR-449 is a potent inducer of cell cycle arrest, and this may contribute to terminal differentiation. In addition, miR-449 reduces the levels of the histone deacetylases SIRT1 and HDAC1, pleiotropic regulators of

transcription, possibly contributing to a differentiation-associated gene expression program. An active function of miR-449a in mucociliary cell differentiation would be in agreement with its high expression levels shortly before and after birth, when the demand for such a differentiation program is the highest.

The cellular origin of cancer has been discussed heavily during the past 100 years. There are two main theories: reprogramming of differentiated cells or blockage of differentiation programming (Sell, 1993; Trosko, 2009). The downregulation of HDACs by miR-449 could contribute to such a reprogramming, pushing the cells toward differentiation. In fact, besides histone deacetylases, I found several regulators of differentiation among the putative miR-449 targets (Tab. 5.1). For instance, KLF4 was shown recently to be one of the four genes sufficient to reprogram fibroblasts into embryonic stem-like cells (Takahashi and Yamanaka, 2006). Additionally, HMGA2 has been involved in the maintenance of an undifferentiated state in cancer (Droge and Davey, 2008). An active Notch signalling has been associated with immature, proliferating cells (Axelson et al., 2005) and Notch1 is found among the putative miR-449 targets (Tab. 5.1). Also the activation of p53 by miR-449 can suppress cellular dedifferentiation (Zhao and Xu, 2010) through the suppression of the pluripotency factor Nanog (Lin et al., 2005). Finally, miR-449 was shown to be involved in development in another report (Redshaw et al., 2009), in this case implicating the down-regulation of another member of the E2F family, E2F5.

Besides differentiation, miR-449a is also capable of inducing apoptosis, and this activity may help miR-449a to provide a first line defence mechanism upon genotoxic stress (as seen in response to cigarette smoke) or virus infection (Wang et al., 2009) in airways. The further up-regulation of miR-449 upon smoke exposure may ensure the elimination of cells with damaged DNA and thus prevent the occurrence of malignancies. While miR-34 acts as a general effector of p53-induced apoptosis in a broad range of tissues, its cousin miR-449 appears to exert a comparable tumour suppressive role specifically in airway epithelia.

6.5. Outlook

The E2F family is essential for cell proliferation. However, its uncontrolled activity is one of the most widely acknowledged reasons for malignant growth. MiR-449 prevents the accumulation of cells with excessive E2F1 activity in two ways. Firstly, it directly antagonises E2F1. Secondly, it eliminates those cells when necessary through the induction of apoptosis. As both mechanisms can occur independently of p53, miR-449 may represent an essential barrier to cancer progression in cells that have already lost p53 function through mutations.

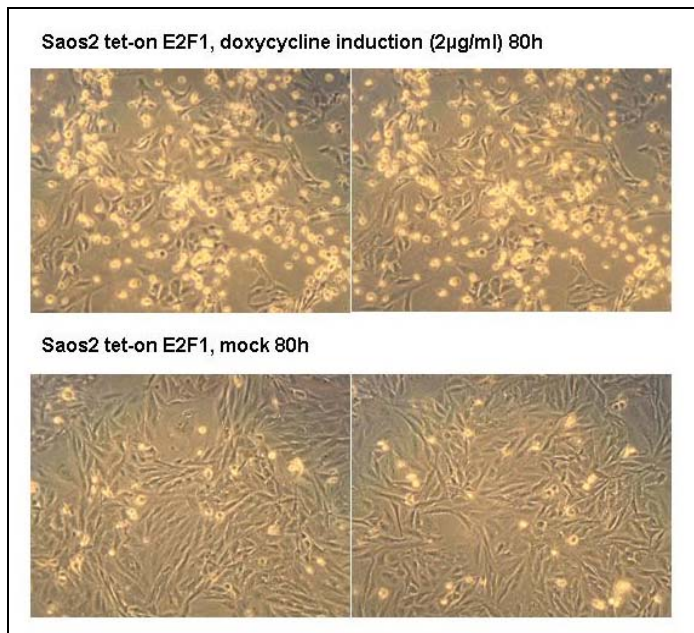
Since tumour cells are generally prone to a constitutive DNA damage response (Bartkova et al., 2005), they might undergo apoptosis in response to miR-449 or miR-34 at an enhanced

rate compared to normal cells. This is supported by the fact that, while little reexpression of miR-449 in tumour cells already stimulates an apoptotic response, non-cancerous tissues tolerate very high levels of miR-449. This makes miR-449 an interesting candidate for cancer therapy. HDAC inhibitors are already being tested in clinical trials. However, their lack of specificity could lead to several side effects. Also drugs targeting the DNA repair machinery are currently under study. MiR-449, by targeting not only HDACS but also several members of the DNA repair machinery, might offer a more tumour-specific, safer therapeutic approach.

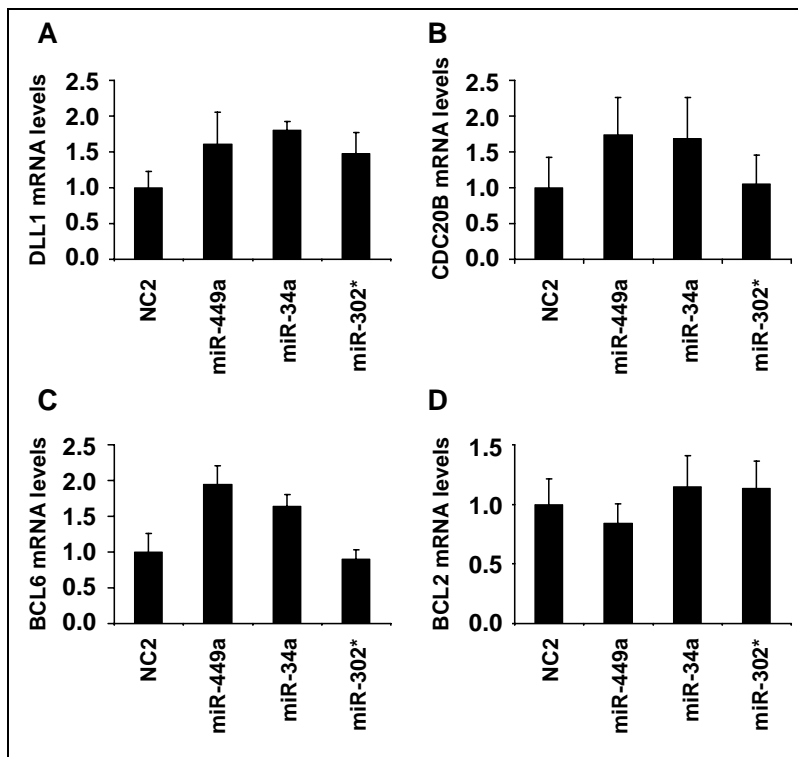
Additionally, residual expression levels of miR-449 and miR-34a, and their inducibility by E2F1 and p53, may represent a determinant for cancer cell death in response to irradiation or chemotherapy. The assessment of miR-449 expression might therefore be of interest in tumour diagnostics and in the prognosis of the outcome of DNA damaging treatments.

Finally, these results identify miR-449a as an exquisitely specific biomarker of differentiated airway epithelia, and moreover suggest a role for miR-449 in the differentiation of airway epithelium and its first line defence *in vivo*.

7. Supplementary data



Suppl. Fig. S 1: Apoptotic phenotype of Saos2 tet-on E2F1 cells after E2F1 induction



Suppl. Fig. S 2: rejected targets

H1299 cells were transfected with the indicated microRNAs, followed by RT-PCR to determine the mRNA levels of DLL1 (A), the microRNAs-449 host gene CDC20B (B), BCL6 (C) and BCL2 (D). Displayed are the mean results of 3 independent experiments with error bars normalised to the 18S rRNA levels in each sample.

Supp. Tab. 1: microRNA micro-array data

The area shaded in grey is considered as non-responsive for it contains the negative controls, and the induction is not significant.

Name	log2(Cy3) Control	Cy3 SD Control	log2(Cy5) E2F	Cy5 SD E2F	Difference: Control-E2F	log induction	fold induction
mmu-miR-449a	7,402	0,061	10,047	0,059	-2,645	2,645	6,253
hsa-miR-449b	6,885	0,097	8,914	0,060	-2,028	2,028	4,080
hsa-miR-492	9,240	0,079	10,481	0,073	-1,241	1,241	2,364
mmu-let-7b	9,177	0,069	10,344	0,113	-1,167	1,167	2,245
mmu-let-7c	9,457	0,046	10,620	0,052	-1,162	1,162	2,238
hsa-miR-663	10,188	0,042	11,317	0,091	-1,130	1,130	2,188
mmu-miR-19b	9,813	0,109	10,882	0,153	-1,069	1,069	2,098
mmu-miR-30b	9,213	0,116	10,223	0,108	-1,010	1,010	2,014
mmu-miR-16	9,809	0,051	10,816	0,099	-1,007	1,007	2,009
mmu-miR-762	7,920	0,057	8,918	0,079	-0,998	0,998	1,997
mmu-miR-17	9,422	0,083	10,414	0,091	-0,992	0,992	1,989
hsa-miR-106a	9,232	0,066	10,200	0,093	-0,967	0,967	1,955
mmu-miR-23a	10,007	0,055	10,942	0,120	-0,936	0,936	1,913
miRPlus_17952	8,114	0,096	9,048	0,171	-0,934	0,934	1,911
mmu-miR-20a	9,568	0,042	10,482	0,072	-0,915	0,915	1,885
mmu-miR-106b	8,910	0,042	9,819	0,066	-0,908	0,908	1,877
mmu-let-7a	11,453	0,094	12,355	0,113	-0,902	0,902	1,869
mmu-miR-23b	9,715	0,087	10,614	0,130	-0,899	0,899	1,865
miRPlus_27561	11,528	0,074	12,403	0,133	-0,875	0,875	1,834
miRPlus_21472	11,565	0,116	12,434	0,165	-0,869	0,869	1,826
hsa-let-7a	9,897	0,063	10,763	0,064	-0,867	0,867	1,824
miRPlus_17890	9,605	0,052	10,468	0,039	-0,862	0,862	1,818
mmu-miR-711	11,617	0,068	12,476	0,100	-0,859	0,859	1,814
mmu-miR-21	9,845	0,030	10,699	0,078	-0,854	0,854	1,808
mmu-miR-494	11,018	0,154	11,867	0,133	-0,849	0,849	1,801
mmu-miR-15b	9,727	0,064	10,571	0,112	-0,845	0,845	1,796
mmu-let-7d	9,915	0,041	10,755	0,042	-0,840	0,840	1,790
mmu-miR-720	8,609	0,085	9,443	0,098	-0,834	0,834	1,783
mmu-miR-93	8,158	0,172	8,992	0,124	-0,834	0,834	1,782
miRPlus_28431	8,967	0,140	9,766	0,155	-0,800	0,800	1,741
mmu-miR-101a	7,433	0,106	8,220	0,112	-0,788	0,788	1,726
hsa_SNORD3@	10,468	0,023	11,253	0,014	-0,785	0,785	1,723
hsa-miR-623	8,681	0,044	9,463	0,083	-0,782	0,782	1,719
spike_control_i	12,057	0,235	12,837	0,106	-0,780	0,780	1,717
mmu-miR-24	9,666	0,045	10,441	0,072	-0,775	0,775	1,711
mmu-miR-26a	8,636	0,171	9,407	0,137	-0,771	0,771	1,707
mmu-miR-29a	9,284	0,145	10,041	0,073	-0,757	0,757	1,690
mmu-miR-667	7,167	0,142	7,921	0,076	-0,755	0,755	1,687
mmu-let-7i	9,443	0,097	10,192	0,123	-0,749	0,749	1,681
mmu-miR-19a	8,310	0,096	9,035	0,111	-0,725	0,725	1,653
hsa-miR-498	8,613	0,101	9,337	0,040	-0,723	0,723	1,651
mmu-miR-30a	8,188	0,027	8,909	0,064	-0,721	0,721	1,648
mmu-miR-301a	8,626	0,082	9,323	0,127	-0,697	0,697	1,621
mmu-miR-30c	8,426	0,033	9,118	0,018	-0,693	0,693	1,616
hsa-miR-671-5p	8,630	0,037	9,311	0,045	-0,682	0,682	1,604
hsa-miR-665	9,073	0,028	9,753	0,040	-0,680	0,680	1,602
U6-snRNA-2	12,075	0,036	12,753	0,020	-0,678	0,678	1,600
mmu-miR-212	8,491	0,066	9,169	0,064	-0,678	0,678	1,600
U6-snRNA-1	8,029	0,032	8,705	0,039	-0,677	0,677	1,598
mmu-miR-185	7,972	0,200	8,636	0,131	-0,664	0,664	1,584

mmu-miR-107	8,086	0,079	8,738	0,110	-0,652	0,652	1,571
spike_control_b	8,163	0,152	8,810	0,102	-0,648	0,648	1,567
rno-miR-93	8,442	0,060	9,085	0,087	-0,643	0,643	1,562
mmu-miR-26a_MM1	7,838	0,059	8,475	0,061	-0,638	0,638	1,556
mmu-miR-106a	7,938	0,064	8,570	0,072	-0,633	0,633	1,550
mmu-miR-15a	8,129	0,058	8,755	0,028	-0,626	0,626	1,543
mmu-miR-22	8,386	0,023	9,001	0,041	-0,615	0,615	1,531
mmu-miR-320	8,410	0,216	9,020	0,053	-0,610	0,610	1,526
mmu-miR-99b	7,553	0,272	8,151	0,079	-0,598	0,598	1,513
mmu-miR-207	7,269	0,583	7,863	0,055	-0,594	0,594	1,509
hsa-miR-330-3p	6,097	0,526	6,688	0,227	-0,591	0,591	1,506
hsa-miR-602	7,121	0,158	7,696	0,047	-0,575	0,575	1,490
hsa_SNORD6	8,479	0,042	9,053	0,040	-0,574	0,574	1,489
mmu-miR-210	7,962	0,051	8,531	0,012	-0,568	0,568	1,483
mmu-miR-27b	8,673	0,027	9,236	0,084	-0,562	0,562	1,477
spike_control_b	8,016	0,142	8,561	0,431	-0,545	0,545	1,459
mmu-miR-709	7,593	0,038	8,135	0,038	-0,542	0,542	1,456
miRPlus_27564	8,026	0,055	8,566	0,084	-0,540	0,540	1,454
miRPlus_17921	6,511	0,495	7,047	0,322	-0,537	0,537	1,450
spike_control_i	12,091	0,080	12,627	0,087	-0,536	0,536	1,450
miRPlus_17832	8,355	0,119	8,889	0,137	-0,534	0,534	1,448
mmu-miR-103	7,442	0,181	7,974	0,045	-0,531	0,531	1,445
spike_control_a	6,553	0,445	7,077	0,258	-0,524	0,524	1,438
spike_control_b	8,195	0,235	8,717	0,292	-0,522	0,522	1,436
spike_control_j	13,347	0,052	13,865	0,038	-0,518	0,518	1,432
mmu-miR-689	7,774	0,131	8,289	0,047	-0,514	0,514	1,428
mmu-miR-668	10,902	0,440	11,407	0,469	-0,505	0,505	1,419
mmu-miR-546	9,866	0,063	10,364	0,042	-0,498	0,498	1,412
spike_control_i	11,991	0,063	12,487	0,150	-0,496	0,496	1,411
mmu-miR-770-3p	6,258	0,380	6,751	0,114	-0,493	0,493	1,408
spike_control_h	10,945	0,197	11,437	0,157	-0,492	0,492	1,406
spike_control_h	10,971	0,111	11,462	0,224	-0,490	0,490	1,405
mmu-miR-125b-5p	8,090	0,079	8,580	0,030	-0,490	0,490	1,404
spike_control_i	11,992	0,039	12,480	0,113	-0,489	0,489	1,403
rno-miR-347	8,319	0,088	8,806	0,131	-0,487	0,487	1,401
spike_control_b	8,111	0,194	8,597	0,420	-0,487	0,487	1,401
hsa_SNORD2	8,578	0,051	9,064	0,080	-0,486	0,486	1,401
hsa-miR-371-5p	7,255	0,063	7,741	0,587	-0,486	0,486	1,401
spike_control_i	11,970	0,102	12,455	0,126	-0,485	0,485	1,399
mmu-miR-467b*	6,596	0,075	7,071	0,298	-0,474	0,474	1,389
mmu-miR-20b	7,803	0,059	8,274	0,108	-0,471	0,471	1,386
spike_control_c	6,888	0,296	7,358	0,093	-0,470	0,470	1,385
spike_control_i	11,984	0,036	12,454	0,064	-0,470	0,470	1,385
hsa-miR-615-3p	6,583	0,118	7,051	0,639	-0,468	0,468	1,383
spike_control_i	12,015	0,086	12,480	0,169	-0,465	0,465	1,380
spike_control_i	12,028	0,049	12,491	0,064	-0,462	0,462	1,378
spike_control_b	8,174	0,110	8,636	0,202	-0,462	0,462	1,377
spike_control_h	11,078	0,035	11,538	0,029	-0,460	0,460	1,376
mmu-miR-143	8,296	0,021	8,754	0,035	-0,459	0,459	1,374
mmu-miR-675-5p	6,496	0,260	6,954	0,792	-0,458	0,458	1,374
spike_control_c	6,866	0,293	7,323	0,058	-0,457	0,457	1,373
spike_control_b	8,049	0,168	8,506	0,133	-0,457	0,457	1,373
spike_control_j	13,097	0,348	13,548	0,337	-0,451	0,451	1,367
spike_control_j	13,240	0,034	13,685	0,062	-0,445	0,445	1,361
mmu-miR-98	8,340	0,024	8,783	0,031	-0,444	0,444	1,360
hsa-miR-768-3p	7,369	0,101	7,812	0,133	-0,443	0,443	1,360
spike_control_b	8,025	0,105	8,468	0,179	-0,442	0,442	1,359

spike_control_j	13,213	0,031	13,650	0,103	-0,437	0,437	1,354
spike_control_j	13,166	0,072	13,603	0,121	-0,437	0,437	1,354
mmu-miR-330*	6,306	0,526	6,739	0,028	-0,433	0,433	1,350
spike_control_j	13,231	0,078	13,660	0,115	-0,429	0,429	1,346
hsa-miR-500*	7,084	0,092	7,511	0,047	-0,427	0,427	1,344
mmu-miR-27a	7,618	0,065	8,044	0,076	-0,426	0,426	1,344
spike_control_h	10,999	0,139	11,424	0,127	-0,425	0,425	1,343
spike_control_d	9,683	0,056	10,107	0,050	-0,425	0,425	1,342
spike_control_j	13,168	0,091	13,592	0,080	-0,424	0,424	1,342
spike_control_h	11,049	0,058	11,463	0,100	-0,414	0,414	1,333
mmu-miR-222	8,070	0,134	8,481	0,121	-0,411	0,411	1,330
mmu-miR-340-5p	7,413	0,036	7,825	0,063	-0,411	0,411	1,330
mmu-miR-690	6,327	0,414	6,735	0,190	-0,407	0,407	1,326
spike_control_h	10,949	0,045	11,355	0,055	-0,406	0,406	1,325
spike_control_h	10,889	0,032	11,294	0,089	-0,405	0,405	1,324
spike_control_d	9,561	0,120	9,965	0,143	-0,405	0,405	1,324
spike_control_h	10,880	0,107	11,282	0,100	-0,402	0,402	1,321
mmu-miR-32	7,486	0,028	7,888	0,048	-0,401	0,401	1,321
mmu-miR-342-3p	6,947	0,034	7,348	0,031	-0,401	0,401	1,321
spike_control_d	9,598	0,033	9,999	0,056	-0,401	0,401	1,321
spike_control_d	9,595	0,121	9,996	0,105	-0,401	0,401	1,320
mmu-miR-18a	7,623	0,051	8,024	0,025	-0,401	0,401	1,320
spike_control_j	13,076	0,193	13,475	0,143	-0,398	0,398	1,318
hsa_negative_control_3	6,632	0,467	7,030	0,835	-0,398	0,398	1,318
mmu-miR-191	7,647	0,088	8,044	0,110	-0,397	0,397	1,317
spike_control_d	9,647	0,057	10,043	0,074	-0,396	0,396	1,316
mmu-miR-706	6,521	0,360	6,916	0,646	-0,395	0,395	1,315
mmu-miR-30d	7,524	0,054	7,918	0,035	-0,394	0,394	1,314
spike_control_d	9,528	0,161	9,917	0,157	-0,389	0,389	1,309
hsa-miR-32*	7,922	0,084	8,309	0,092	-0,387	0,387	1,308
mmu-miR-100	7,547	0,037	7,933	0,096	-0,386	0,386	1,307
spike_control_d	9,610	0,118	9,995	0,149	-0,385	0,385	1,306
mmu-miR-452	7,141	0,056	7,524	0,051	-0,383	0,383	1,304
spike_control_a	6,605	0,317	6,985	0,242	-0,380	0,380	1,302
hsa-miR-18b	7,462	0,027	7,841	0,077	-0,379	0,379	1,301
spike_control_a	6,451	0,060	6,830	0,040	-0,379	0,379	1,300
mmu-miR-374	7,327	0,046	7,705	0,047	-0,378	0,378	1,299
miRPlus_17867	6,549	0,261	6,926	0,686	-0,377	0,377	1,298
mmu-miR-666-5p	6,510	0,034	6,886	0,022	-0,376	0,376	1,298
spike_control_d	9,603	0,115	9,976	0,111	-0,374	0,374	1,296
spike_control_c	6,993	0,104	7,363	0,033	-0,370	0,370	1,292
mmu-miR-300	6,136	0,456	6,505	0,056	-0,369	0,369	1,291
mmu-miR-130a	8,308	0,042	8,675	0,059	-0,367	0,367	1,290
hsa-miR-557	7,079	0,047	7,442	0,006	-0,363	0,363	1,286
spike_control_g	7,080	0,105	7,443	0,046	-0,363	0,363	1,286
spike_control_g	7,046	0,202	7,408	0,049	-0,362	0,362	1,285
spike_control_a	6,695	0,260	7,056	0,215	-0,361	0,361	1,284
mmu-miR-744	7,268	0,059	7,623	0,044	-0,355	0,355	1,279
mmu-miR-199a-3p/199b	7,744	0,097	8,093	0,111	-0,350	0,350	1,274
miRPlus_17947	6,495	0,316	6,842	0,532	-0,347	0,347	1,272
spike_control_c	7,054	0,079	7,400	0,034	-0,346	0,346	1,271
spike_control_a	6,437	0,029	6,780	0,087	-0,343	0,343	1,268
spike_control_c	7,131	0,046	7,471	0,056	-0,340	0,340	1,266
hsa-miR-502-3p	7,083	0,030	7,418	0,025	-0,336	0,336	1,262
hsa-miR-635	6,459	0,317	6,791	0,340	-0,332	0,332	1,259
spike_control_c	7,089	0,034	7,420	0,034	-0,331	0,331	1,258
miRPlus_30271	6,536	0,056	6,865	0,591	-0,328	0,328	1,256

spike_control_a	6,471	0,039	6,795	0,045	-0,324	0,324	1,252
mmu-miR-801	8,733	0,169	9,057	0,180	-0,324	0,324	1,252
hsa-miR-503	7,684	0,066	8,003	0,109	-0,318	0,318	1,247
spike_control_b	7,727	0,531	8,043	0,607	-0,316	0,316	1,245
hsa-miR-518a-5p/527	6,778	0,369	7,092	0,123	-0,314	0,314	1,243
hsa-miR-802	6,289	0,497	6,603	0,039	-0,314	0,314	1,243
spike_control_g	7,214	0,105	7,520	0,147	-0,306	0,306	1,237
miRPlus_17869	7,315	0,040	7,620	0,026	-0,304	0,304	1,235
mmu-miR-31*	6,806	0,095	7,108	0,889	-0,302	0,302	1,233
spike_control_c	6,923	0,259	7,223	0,202	-0,300	0,300	1,231
hsa-miR-486-3p	7,066	0,051	7,365	0,146	-0,300	0,300	1,231
spike_control_a	6,603	0,232	6,899	0,175	-0,296	0,296	1,228
mmu-miR-703	6,325	0,053	6,620	0,068	-0,295	0,295	1,227
hsa-miR-362-3p	7,063	0,028	7,357	0,040	-0,294	0,294	1,226
spike_control_g	7,188	0,018	7,480	0,027	-0,292	0,292	1,224
mmu-miR-466d-3p_MM1	6,461	0,402	6,751	0,050	-0,289	0,289	1,222
spike_control_c	7,093	0,050	7,383	0,066	-0,289	0,289	1,222
miRPlus_28575	7,372	0,095	7,659	0,027	-0,287	0,287	1,220
spike_control_g	7,202	0,066	7,486	0,041	-0,284	0,284	1,218
spike_control_g	7,144	0,042	7,428	0,058	-0,283	0,283	1,217
hsa-miR-658	7,820	0,147	8,102	0,140	-0,282	0,282	1,216
hsa-miR-765	8,037	0,142	8,318	0,055	-0,281	0,281	1,215
mmu-miR-423-5p	7,897	0,078	8,177	0,064	-0,280	0,280	1,215
mmu-miR-361	7,961	0,132	8,241	0,062	-0,280	0,280	1,215
hsa-miR-320	7,808	0,072	8,080	0,072	-0,272	0,272	1,208
hsa-miR-501-3p	6,613	0,360	6,878	0,319	-0,265	0,265	1,201
hsa_SNORD10	7,661	0,038	7,925	0,036	-0,263	0,263	1,200
spike_control_g	7,180	0,056	7,442	0,039	-0,261	0,261	1,198
rno-miR-376b-3p	6,249	0,500	6,506	0,073	-0,257	0,257	1,195
mmu-miR-410	6,718	0,020	6,970	0,871	-0,252	0,252	1,191
spike_control_g	7,238	0,041	7,488	0,013	-0,250	0,250	1,189
spike_control_a	6,723	0,184	6,968	0,262	-0,245	0,245	1,185
mmu-miR-574-3p	6,478	0,095	6,723	0,270	-0,245	0,245	1,185
rno-miR-541	7,023	0,361	7,267	0,134	-0,244	0,244	1,184
mmu-miR-363	6,685	0,351	6,928	0,106	-0,243	0,243	1,184
hsa-miR-422a_MM2	6,959	0,040	7,201	0,033	-0,243	0,243	1,183
mmu-miR-467a*/467d*	6,792	0,063	7,034	0,049	-0,242	0,242	1,183
mmu-miR-744	7,317	0,024	7,558	0,044	-0,241	0,241	1,181
mmu-miR-370	6,727	0,194	6,966	0,176	-0,238	0,238	1,180
miRPlus_28454	6,672	0,227	6,908	0,151	-0,236	0,236	1,178
hsa-miR-625	6,893	0,076	7,129	0,056	-0,236	0,236	1,178
hsa-miR-519d	7,831	0,087	8,065	0,078	-0,234	0,234	1,176
No known hsa target	7,745	0,045	7,972	0,080	-0,226	0,226	1,170
mmu-miR-590-5p	6,995	0,046	7,218	0,030	-0,223	0,223	1,167
mmu-miR-92b	6,835	0,018	7,058	0,027	-0,223	0,223	1,167
miRPlus_17896	7,015	0,068	7,237	0,483	-0,222	0,222	1,166
mmu-miR-125a-5p	8,267	0,067	8,488	0,096	-0,221	0,221	1,165
hsa-miR-96*	7,158	0,021	7,375	0,026	-0,218	0,218	1,163
spike_control_f	8,997	0,155	9,212	0,110	-0,216	0,216	1,161
hsa-miR-9*	6,722	0,059	6,937	0,313	-0,215	0,215	1,161
mmu-miR-10b	7,044	0,280	7,259	0,062	-0,215	0,215	1,161
miRPlus_11201	7,277	0,298	7,491	0,069	-0,214	0,214	1,160
mmu-miR-30a*	6,671	0,102	6,884	0,089	-0,213	0,213	1,159
rno-miR-376c	6,354	0,045	6,564	0,027	-0,210	0,210	1,157
mmu-miR-138	7,637	0,040	7,846	0,078	-0,209	0,209	1,156
mmu-miR-489	6,497	0,022	6,706	0,022	-0,208	0,208	1,155
mmu-miR-134	6,618	0,316	6,825	0,434	-0,207	0,207	1,154

mmu-miR-874	6,338	0,065	6,543	0,023	-0,205	0,205	1,153
miRPlus_17834	6,685	0,060	6,889	0,602	-0,204	0,204	1,152
mmu-miR-378	7,090	0,120	7,293	0,088	-0,202	0,202	1,151
spike_control_e	11,179	0,203	11,379	0,154	-0,199	0,199	1,148
mmu-miR-805	6,359	0,012	6,557	0,017	-0,198	0,198	1,147
hsa-miR-630	6,676	0,420	6,870	0,354	-0,194	0,194	1,144
hsa-miR-483-5p	7,422	0,072	7,616	0,045	-0,194	0,194	1,144
hsa_negative_control_7	6,432	0,285	6,626	0,284	-0,193	0,193	1,144
spike_control_e	11,234	0,035	11,422	0,074	-0,188	0,188	1,139
spike_control_e	11,269	0,087	11,455	0,072	-0,186	0,186	1,138
spike_control_f	8,929	0,068	9,113	0,074	-0,184	0,184	1,136
mmu-miR-219	6,420	0,354	6,604	0,161	-0,184	0,184	1,136
hsa-miR-374b	6,729	0,033	6,910	0,042	-0,181	0,181	1,133
hsa-miR-526b*	6,519	0,394	6,698	0,339	-0,179	0,179	1,132
hsa-miR-95	6,616	0,368	6,794	0,352	-0,179	0,179	1,132
mmu-miR-9*	6,728	0,300	6,906	0,065	-0,178	0,178	1,131
hsa-miR-886-5p	6,723	0,163	6,899	0,562	-0,176	0,176	1,129
mmu-miR-322*	6,697	0,127	6,871	0,559	-0,175	0,175	1,129
rno-miR-503	6,771	0,063	6,945	0,053	-0,174	0,174	1,128
mmu-miR-193	6,949	0,249	7,123	0,057	-0,174	0,174	1,128
rno-miR-352	7,172	0,060	7,345	0,030	-0,174	0,174	1,128
hsa-miR-1	6,624	0,365	6,797	0,469	-0,173	0,173	1,128
hsa-miR-548a-5p	6,499	0,244	6,672	0,317	-0,173	0,173	1,127
mmu-miR-455	6,802	0,095	6,975	0,017	-0,173	0,173	1,127
hsa-miR-656	6,423	0,045	6,595	0,020	-0,172	0,172	1,127
hsa-miR-30b*	7,661	0,030	7,833	0,032	-0,172	0,172	1,126
hsa-miR-302b	6,747	0,048	6,916	0,602	-0,169	0,169	1,124
miRPlus_30209	6,407	0,033	6,576	0,015	-0,169	0,169	1,124
mmu-miR-30e	7,672	0,200	7,840	0,098	-0,168	0,168	1,124
hsa-let-7d	7,216	0,137	7,381	0,077	-0,165	0,165	1,121
mmu-miR-761	6,451	0,013	6,614	0,003	-0,164	0,164	1,120
mmu-miR-183	6,767	0,025	6,930	0,026	-0,163	0,163	1,119
mmu-miR-182	6,795	0,058	6,957	0,087	-0,162	0,162	1,119
mmu-miR-34b-5p	6,340	0,320	6,502	0,029	-0,162	0,162	1,119
hsa-miR-566	6,605	0,064	6,766	0,310	-0,160	0,160	1,117
hsa-miR-583	7,121	0,238	7,279	0,115	-0,158	0,158	1,116
spike_control_f	9,012	0,117	9,170	0,127	-0,158	0,158	1,116
mmu-miR-365	7,267	0,012	7,424	0,005	-0,157	0,157	1,115
mmu-miR-129-5p	7,343	0,046	7,498	0,038	-0,155	0,155	1,113
spike_control_f	9,006	0,036	9,160	0,104	-0,154	0,154	1,113
hsa-miR-515-5p	6,624	0,220	6,777	0,270	-0,154	0,154	1,112
spike_control_f	9,019	0,077	9,171	0,102	-0,153	0,153	1,112
mmu-miR-199a-5p	7,996	0,063	8,144	0,098	-0,148	0,148	1,108
spike_control_e	11,175	0,162	11,322	0,132	-0,147	0,147	1,107
miRPlus_28232	6,982	0,027	7,129	0,032	-0,147	0,147	1,107
hsa-miR-559	6,475	0,083	6,621	0,022	-0,147	0,147	1,107
mmu-miR-543	6,643	0,426	6,790	0,413	-0,147	0,147	1,107
mmu-miR-130b	7,621	0,119	7,767	0,092	-0,146	0,146	1,106
spike_control_e	11,176	0,038	11,321	0,097	-0,145	0,145	1,106
mmu-miR-693-5p	6,664	0,071	6,808	0,272	-0,144	0,144	1,105
rno-miR-376a	6,418	0,380	6,562	0,115	-0,144	0,144	1,105
mmu-miR-708	6,750	0,189	6,893	0,148	-0,144	0,144	1,105
miRPlus_17900	6,778	0,275	6,920	0,032	-0,142	0,142	1,103
hsa-miR-887	6,615	0,421	6,755	0,050	-0,140	0,140	1,102
miRPlus_17941	6,837	0,411	6,976	0,666	-0,139	0,139	1,101
hsa-miR-151-3p	6,944	0,313	7,076	0,048	-0,132	0,132	1,096
mmu-miR-700	6,864	0,030	6,994	0,084	-0,130	0,130	1,094

mmu-miR-291b-5p	6,517	0,067	6,645	0,131	-0,129	0,129	1,093
mmu-miR-431	6,696	0,065	6,824	0,401	-0,128	0,128	1,093
spike_control_e	11,163	0,103	11,291	0,062	-0,128	0,128	1,093
hsa-miR-525-3p	6,468	0,105	6,596	0,048	-0,127	0,127	1,092
hsa-miR-518f*	6,847	0,512	6,974	0,271	-0,127	0,127	1,092
miRPlus_17930	6,669	0,314	6,795	0,272	-0,126	0,126	1,091
spike_control_e	11,276	0,049	11,400	0,080	-0,124	0,124	1,090
mmu-miR-298	8,269	0,074	8,393	0,019	-0,124	0,124	1,090
mmu-miR-741	6,382	0,504	6,506	0,090	-0,124	0,124	1,089
miRPlus_30317	6,435	0,065	6,557	0,039	-0,123	0,123	1,089
hsa_negative_control_2	6,919	0,049	7,041	0,769	-0,122	0,122	1,088
spike_control_e	11,153	0,057	11,274	0,036	-0,121	0,121	1,088
hsa-miR-193b	7,381	0,085	7,501	0,056	-0,120	0,120	1,087
mmu-miR-760	6,808	0,041	6,927	0,007	-0,119	0,119	1,086
mmu-miR-29b	7,070	0,238	7,188	0,052	-0,118	0,118	1,085
mmu-miR-551b	7,247	0,191	7,363	0,075	-0,116	0,116	1,084
miRPlus_17653	6,692	0,170	6,807	0,425	-0,116	0,116	1,084
mmu-miR-183*	6,602	0,065	6,713	0,017	-0,110	0,110	1,080
mmu-miR-873	7,002	0,119	7,111	0,154	-0,109	0,109	1,078
mmu-miR-141	6,720	0,166	6,829	0,416	-0,108	0,108	1,078
hsa-miR-621	6,483	0,048	6,590	0,027	-0,108	0,108	1,077
hsa-miR-373*	6,647	0,051	6,752	0,225	-0,105	0,105	1,075
hsa-miR-193a-5p	7,444	0,065	7,547	0,024	-0,103	0,103	1,074
hsa-miR-455-3p	6,652	0,040	6,754	0,059	-0,102	0,102	1,074
hsa-miR-629*	6,725	0,037	6,826	0,035	-0,101	0,101	1,072
mmu-miR-215	6,465	0,060	6,564	0,019	-0,099	0,099	1,071
spike_control_f	8,933	0,054	9,029	0,043	-0,097	0,097	1,069
hsa-miR-215	6,576	0,258	6,672	0,128	-0,096	0,096	1,069
mmu-miR-195	6,930	0,066	7,021	0,043	-0,091	0,091	1,065
miRPlus_17945	6,797	0,053	6,886	0,037	-0,089	0,089	1,064
mmu-miR-181a	6,952	0,283	7,041	0,071	-0,089	0,089	1,064
miRPlus_17951	6,470	0,028	6,556	0,030	-0,086	0,086	1,061
rno-miR-382*	6,558	0,057	6,640	0,018	-0,082	0,082	1,058
miRPlus_30908	6,542	0,026	6,622	0,014	-0,080	0,080	1,057
mmu-miR-381	6,612	0,029	6,692	0,020	-0,080	0,080	1,057
spike_control_f	8,938	0,057	9,017	0,060	-0,079	0,079	1,057
mmu-miR-151-5p	6,870	0,049	6,950	0,035	-0,079	0,079	1,056
hsa-miR-20b*	6,773	0,402	6,851	0,090	-0,078	0,078	1,056
mmu-miR-697	6,670	0,430	6,745	0,262	-0,075	0,075	1,054
miRPlus_17865	7,095	0,254	7,170	0,053	-0,075	0,075	1,053
hsa-miR-499-3p	6,509	0,552	6,584	0,170	-0,075	0,075	1,053
spike_control_f	8,993	0,041	9,068	0,046	-0,075	0,075	1,053
No known hsa target	6,539	0,052	6,613	0,029	-0,074	0,074	1,053
hsa-miR-384	6,498	0,244	6,569	0,059	-0,071	0,071	1,051
rno-miR-542-5p	7,501	0,072	7,572	0,034	-0,071	0,071	1,050
hsa-miR-519e*	6,849	0,412	6,916	0,130	-0,067	0,067	1,048
mmu-miR-214	7,654	0,120	7,719	0,128	-0,066	0,066	1,046
mmu-miR-184	6,924	0,125	6,989	0,142	-0,065	0,065	1,046
mmu-miR-691	6,871	0,052	6,935	0,042	-0,064	0,064	1,046
hsa-miR-647	6,429	0,460	6,491	0,041	-0,062	0,062	1,044
mmu-miR-20b*	6,817	0,402	6,879	0,544	-0,062	0,062	1,044
mmu-miR-202-3p	6,803	0,126	6,864	0,452	-0,061	0,061	1,043
mmu-miR-362-5p	6,776	0,028	6,837	0,019	-0,061	0,061	1,043
hsa-miR-520g	6,737	0,068	6,795	0,362	-0,058	0,058	1,041
mmu-miR-804	6,710	0,259	6,766	0,351	-0,056	0,056	1,040
hsa-miR-589*	6,526	0,034	6,582	0,026	-0,055	0,055	1,039
miRPlus_28534	6,453	0,023	6,507	0,040	-0,055	0,055	1,039

mmu-miR-675-3p	6,517	0,052	6,570	0,046	-0,053	0,053	1,037
hsa-miR-640	6,533	0,017	6,585	0,036	-0,052	0,052	1,037
mmu-miR-429	6,550	0,025	6,600	0,030	-0,050	0,050	1,035
hsa-miR-487a	6,562	0,021	6,612	0,041	-0,049	0,049	1,035
rno-miR-101a_MM1	6,781	0,314	6,826	0,355	-0,044	0,044	1,031
hsa-miR-199a-3p/199b-3p	6,982	0,026	7,026	0,036	-0,044	0,044	1,031
hsa-miR-574-5p	7,470	0,097	7,514	0,136	-0,043	0,043	1,030
mmu-miR-125b-3p	6,714	0,288	6,755	0,203	-0,041	0,041	1,029
hsa-miR-610	6,688	0,599	6,727	0,202	-0,040	0,040	1,028
hsa-miR-493	6,542	0,037	6,579	0,028	-0,037	0,037	1,026
miRPlus_17956	6,666	0,381	6,702	0,064	-0,036	0,036	1,025
hsa-miR-185*	7,110	0,199	7,146	0,173	-0,036	0,036	1,025
mmu-miR-673-5p	6,432	0,398	6,467	0,088	-0,035	0,035	1,024
hsa-miR-222*	6,596	0,047	6,628	0,243	-0,033	0,033	1,023
miRPlus_32832	6,538	0,112	6,570	0,061	-0,032	0,032	1,023
mmu-miR-369-5p	6,581	0,059	6,612	0,033	-0,031	0,031	1,022
mmu-miR-376c	6,641	0,022	6,671	0,025	-0,030	0,030	1,021
mmu-miR-153	6,538	0,040	6,568	0,016	-0,030	0,030	1,021
hsa-miR-105	6,807	0,023	6,829	0,025	-0,022	0,022	1,015
hsa-miR-19b-1*	6,584	0,049	6,605	0,012	-0,021	0,021	1,014
hsa-miR-576-3p	6,571	0,043	6,592	0,013	-0,021	0,021	1,014
hsa-miR-891a	6,811	0,079	6,829	0,044	-0,018	0,018	1,013
mmu-miR-181b	7,753	0,070	7,770	0,048	-0,018	0,018	1,012
hsa-miR-192	6,666	0,016	6,682	0,015	-0,016	0,016	1,011
miRPlus_17861	7,572	0,063	7,588	0,028	-0,016	0,016	1,011
hsa-miR-541*	6,533	0,056	6,549	0,022	-0,015	0,015	1,011
mmu-miR-713	6,609	0,045	6,624	0,019	-0,015	0,015	1,011
mmu-miR-500	6,818	0,019	6,831	0,023	-0,013	0,013	1,009
hsa-miR-217	6,568	0,021	6,580	0,010	-0,013	0,013	1,009
hsa-miR-638	6,898	0,123	6,910	0,010	-0,012	0,012	1,008
mmu-miR-99b*	6,775	0,055	6,787	0,035	-0,012	0,012	1,008
hsa-miR-302c*	7,006	0,327	7,018	0,038	-0,011	0,011	1,008
mmu-miR-126-3p	6,979	0,041	6,988	0,015	-0,010	0,010	1,007
mmu-miR-425*	6,597	0,434	6,604	0,047	-0,007	0,007	1,005
hsa-miR-675	6,613	0,016	6,619	0,023	-0,006	0,006	1,004
mmu-miR-196a	7,451	0,237	7,457	0,072	-0,006	0,006	1,004
hsa-miR-519b-3p	6,609	0,494	6,613	0,206	-0,004	0,004	1,003
mmu-miR-490	6,604	0,067	6,608	0,031	-0,004	0,004	1,002
mmu-miR-743a	6,591	0,060	6,595	0,014	-0,003	0,003	1,002
mmu-let-7f	7,030	0,028	7,030	0,016	0,000	0,000	1,000
mmu-miR-496	6,607	0,068	6,606	0,011	0,001	-0,001	0,999
hsa_SNORD13	7,235	0,171	7,233	0,059	0,003	-0,003	0,998
hsa-miR-544	6,584	0,021	6,581	0,014	0,003	-0,003	0,998
mmu-miR-495	6,521	0,458	6,517	0,042	0,004	-0,004	0,997
hsa-miR-526b	6,720	0,202	6,716	0,039	0,004	-0,004	0,997
rno-miR-336	6,714	0,434	6,708	0,012	0,006	-0,006	0,996
mmu-miR-714	6,695	0,048	6,690	0,011	0,006	-0,006	0,996
mmu-miR-704	6,624	0,064	6,618	0,018	0,006	-0,006	0,996
hsa_SNORD4A	7,295	0,066	7,289	0,046	0,006	-0,006	0,996
hsa-miR-599	6,617	0,021	6,610	0,010	0,007	-0,007	0,995
mmu-miR-146b	6,871	0,023	6,864	0,013	0,007	-0,007	0,995
mmu-miR-699	6,536	0,075	6,528	0,017	0,008	-0,008	0,995
hsa-miR-518c*	7,275	0,034	7,266	0,037	0,009	-0,009	0,994
hsa-miR-550*	6,687	0,029	6,675	0,033	0,012	-0,012	0,992
mmu-miR-763	7,006	0,216	6,994	0,734	0,012	-0,012	0,992
hsa-miR-662	6,561	0,476	6,546	0,122	0,015	-0,015	0,990
hsa-miR-876-5p	6,764	0,330	6,746	0,317	0,018	-0,018	0,988

miRPlus_17847	6,766	0,209	6,747	0,229	0,018	-0,018	0,987
hsa-miR-325	6,760	0,352	6,741	0,242	0,020	-0,020	0,987
mmu-miR-421	6,918	0,041	6,898	0,031	0,020	-0,020	0,986
miRPlus_32953	6,731	0,060	6,710	0,029	0,021	-0,021	0,986
mmu-miR-295	6,622	0,379	6,601	0,092	0,021	-0,021	0,985
mmu-miR-764-5p	6,651	0,083	6,630	0,020	0,022	-0,022	0,985
hsa_SNORD15A	8,056	2,194	8,034	2,800	0,022	-0,022	0,985
hsa-miR-564	6,635	0,058	6,613	0,059	0,023	-0,023	0,984
mmu-miR-221	7,303	0,037	7,279	0,035	0,023	-0,023	0,984
mmu-miR-379	6,781	0,144	6,757	0,307	0,024	-0,024	0,984
mmu-miR-455*	6,900	0,274	6,875	0,061	0,025	-0,025	0,983
hsa-miR-617	6,746	0,016	6,721	0,024	0,025	-0,025	0,983
miRPlus_17841	6,610	0,063	6,584	0,016	0,026	-0,026	0,982
hsa-miR-517*	6,595	0,470	6,567	0,151	0,028	-0,028	0,981
hsa-miR-619	6,660	0,461	6,629	0,280	0,031	-0,031	0,979
mmu-miR-142-5p	6,670	0,070	6,638	0,029	0,033	-0,033	0,978
mmu-miR-144	6,644	0,065	6,611	0,015	0,033	-0,033	0,977
mmu-miR-718	6,678	0,038	6,644	0,028	0,034	-0,034	0,977
hsa-miR-302d	6,709	0,420	6,673	0,254	0,036	-0,036	0,975
hsa-miR-16-1*	6,661	0,016	6,625	0,007	0,036	-0,036	0,975
hsa-miR-516b	6,775	0,027	6,738	0,024	0,036	-0,036	0,975
hsa-miR-641	6,623	0,014	6,585	0,019	0,038	-0,038	0,974
mmu-miR-148a*	6,591	0,042	6,553	0,026	0,038	-0,038	0,974
mmu-miR-194	6,642	0,023	6,603	0,034	0,039	-0,039	0,973
mmu-miR-208	6,819	0,045	6,778	0,021	0,041	-0,041	0,972
mmu-miR-9	7,447	0,044	7,405	0,036	0,041	-0,041	0,972
hsa-miR-628-3p	6,821	0,229	6,778	0,054	0,043	-0,043	0,971
mmu-miR-448	6,749	0,043	6,705	0,210	0,044	-0,044	0,970
mmu-miR-409-3p	6,647	0,023	6,602	0,025	0,044	-0,044	0,970
No known hsa target	6,668	0,050	6,621	0,008	0,047	-0,047	0,968
mmu-miR-670	6,672	0,037	6,624	0,016	0,048	-0,048	0,967
miRPlus_17868	6,624	0,039	6,575	0,020	0,049	-0,049	0,966
mmu-miR-486	6,751	0,028	6,701	0,013	0,050	-0,050	0,966
hsa-let-7e*	6,626	0,063	6,576	0,041	0,051	-0,051	0,965
hsa-miR-542-3p	6,750	0,062	6,697	0,035	0,053	-0,053	0,964
hsa-miR-337-5p	6,589	0,505	6,536	0,123	0,053	-0,053	0,964
mmu-miR-380-5p	6,604	0,063	6,551	0,037	0,053	-0,053	0,964
mmu-miR-190	7,034	0,108	6,980	0,083	0,053	-0,053	0,964
mmu-miR-875-5p	6,659	0,054	6,605	0,022	0,054	-0,054	0,964
hsa-miR-489	6,646	0,079	6,592	0,057	0,054	-0,054	0,963
hsa-miR-649	6,663	0,029	6,608	0,016	0,055	-0,055	0,963
mmu-miR-423-3p	6,670	0,034	6,614	0,019	0,056	-0,056	0,962
miRPlus_31515	6,623	0,034	6,567	0,008	0,056	-0,056	0,962
hsa-miR-181a-2*	6,782	0,019	6,726	0,022	0,056	-0,056	0,962
hsa-miR-525-5p	7,033	0,018	6,975	0,023	0,058	-0,058	0,961
hsa-miR-768-5p	7,781	0,214	7,721	0,085	0,059	-0,059	0,960
mmu-miR-331-5p	6,620	0,045	6,560	0,041	0,060	-0,060	0,960
hsa-miR-607	6,650	0,025	6,591	0,008	0,060	-0,060	0,960
hsa-miR-657	6,692	0,071	6,632	0,013	0,060	-0,060	0,959
mmu-miR-742	6,728	0,056	6,668	0,023	0,060	-0,060	0,959
hsa-miR-552	6,686	0,057	6,624	0,015	0,061	-0,061	0,958
mmu-miR-137	6,811	0,024	6,747	0,238	0,064	-0,064	0,957
mmu-miR-540-3p	6,810	0,351	6,746	0,251	0,064	-0,064	0,957
hsa-miR-885-5p	6,798	0,059	6,733	0,033	0,065	-0,065	0,956
hsa-miR-33b*	6,678	0,135	6,613	0,027	0,065	-0,065	0,956
mmu-miR-568	6,592	0,046	6,524	0,065	0,068	-0,068	0,954
hsa-miR-299-3p	6,692	0,029	6,624	0,008	0,068	-0,068	0,954

mmu-miR-139-5p	6,575	0,428	6,505	0,056	0,069	-0,069	0,953
hsa-miR-500	7,138	0,053	7,069	0,006	0,069	-0,069	0,953
mmu-miR-10a	7,222	0,074	7,153	0,045	0,070	-0,070	0,953
mmu-miR-7a	7,218	0,076	7,148	0,065	0,070	-0,070	0,953
rno-miR-346	6,642	0,034	6,570	0,015	0,072	-0,072	0,952
mmu-miR-1	6,862	0,041	6,790	0,073	0,072	-0,072	0,951
hsa-miR-614	6,637	0,119	6,564	0,013	0,072	-0,072	0,951
mmu-miR-384-3p	6,795	0,633	6,722	0,264	0,073	-0,073	0,950
hsa-miR-554	6,691	0,024	6,616	0,018	0,076	-0,076	0,949
mmu-miR-24-1*/24-2*	6,832	0,055	6,757	0,038	0,076	-0,076	0,949
hsa-miR-624	6,668	0,056	6,592	0,023	0,076	-0,076	0,949
mmu-miR-324-5p	7,127	0,022	7,051	0,022	0,076	-0,076	0,949
miRPlus_17932	6,991	0,070	6,915	0,500	0,076	-0,076	0,949
hsa-miR-645	6,706	0,025	6,629	0,019	0,077	-0,077	0,948
hsa_SNORD11B	7,527	0,055	7,450	0,075	0,077	-0,077	0,948
hsa-miR-577	6,611	0,073	6,533	0,056	0,077	-0,077	0,948
hsa-miR-604	6,671	0,016	6,593	0,031	0,077	-0,077	0,948
mmu-miR-196b	7,127	0,033	7,049	0,016	0,078	-0,078	0,948
mmu-miR-127	6,931	0,092	6,850	0,033	0,080	-0,080	0,946
rno-miR-489	6,629	0,080	6,549	0,014	0,080	-0,080	0,946
hsa-miR-758	6,786	0,025	6,704	0,379	0,081	-0,081	0,945
hsa-miR-549	6,656	0,056	6,574	0,020	0,082	-0,082	0,945
mmu-miR-148b	7,362	0,041	7,279	0,037	0,082	-0,082	0,945
miRPlus_28993	6,990	0,023	6,907	0,028	0,083	-0,083	0,944
hsa-miR-412	6,667	0,048	6,583	0,019	0,084	-0,084	0,944
hsa-miR-17*	6,911	0,039	6,828	0,043	0,084	-0,084	0,944
miRPlus_17820	6,585	0,432	6,500	0,089	0,084	-0,084	0,943
hsa-miR-582-3p	6,630	0,041	6,544	0,030	0,085	-0,085	0,943
mmu-miR-688	6,929	0,023	6,843	0,024	0,086	-0,086	0,942
mmu-miR-488*	6,695	0,072	6,609	0,023	0,086	-0,086	0,942
hsa-miR-596	6,659	0,091	6,573	0,039	0,087	-0,087	0,942
mmu-miR-188-3p	6,655	0,030	6,567	0,022	0,088	-0,088	0,941
mmu-miR-31	7,012	0,011	6,924	0,070	0,088	-0,088	0,941
hsa-miR-769-5p	6,786	0,035	6,696	0,012	0,089	-0,089	0,940
rno-miR-1	6,861	0,129	6,771	0,309	0,090	-0,090	0,940
hsa-miR-490-5p	6,708	0,032	6,618	0,023	0,090	-0,090	0,939
hsa-miR-454*	6,751	0,089	6,660	0,026	0,091	-0,091	0,939
hsa-miR-661	6,788	0,131	6,695	0,141	0,093	-0,093	0,938
hsa-miR-520g/520h	6,698	0,330	6,605	0,051	0,093	-0,093	0,937
hsa-miR-637	6,794	0,029	6,700	0,021	0,094	-0,094	0,937
hsa-miR-376c	6,590	0,413	6,496	0,060	0,094	-0,094	0,937
hsa-miR-452	7,296	0,391	7,201	0,052	0,095	-0,095	0,936
miRPlus_11239	6,709	0,069	6,613	0,032	0,096	-0,096	0,935
miRPlus_17880	6,893	0,139	6,796	0,335	0,097	-0,097	0,935
hsa-miR-432*	6,684	0,014	6,586	0,033	0,098	-0,098	0,934
mmu-miR-186	7,679	0,213	7,581	0,040	0,098	-0,098	0,934
hsa-miR-297	6,743	0,028	6,645	0,026	0,099	-0,099	0,934
hsa-miR-562	6,702	0,040	6,604	0,018	0,099	-0,099	0,934
hsa-miR-767-5p	6,770	0,011	6,671	0,012	0,099	-0,099	0,933
mmu-miR-203	6,876	0,055	6,776	0,028	0,099	-0,099	0,933
hsa-miR-654-5p	6,718	0,060	6,618	0,017	0,099	-0,099	0,933
hsa-miR-521	6,650	0,037	6,550	0,026	0,100	-0,100	0,933
miRPlus_28790	6,606	0,392	6,505	0,020	0,101	-0,101	0,933
hsa-miR-606	6,617	0,080	6,516	0,043	0,101	-0,101	0,932
hsa-miR-556-5p	6,710	0,090	6,608	0,036	0,102	-0,102	0,932
miRPlus_27560	7,005	0,047	6,904	0,038	0,102	-0,102	0,932
rno-miR-664	6,915	0,061	6,810	0,032	0,104	-0,104	0,930

mmu-miR-464	6,686	0,056	6,581	0,022	0,105	-0,105	0,930
mmu-miR-132	6,782	0,123	6,677	0,045	0,105	-0,105	0,930
mmu-miR-154*	6,676	0,404	6,570	0,104	0,106	-0,106	0,929
mmu-miR-146a	6,661	0,060	6,554	0,017	0,107	-0,107	0,929
hsa-miR-198	6,910	0,025	6,802	0,109	0,108	-0,108	0,928
hsa-miR-192*	6,688	0,052	6,579	0,013	0,109	-0,109	0,927
mmu-miR-671-3p	6,702	0,043	6,592	0,040	0,111	-0,111	0,926
mmu-miR-152	7,083	0,045	6,972	0,014	0,111	-0,111	0,926
miRPlus_17955	6,689	0,045	6,578	0,036	0,111	-0,111	0,926
mmu-miR-491	6,779	0,018	6,668	0,040	0,111	-0,111	0,926
mmu-miR-539	6,883	0,279	6,770	0,252	0,114	-0,114	0,924
hsa-miR-345	6,866	0,021	6,752	0,010	0,114	-0,114	0,924
hsa-miR-422a	6,732	0,272	6,616	0,084	0,116	-0,116	0,923
hsa-miR-133a/133b	6,830	0,016	6,714	0,051	0,116	-0,116	0,923
miRPlus_17840	6,855	0,041	6,738	0,098	0,116	-0,116	0,923
hsa-miR-453	6,750	0,057	6,633	0,023	0,117	-0,117	0,922
hsa-miR-593*	6,708	0,063	6,590	0,033	0,117	-0,117	0,922
mmu-let-7i*	6,717	0,031	6,599	0,017	0,117	-0,117	0,922
hsa-miR-585	6,843	0,023	6,726	0,013	0,117	-0,117	0,922
hsa-miR-518e*/519a*/519b-5p/519c-5p/522*/523*	6,887	0,051	6,767	0,021	0,120	-0,120	0,920
mmu-let-7e	7,017	0,017	6,896	0,065	0,120	-0,120	0,920
hsa-miR-600	6,731	0,064	6,610	0,029	0,121	-0,121	0,919
hsa-miR-376a	6,719	0,036	6,598	0,021	0,122	-0,122	0,919
miRPlus_17933	6,779	0,024	6,656	0,035	0,122	-0,122	0,919
mmu-miR-684	6,742	0,062	6,619	0,019	0,123	-0,123	0,918
mmu-miR-197	7,177	0,058	7,053	0,031	0,124	-0,124	0,918
mmu-miR-676*	6,699	0,040	6,574	0,064	0,125	-0,125	0,917
miRPlus_17824	6,708	0,027	6,582	0,016	0,125	-0,125	0,917
hsa-miR-934	7,063	0,193	6,937	0,076	0,126	-0,126	0,916
mmu-miR-29c	6,843	0,045	6,715	0,023	0,128	-0,128	0,915
hsa-miR-567	6,595	0,331	6,467	0,105	0,128	-0,128	0,915
hsa-miR-515-3p	6,775	0,115	6,647	0,074	0,128	-0,128	0,915
mmu-miR-409-5p	6,735	0,028	6,606	0,020	0,129	-0,129	0,914
mmu-miR-712*	6,812	0,036	6,682	0,005	0,130	-0,130	0,914
hsa-miR-597	6,779	0,163	6,648	0,050	0,131	-0,131	0,913
hsa_negative_control_8	6,668	0,023	6,537	0,021	0,131	-0,131	0,913
hsa-miR-520b/520c-3p	6,744	0,023	6,612	0,018	0,132	-0,132	0,913
mmu-miR-377	6,705	0,047	6,573	0,019	0,132	-0,132	0,913
hsa-miR-613	6,758	0,122	6,626	0,038	0,132	-0,132	0,912
mmu-miR-28	6,935	0,136	6,801	0,233	0,134	-0,134	0,911
mmu-miR-378*	6,762	0,021	6,628	0,035	0,134	-0,134	0,911
hsa-miR-565	6,935	0,017	6,801	0,019	0,135	-0,135	0,911
hsa-miR-182*	6,669	0,040	6,532	0,020	0,136	-0,136	0,910
hsa-miR-555	6,631	0,084	6,494	0,044	0,136	-0,136	0,910
miRPlus_17860	6,749	0,088	6,612	0,107	0,137	-0,137	0,909
mmu-miR-99a	6,849	0,033	6,711	0,019	0,138	-0,138	0,909
miRPlus_17899	6,861	0,054	6,718	0,016	0,143	-0,143	0,905
mmu-miR-33	7,026	0,063	6,883	0,371	0,143	-0,143	0,905
mmu-miR-687	6,702	0,047	6,559	0,021	0,143	-0,143	0,905
mmu-miR-501-5p	6,809	0,033	6,665	0,058	0,144	-0,144	0,905
rno-miR-369-3p	6,708	0,031	6,564	0,029	0,144	-0,144	0,905
mmu-miR-674	6,828	0,038	6,684	0,106	0,144	-0,144	0,905
mmu-let-7g	6,843	0,019	6,699	0,014	0,144	-0,144	0,905
mmu-miR-710	7,236	0,069	7,091	0,040	0,145	-0,145	0,905
hsa-miR-519c-5p_MM1	6,855	0,034	6,710	0,020	0,145	-0,145	0,904
hsa-miR-346	6,875	0,027	6,728	0,027	0,147	-0,147	0,903
rno-miR-337	6,996	0,197	6,849	0,316	0,148	-0,148	0,903

mmu-miR-346	6,862	0,253	6,714	0,224	0,148	-0,148	0,903
hsa-miR-769-3p	6,955	0,060	6,807	0,093	0,148	-0,148	0,903
hsa-miR-524-3p	6,770	0,032	6,621	0,012	0,149	-0,149	0,902
mmu-miR-671-5p	6,814	0,063	6,664	0,055	0,150	-0,150	0,901
hsa-miR-569	6,770	0,032	6,619	0,019	0,151	-0,151	0,900
mmu-miR-434-3p	6,815	0,052	6,661	0,133	0,154	-0,154	0,899
mmu-miR-200c	6,788	0,025	6,633	0,012	0,155	-0,155	0,898
hsa-miR-302c	6,759	0,023	6,604	0,037	0,155	-0,155	0,898
mmu-miR-223	6,921	0,042	6,765	0,044	0,156	-0,156	0,898
rno-miR-369-5p	6,632	0,286	6,476	0,065	0,156	-0,156	0,897
mmu-miR-34a	6,809	0,102	6,653	0,041	0,156	-0,156	0,897
hsa-miR-369-5p	6,800	0,035	6,644	0,076	0,156	-0,156	0,897
hsa-miR-518a-3p	6,783	0,026	6,624	0,036	0,159	-0,159	0,895
mmu-miR-669c	6,908	0,061	6,749	0,015	0,159	-0,159	0,895
mmu-miR-695	7,075	0,295	6,915	0,483	0,160	-0,160	0,895
mmu-miR-193b	6,855	0,031	6,693	0,041	0,162	-0,162	0,894
hsa-miR-636	6,798	0,018	6,636	0,036	0,162	-0,162	0,894
mmu-miR-759	6,737	0,033	6,573	0,008	0,164	-0,164	0,892
mmu-miR-532-5p	7,169	0,036	7,003	0,033	0,166	-0,166	0,891
mmu-miR-145*	6,684	0,040	6,518	0,027	0,166	-0,166	0,891
mmu-miR-298	6,723	0,062	6,557	0,045	0,166	-0,166	0,891
rno-miR-20a*	6,774	0,034	6,607	0,017	0,167	-0,167	0,891
hsa-miR-34b*	6,778	0,056	6,610	0,153	0,167	-0,167	0,890
mmu-miR-149	6,808	0,051	6,638	0,011	0,170	-0,170	0,889
rno-miR-142-5p	6,752	0,026	6,582	0,041	0,171	-0,171	0,888
mmu-miR-678	6,840	0,023	6,669	0,036	0,171	-0,171	0,888
hsa-miR-512-3p	6,768	0,033	6,596	0,009	0,173	-0,173	0,887
mmu-miR-487b	7,235	0,049	7,062	0,082	0,173	-0,173	0,887
miRPlus_28535	6,933	0,054	6,759	0,023	0,173	-0,173	0,887
mmu-miR-433	6,790	0,039	6,617	0,053	0,174	-0,174	0,887
hsa-miR-660	7,033	0,053	6,859	0,087	0,174	-0,174	0,886
miRPlus_32902	6,880	0,030	6,705	0,057	0,174	-0,174	0,886
mmu-miR-34c	6,901	0,057	6,725	0,029	0,176	-0,176	0,885
No known hsa target	7,212	0,022	7,036	0,038	0,176	-0,176	0,885
hsa-miR-506	6,773	0,260	6,596	0,095	0,177	-0,177	0,885
mmu-miR-669a	6,848	0,357	6,670	0,099	0,178	-0,178	0,884
hsa-miR-542-5p	6,808	0,260	6,629	0,047	0,178	-0,178	0,884
hsa-miR-519e	7,031	0,033	6,853	0,016	0,179	-0,179	0,883
rno-miR-291a-5p	6,888	0,039	6,709	0,021	0,180	-0,180	0,883
hsa-miR-558	6,792	0,093	6,612	0,032	0,181	-0,181	0,882
mmu-miR-686	6,736	0,344	6,555	0,058	0,181	-0,181	0,882
mmu-miR-693-3p	6,814	0,036	6,633	0,025	0,181	-0,181	0,882
mmu-miR-34c	6,836	0,081	6,655	0,027	0,181	-0,181	0,882
hsa-miR-518d-3p	6,753	0,302	6,570	0,065	0,183	-0,183	0,881
mmu-miR-200a	6,833	0,052	6,650	0,021	0,183	-0,183	0,881
mmu-miR-33*	6,824	0,093	6,640	0,013	0,183	-0,183	0,881
mmu-miR-376a*	6,886	0,145	6,702	0,206	0,183	-0,183	0,881
mmu-miR-877	7,412	0,062	7,228	0,054	0,183	-0,183	0,881
mmu-miR-467b	6,804	0,013	6,618	0,010	0,186	-0,186	0,879
mmu-miR-188-5p	7,049	0,146	6,863	0,431	0,186	-0,186	0,879
mmu-miR-411	6,773	0,037	6,586	0,037	0,187	-0,187	0,879
hsa-miR-329	6,816	0,027	6,626	0,020	0,191	-0,191	0,876
hsa-miR-339-3p	6,767	0,056	6,576	0,050	0,191	-0,191	0,876
hsa-miR-560	6,730	0,028	6,539	0,048	0,191	-0,191	0,876
hsa-miR-429	6,817	0,019	6,624	0,046	0,193	-0,193	0,875
mmu-miR-350	6,776	0,020	6,583	0,020	0,194	-0,194	0,874
mmu-miR-369-3p	7,013	0,504	6,817	0,302	0,195	-0,195	0,873

mmu-miR-92a	6,995	0,078	6,800	0,046	0,196	-0,196	0,873
hsa-miR-220	6,809	0,022	6,613	0,026	0,196	-0,196	0,873
hsa-miR-631	6,690	0,070	6,494	0,045	0,196	-0,196	0,873
hsa-miR-587	6,695	0,028	6,497	0,058	0,198	-0,198	0,872
hsa-miR-767-3p	6,740	0,120	6,541	0,049	0,199	-0,199	0,871
mmu-miR-451	6,713	0,042	6,513	0,120	0,200	-0,200	0,870
mmu-miR-681	6,845	0,078	6,645	0,025	0,200	-0,200	0,870
mmu-miR-217	6,831	0,022	6,630	0,010	0,201	-0,201	0,870
mmu-miR-331-3p	6,878	0,036	6,676	0,015	0,202	-0,202	0,869
hsa-miR-890	6,905	0,030	6,703	0,021	0,202	-0,202	0,869
mmu-miR-140	7,122	0,018	6,918	0,024	0,204	-0,204	0,868
hsa-miR-876-3p	6,991	0,059	6,786	0,024	0,205	-0,205	0,868
mmu-miR-425	7,162	0,067	6,956	0,056	0,206	-0,206	0,867
hsa-miR-611	6,908	0,038	6,701	0,075	0,207	-0,207	0,867
hsa-miR-891b	6,814	0,043	6,606	0,033	0,208	-0,208	0,866
hsa-miR-15a*	6,722	0,055	6,512	0,026	0,209	-0,209	0,865
mmu-miR-25	7,107	0,035	6,897	0,026	0,210	-0,210	0,864
hsa-miR-143*	6,834	0,056	6,623	0,039	0,211	-0,211	0,864
mmu-miR-205	7,131	0,514	6,920	0,352	0,211	-0,211	0,864
hsa-miR-770-5p	6,815	0,059	6,603	0,019	0,212	-0,212	0,863
mmu-miR-380-3p	6,910	0,045	6,697	0,021	0,212	-0,212	0,863
mmu-miR-465a-3p/465b-3p/465c-3p	6,868	0,078	6,656	0,023	0,213	-0,213	0,863
hsa-miR-605	6,859	0,032	6,646	0,042	0,213	-0,213	0,863
hsa-miR-548c-3p	6,843	0,044	6,630	0,022	0,213	-0,213	0,863
hsa-miR-572	6,979	0,040	6,766	0,060	0,213	-0,213	0,863
hsa-miR-766	6,996	0,061	6,782	0,028	0,214	-0,214	0,862
miRPlus_17811	6,846	0,034	6,630	0,020	0,215	-0,215	0,861
hsa-miR-644	6,803	0,075	6,587	0,014	0,216	-0,216	0,861
mmu-miR-674*	6,798	0,004	6,582	0,022	0,216	-0,216	0,861
rno-miR-421	6,829	0,048	6,612	0,013	0,217	-0,217	0,860
mmu-miR-721	6,859	0,061	6,642	0,014	0,217	-0,217	0,860
rno-miR-450a	6,949	0,315	6,732	0,041	0,217	-0,217	0,860
mmu-miR-192	6,855	0,043	6,638	0,031	0,218	-0,218	0,860
rno-miR-505	6,863	0,021	6,644	0,025	0,220	-0,220	0,859
miRPlus_32900	6,939	0,621	6,719	0,104	0,220	-0,220	0,859
hsa-miR-18b*	6,866	0,026	6,645	0,033	0,221	-0,221	0,858
miRPlus_17891	7,015	0,145	6,792	0,047	0,224	-0,224	0,856
rno-miR-148b-5p	6,858	0,059	6,634	0,020	0,224	-0,224	0,856
mmu-miR-450b-5p	6,747	0,282	6,522	0,053	0,225	-0,225	0,856
hsa-miR-551a	7,115	0,070	6,890	0,034	0,225	-0,225	0,856
mmu-miR-133a	6,834	0,149	6,609	0,010	0,225	-0,225	0,856
hsa-miR-643	6,845	0,060	6,619	0,046	0,226	-0,226	0,855
miRPlus_27869	6,943	0,059	6,716	0,020	0,227	-0,227	0,855
mmu-miR-218	7,133	0,043	6,901	0,033	0,232	-0,232	0,851
mmu-miR-705	6,977	0,211	6,744	0,066	0,233	-0,233	0,851
hsa-miR-488*	6,846	0,045	6,613	0,156	0,233	-0,233	0,851
mmu-miR-335-5p	6,855	0,115	6,621	0,004	0,234	-0,234	0,850
hsa-miR-502-5p	6,967	0,049	6,734	0,038	0,234	-0,234	0,850
No known hsa target	6,835	0,043	6,599	0,025	0,236	-0,236	0,849
mmu-miR-582-5p	6,906	0,084	6,668	0,059	0,237	-0,237	0,848
mmu-miR-504	6,832	0,022	6,594	0,034	0,238	-0,238	0,848
miRPlus_17819	6,810	0,084	6,571	0,044	0,239	-0,239	0,847
hsa-miR-595	7,283	0,088	7,043	0,877	0,239	-0,239	0,847
mmu-miR-470	6,927	0,041	6,688	0,042	0,239	-0,239	0,847
miRPlus_27839	7,026	0,016	6,786	0,047	0,240	-0,240	0,847
mmu-miR-680	6,867	0,051	6,627	0,029	0,240	-0,240	0,847

hsa-miR-655	6,735	0,037	6,490	0,027	0,244	-0,244	0,844
mmu-miR-29b*	6,927	0,021	6,682	0,039	0,246	-0,246	0,843
hsa-miR-646	6,876	0,061	6,628	0,014	0,248	-0,248	0,842
hsa-miR-100*	6,899	0,041	6,651	0,023	0,248	-0,248	0,842
hsa-miR-34a*	6,764	0,081	6,516	0,067	0,248	-0,248	0,842
mmu-miR-150	7,063	0,078	6,814	0,032	0,248	-0,248	0,842
mmu-miR-329	7,055	0,037	6,806	0,021	0,249	-0,249	0,842
hsa-miR-650	6,873	0,131	6,623	0,045	0,250	-0,250	0,841
mmu-miR-293	6,858	0,041	6,606	0,013	0,252	-0,252	0,840
miRPlus_17926	6,788	0,024	6,536	0,050	0,252	-0,252	0,839
mmu-miR-374*	6,884	0,100	6,629	0,027	0,255	-0,255	0,838
mmu-miR-96	7,302	0,165	7,047	0,081	0,255	-0,255	0,838
mmu-miR-216a	6,815	0,090	6,560	0,023	0,255	-0,255	0,838
mmu-miR-345-5p	6,912	0,240	6,656	0,052	0,256	-0,256	0,837
hsa_negative_control_1	6,890	0,025	6,634	0,031	0,256	-0,256	0,837
hsa-miR-372	6,832	0,106	6,576	0,044	0,256	-0,256	0,837
miRPlus_17925	6,874	0,046	6,616	0,011	0,258	-0,258	0,836
hsa-miR-553	6,959	0,069	6,701	0,029	0,258	-0,258	0,836
mmu-miR-148a	6,773	0,060	6,515	0,040	0,258	-0,258	0,836
mmu-miR-758	6,894	0,037	6,635	0,002	0,259	-0,259	0,836
hsa-let-7f-2*	6,824	0,344	6,565	0,124	0,259	-0,259	0,835
hsa-miR-563	6,830	0,056	6,570	0,039	0,260	-0,260	0,835
rno-miR-333	6,886	0,025	6,625	0,016	0,261	-0,261	0,835
mmu-miR-124	6,925	0,250	6,663	0,057	0,262	-0,262	0,834
hsa-miR-629	6,982	0,037	6,718	0,018	0,264	-0,264	0,833
hsa-miR-30d*	6,890	0,065	6,625	0,030	0,265	-0,265	0,832
mmu-miR-712	6,979	0,097	6,713	0,014	0,265	-0,265	0,832
hsa-miR-518c	6,855	0,299	6,590	0,034	0,266	-0,266	0,832
hsa-miR-520a-3p	6,829	0,032	6,561	0,028	0,268	-0,268	0,831
mmu-miR-199b*	7,126	0,035	6,858	0,034	0,268	-0,268	0,830
hsa-miR-374a	6,977	0,058	6,709	0,031	0,269	-0,269	0,830
mmu-miR-497	6,928	0,048	6,659	0,041	0,269	-0,269	0,830
miRPlus_17827	7,055	0,035	6,785	0,007	0,270	-0,270	0,830
mmu-miR-652	6,829	0,047	6,559	0,021	0,270	-0,270	0,829
hsa_negative_control_6	6,933	0,095	6,662	0,027	0,271	-0,271	0,829
mmu-miR-325*	6,869	0,310	6,599	0,037	0,271	-0,271	0,829
hsa-miR-520a-5p	6,905	0,017	6,633	0,052	0,272	-0,272	0,828
miRPlus_17957	6,877	0,290	6,604	0,058	0,273	-0,273	0,827
hsa-miR-505	7,212	0,042	6,938	0,043	0,274	-0,274	0,827
hsa-miR-380	6,829	0,068	6,554	0,053	0,275	-0,275	0,826
hsa-miR-586	6,898	0,037	6,622	0,016	0,276	-0,276	0,826
hsa-miR-601	7,001	0,028	6,722	0,034	0,278	-0,278	0,825
mmu-miR-7a*	6,878	0,122	6,599	0,043	0,279	-0,279	0,824
mmu-miR-126-5p	6,922	0,036	6,642	0,051	0,280	-0,280	0,824
mmu-miR-216b	6,916	0,035	6,635	0,038	0,281	-0,281	0,823
mmu-miR-707	6,858	0,025	6,577	0,018	0,281	-0,281	0,823
hsa-miR-301b	7,305	0,065	7,023	0,046	0,283	-0,283	0,822
mmu-miR-764-3p	6,932	0,046	6,649	0,040	0,283	-0,283	0,822
mmu-miR-130b*	6,843	0,100	6,560	0,045	0,283	-0,283	0,822
hsa-miR-633	6,934	0,062	6,651	0,031	0,283	-0,283	0,822
hsa-miR-598	7,134	0,118	6,850	0,359	0,285	-0,285	0,821
mmu-miR-615-3p	7,083	0,036	6,798	0,024	0,285	-0,285	0,821
rno-miR-344-3p	6,913	0,051	6,627	0,034	0,287	-0,287	0,820
hsa-miR-523	6,915	0,053	6,628	0,024	0,287	-0,287	0,820
mmu-miR-698	7,361	0,043	7,073	0,651	0,287	-0,287	0,819
mmu-miR-200b	6,873	0,069	6,584	0,013	0,290	-0,290	0,818
mmu-miR-682	6,789	0,017	6,498	0,042	0,291	-0,291	0,818

mmu-miR-382	6,971	0,040	6,680	0,016	0,291	-0,291	0,817
hsa-miR-642	7,490	0,357	7,199	0,106	0,291	-0,291	0,817
hsa-miR-548d-3p	6,974	0,071	6,683	0,025	0,292	-0,292	0,817
hsa-miR-588	6,877	0,031	6,584	0,016	0,292	-0,292	0,817
hsa-miR-634	7,122	0,067	6,828	0,178	0,294	-0,294	0,815
mmu-miR-18a*	6,931	0,051	6,635	0,013	0,296	-0,296	0,814
mmu-let-7g*	6,908	0,014	6,612	0,011	0,296	-0,296	0,814
hsa-miR-28-3p	6,842	0,059	6,546	0,026	0,297	-0,297	0,814
mmu-miR-30e*	7,223	0,034	6,925	0,025	0,298	-0,298	0,813
mmu-miR-200b*	7,041	0,051	6,741	0,037	0,300	-0,300	0,812
hsa-miR-581	6,948	0,050	6,647	0,049	0,301	-0,301	0,812
mmu-miR-128a/128b	7,196	0,073	6,895	0,028	0,301	-0,301	0,812
hsa-miR-363*	6,915	0,040	6,614	0,008	0,301	-0,301	0,812
hsa-miR-651	6,799	0,405	6,496	0,081	0,303	-0,303	0,811
miRPlus_17897	7,026	0,039	6,719	0,027	0,307	-0,307	0,808
mmu-miR-200a*	6,951	0,048	6,644	0,139	0,307	-0,307	0,808
mmu-miR-590-3p	6,889	0,019	6,582	0,046	0,307	-0,307	0,808
hsa-miR-612	6,929	0,195	6,621	0,053	0,308	-0,308	0,808
mmu-miR-106b*	6,994	0,151	6,685	0,029	0,309	-0,309	0,807
mmu-miR-367	6,965	0,032	6,654	0,056	0,311	-0,311	0,806
hsa-miR-632	6,895	0,138	6,582	0,037	0,313	-0,313	0,805
rno-miR-292-5p	6,960	0,087	6,646	0,016	0,314	-0,314	0,804
hsa-miR-511	6,937	0,249	6,623	0,043	0,315	-0,315	0,804
hsa-miR-454	6,921	0,039	6,606	0,011	0,315	-0,315	0,804
mmu-miR-872	6,848	0,063	6,533	0,048	0,316	-0,316	0,804
mmu-miR-339-5p	6,983	0,037	6,664	0,012	0,318	-0,318	0,802
mmu-miR-133b	6,957	0,207	6,638	0,063	0,318	-0,318	0,802
mmu-miR-93*	6,986	0,060	6,668	0,017	0,319	-0,319	0,802
hsa-miR-504	6,922	0,251	6,603	0,066	0,319	-0,319	0,802
hsa-miR-362-5p	7,060	0,056	6,740	0,037	0,320	-0,320	0,801
hsa-miR-518d-5p/518f*/520c-5p/526a	7,154	0,032	6,834	0,010	0,320	-0,320	0,801
mmu-miR-434-5p	6,870	0,071	6,549	0,027	0,321	-0,321	0,801
hsa-miR-626	6,945	0,045	6,623	0,029	0,321	-0,321	0,800
mmu-miR-702	7,052	0,311	6,731	0,133	0,322	-0,322	0,800
mmu-miR-328	6,866	0,100	6,544	0,047	0,322	-0,322	0,800
miRPlus_29878	7,050	0,036	6,723	0,034	0,327	-0,327	0,797
mmu-miR-351	7,418	0,032	7,091	0,048	0,328	-0,328	0,797
mmu-miR-344	6,895	0,054	6,568	0,021	0,328	-0,328	0,797
rno-miR-1*	6,908	0,240	6,580	0,077	0,329	-0,329	0,796
mmu-miR-302b*	6,912	0,014	6,583	0,016	0,329	-0,329	0,796
mmu-miR-654-3p	6,925	0,045	6,596	0,010	0,329	-0,329	0,796
mmu-miR-297b-5p	6,954	0,073	6,624	0,018	0,329	-0,329	0,796
hsa-miR-509-3p	6,982	0,042	6,653	0,025	0,330	-0,330	0,796
mmu-miR-27a*	6,971	0,056	6,639	0,030	0,332	-0,332	0,794
mmu-miR-499	6,869	0,300	6,536	0,096	0,333	-0,333	0,794
mmu-miR-485*	6,973	0,037	6,640	0,020	0,334	-0,334	0,794
hsa-miR-516a-3p/516b*	6,928	0,119	6,594	0,016	0,334	-0,334	0,793
hsa-miR-888	6,886	0,043	6,552	0,021	0,334	-0,334	0,793
hsa-miR-886-3p	6,993	0,042	6,658	0,021	0,335	-0,335	0,793
hsa-miR-514	6,937	0,071	6,601	0,053	0,336	-0,336	0,792
mmu-miR-692	6,956	0,024	6,619	0,030	0,338	-0,338	0,791
hsa-miR-508-3p	6,962	0,061	6,624	0,039	0,338	-0,338	0,791
mmu-miR-181a-1*	7,092	0,064	6,754	0,058	0,339	-0,339	0,791
hsa-miR-493*	7,011	0,079	6,672	0,017	0,339	-0,339	0,791
rno-miR-10a-3p	6,990	0,207	6,650	0,041	0,339	-0,339	0,790
hsa-miR-491-3p	7,504	0,086	7,162	0,069	0,341	-0,341	0,789

mmu-miR-669b	6,974	0,014	6,632	0,046	0,342	-0,342	0,789
mmu-miR-708*	6,910	0,370	6,566	0,077	0,344	-0,344	0,788
hsa-miR-561	6,986	0,066	6,641	0,021	0,346	-0,346	0,787
hsa-miR-383	6,883	0,042	6,536	0,042	0,347	-0,347	0,786
miRPlus_17812	7,062	0,089	6,714	0,023	0,348	-0,348	0,786
hsa-miR-608	6,952	0,299	6,604	0,046	0,348	-0,348	0,785
hsa-miR-510	7,011	0,572	6,661	0,093	0,349	-0,349	0,785
mmu-miR-450b-3p	6,944	0,007	6,591	0,109	0,353	-0,353	0,783
hsa-miR-132*	7,021	0,034	6,667	0,017	0,354	-0,354	0,782
mmu-miR-484	7,262	0,030	6,907	0,021	0,355	-0,355	0,782
mmu-miR-101a*	6,882	0,053	6,526	0,068	0,356	-0,356	0,781
No known hsa target	6,872	0,139	6,516	0,055	0,356	-0,356	0,781
mmu-miR-299*	7,059	0,031	6,702	0,011	0,357	-0,357	0,781
miRPlus_17937	7,034	0,057	6,677	0,013	0,357	-0,357	0,781
mmu-miR-201	6,953	0,080	6,596	0,015	0,358	-0,358	0,780
miRPlus_17920	6,986	0,033	6,627	0,010	0,359	-0,359	0,780
rno-miR-349	6,944	0,076	6,584	0,085	0,360	-0,360	0,779
mmu-miR-676	7,010	0,004	6,650	0,025	0,360	-0,360	0,779
mmu-miR-335-3p	7,010	0,031	6,647	0,030	0,363	-0,363	0,777
miRPlus_17828	7,271	0,061	6,905	0,040	0,366	-0,366	0,776
hsa-miR-639	6,891	0,273	6,525	0,071	0,366	-0,366	0,776
mmu-miR-485	6,858	0,112	6,490	0,091	0,368	-0,368	0,775
miRPlus_28350	6,968	0,047	6,599	0,012	0,369	-0,369	0,774
rno-miR-291a-3p	6,966	0,100	6,596	0,020	0,369	-0,369	0,774
hsa-miR-33b	7,018	0,174	6,649	0,009	0,369	-0,369	0,774
hsa-miR-520e	7,017	0,053	6,648	0,031	0,369	-0,369	0,774
mmu-miR-542-3p	7,054	0,099	6,683	0,025	0,371	-0,371	0,773
hsa-miR-517c	6,941	0,057	6,569	0,017	0,372	-0,372	0,773
hsa-miR-524-5p	7,044	0,073	6,672	0,036	0,372	-0,372	0,773
rno-miR-327	7,022	0,035	6,650	0,071	0,372	-0,372	0,773
hsa-miR-627	6,994	0,090	6,622	0,036	0,372	-0,372	0,773
hsa-miR-628-5p	7,010	0,084	6,632	0,031	0,377	-0,377	0,770
hsa-miR-512-5p	7,141	0,022	6,763	0,037	0,377	-0,377	0,770
hsa-miR-573	7,050	0,042	6,672	0,027	0,378	-0,378	0,770
mmu-miR-145	6,978	0,061	6,599	0,036	0,379	-0,379	0,769
mmu-miR-206	6,998	0,332	6,618	0,057	0,380	-0,380	0,769
mmu-miR-292-3p	6,928	0,061	6,547	0,042	0,381	-0,381	0,768
hsa-miR-147	7,043	0,051	6,660	0,040	0,383	-0,383	0,767
mmu-miR-214*	6,976	0,097	6,593	0,047	0,383	-0,383	0,767
mmu-miR-302b	6,991	0,024	6,607	0,017	0,384	-0,384	0,766
mmu-miR-433*	7,272	0,051	6,887	0,013	0,385	-0,385	0,766
rno-miR-224	7,075	0,018	6,689	0,020	0,386	-0,386	0,765
mmu-miR-187	7,061	0,030	6,673	0,023	0,388	-0,388	0,764
hsa-miR-517a/517b	6,914	0,245	6,525	0,081	0,389	-0,389	0,764
hsa-miR-648	7,146	0,561	6,756	0,319	0,391	-0,391	0,763
mmu-miR-302a	7,055	0,033	6,664	0,013	0,391	-0,391	0,763
rno-miR-343	6,982	0,195	6,590	0,039	0,392	-0,392	0,762
mmu-miR-22*	7,140	0,030	6,746	0,022	0,393	-0,393	0,761
hsa-miR-622	7,088	0,037	6,692	0,017	0,396	-0,396	0,760
hsa_negative_control_4	6,976	0,034	6,580	0,029	0,396	-0,396	0,760
hsa-miR-620	6,969	0,027	6,572	0,017	0,397	-0,397	0,760
miRPlus_17838	6,944	0,040	6,547	0,046	0,397	-0,397	0,759
hsa-miR-580	7,009	0,055	6,611	0,022	0,398	-0,398	0,759
mmu-miR-200c*	7,003	0,204	6,604	0,036	0,399	-0,399	0,758
mmu-miR-449c	7,024	0,073	6,625	0,027	0,400	-0,400	0,758
mmu-miR-696	6,996	0,023	6,593	0,028	0,403	-0,403	0,756
mmu-miR-125a-3p	7,132	0,054	6,728	0,027	0,404	-0,404	0,755

mmu-miR-326	7,723	0,028	7,316	0,257	0,407	-0,407	0,754
hsa-miR-376b	6,907	0,345	6,499	0,080	0,409	-0,409	0,753
mmu-miR-154	7,059	0,038	6,648	0,014	0,410	-0,410	0,753
mmu-miR-302c	7,133	0,117	6,723	0,130	0,410	-0,410	0,752
hsa-miR-199b-5p	7,104	0,039	6,694	0,071	0,411	-0,411	0,752
hsa-miR-570	7,111	0,069	6,699	0,013	0,412	-0,412	0,752
hsa-miR-520c-3p/520f	6,981	0,090	6,569	0,052	0,412	-0,412	0,752
mmu-miR-324-3p	7,166	0,131	6,754	0,035	0,413	-0,413	0,751
rno-miR-34b	7,209	0,029	6,796	0,113	0,413	-0,413	0,751
hsa-miR-519c-3p	7,014	0,027	6,600	0,020	0,415	-0,415	0,750
mmu-miR-151-3p	7,036	0,045	6,619	0,027	0,418	-0,418	0,749
mmu-miR-592	7,069	0,050	6,651	0,020	0,418	-0,418	0,749
hsa-miR-507	7,030	0,066	6,611	0,022	0,419	-0,419	0,748
miRPlus_17833	7,178	0,056	6,758	0,007	0,420	-0,420	0,747
mmu-miR-469	7,010	0,039	6,587	0,028	0,423	-0,423	0,746
mmu-miR-685	7,341	0,049	6,917	0,012	0,424	-0,424	0,745
mmu-miR-338-3p	7,133	0,282	6,709	0,081	0,424	-0,424	0,745
mmu-miR-505	7,040	0,056	6,616	0,029	0,424	-0,424	0,745
miRPlus_17848	7,069	0,039	6,645	0,035	0,425	-0,425	0,745
mmu-miR-341	7,010	0,040	6,584	0,049	0,426	-0,426	0,745
hsa-miR-591	7,097	0,123	6,671	0,298	0,426	-0,426	0,744
hsa-miR-520d-3p	7,021	0,068	6,590	0,015	0,431	-0,431	0,742
rno-miR-297	6,957	0,071	6,524	0,056	0,433	-0,433	0,741
miRPlus_17912	7,044	0,073	6,610	0,016	0,433	-0,433	0,740
hsa-miR-624*	7,038	0,092	6,604	0,016	0,434	-0,434	0,740
hsa-miR-575	7,026	0,093	6,590	0,101	0,436	-0,436	0,739
mmu-miR-488	7,126	0,050	6,690	0,100	0,436	-0,436	0,739
mmu-miR-122	7,036	0,077	6,598	0,046	0,438	-0,438	0,738
mmu-miR-468	7,148	0,098	6,706	0,010	0,442	-0,442	0,736
mmu-miR-719	7,119	0,061	6,677	0,032	0,442	-0,442	0,736
hsa-miR-191*	7,033	0,041	6,591	0,033	0,442	-0,442	0,736
mmu-miR-19a*	7,027	0,045	6,584	0,031	0,443	-0,443	0,736
mmu-miR-10a*	7,008	0,067	6,565	0,072	0,443	-0,443	0,736
miRPlus_17821	7,091	0,058	6,647	0,023	0,444	-0,444	0,735
mmu-miR-450a-5p	7,156	0,045	6,707	0,017	0,449	-0,449	0,732
mmu-miR-204	7,133	0,038	6,682	0,024	0,451	-0,451	0,731
hsa-miR-548a-3p	7,040	0,093	6,588	0,050	0,452	-0,452	0,731
hsa-miR-424	7,152	0,037	6,698	0,030	0,454	-0,454	0,730
mmu-miR-29c*	7,135	0,076	6,681	0,024	0,454	-0,454	0,730
mmu-miR-296-5p	7,208	0,041	6,751	0,065	0,456	-0,456	0,729
mmu-miR-701	7,169	0,186	6,712	0,111	0,457	-0,457	0,728
hsa-miR-875-3p	7,084	0,003	6,624	0,025	0,460	-0,460	0,727
mmu-miR-677	7,148	0,078	6,682	0,051	0,466	-0,466	0,724
mmu-let-7a*/mmu-let-7c-2*	7,282	0,069	6,813	0,109	0,469	-0,469	0,722
mmu-let-7d*	7,039	0,055	6,566	0,027	0,473	-0,473	0,721
mmu-miR-463*	7,039	0,053	6,565	0,018	0,474	-0,474	0,720
hsa-miR-940	7,314	0,119	6,837	0,086	0,476	-0,476	0,719
mmu-miR-129-3p	7,150	0,054	6,670	0,025	0,481	-0,481	0,717
hsa-miR-373	7,124	0,023	6,640	0,029	0,484	-0,484	0,715
hsa-miR-518b	7,101	0,082	6,615	0,034	0,486	-0,486	0,714
mmu-miR-135b	7,085	0,118	6,598	0,036	0,487	-0,487	0,714
hsa-miR-155	7,147	0,115	6,659	0,008	0,488	-0,488	0,713
hsa-miR-483-3p	7,395	0,057	6,907	0,020	0,488	-0,488	0,713
mmu-miR-7b	7,112	0,015	6,621	0,013	0,491	-0,491	0,712
mmu-miR-679	7,088	0,080	6,597	0,026	0,491	-0,491	0,712
mmu-miR-181d	7,348	0,068	6,849	0,024	0,499	-0,499	0,708
mmu-miR-181c	7,158	0,242	6,656	0,027	0,501	-0,501	0,706

mmu-miR-29a*	7,134	0,057	6,631	0,028	0,503	-0,503	0,706
hsa-miR-603	7,214	0,285	6,704	0,100	0,510	-0,510	0,702
hsa_SNORD12	7,337	0,028	6,826	0,014	0,511	-0,511	0,702
mmu-miR-376b*	7,104	0,051	6,592	0,015	0,511	-0,511	0,702
hsa-miR-211	7,160	0,132	6,639	0,022	0,521	-0,521	0,697
hsa_SNORD14B	7,503	0,112	6,981	0,167	0,522	-0,522	0,696
mmu-miR-322	7,118	0,062	6,594	0,030	0,524	-0,524	0,695
hsa-miR-374a*	7,133	0,045	6,604	0,039	0,529	-0,529	0,693
mmu-miR-330	7,090	0,080	6,550	0,038	0,540	-0,540	0,688
hsa-miR-518e	7,085	0,115	6,541	0,039	0,544	-0,544	0,686
rno-miR-483	7,634	0,068	7,089	0,029	0,545	-0,545	0,686
mmu-miR-17*	7,190	0,045	6,644	0,124	0,546	-0,546	0,685
mmu-miR-717	7,249	0,028	6,701	0,005	0,547	-0,547	0,684
hsa-miR-548b-3p	7,199	0,043	6,651	0,022	0,548	-0,548	0,684
mmu-miR-547	7,280	0,038	6,728	0,009	0,552	-0,552	0,682
hsa-miR-361-3p	7,173	0,115	6,620	0,018	0,553	-0,553	0,682
mmu-miR-375	7,141	0,121	6,582	0,056	0,560	-0,560	0,678
hsa-miR-141*	7,186	0,060	6,625	0,018	0,561	-0,561	0,678
mmu-miR-294	7,245	0,067	6,679	0,025	0,566	-0,566	0,675
hsa-miR-616*	7,253	0,060	6,686	0,013	0,567	-0,567	0,675
rno-miR-290	7,286	0,030	6,715	0,022	0,572	-0,572	0,673
mmu-miR-338-5p	7,234	0,012	6,658	0,126	0,577	-0,577	0,671
hsa-miR-659	7,327	0,111	6,750	0,040	0,577	-0,577	0,670
hsa-miR-545	7,160	0,040	6,576	0,027	0,584	-0,584	0,667
miRPlus_17858	7,505	0,125	6,917	0,073	0,588	-0,588	0,665
mmu-miR-694	7,212	0,060	6,618	0,058	0,594	-0,594	0,663
hsa-miR-432	7,121	0,146	6,524	0,048	0,597	-0,597	0,661
hsa-miR-578	7,386	0,212	6,786	0,233	0,600	-0,600	0,660
mmu-miR-715	7,446	0,067	6,846	0,202	0,600	-0,600	0,660
mmu-miR-135a	7,173	0,021	6,572	0,040	0,601	-0,601	0,659
No known hsa target	7,380	0,236	6,778	0,052	0,602	-0,602	0,659
hsa-miR-571	7,152	0,169	6,549	0,036	0,603	-0,603	0,659
mmu-miR-136	7,311	0,031	6,704	0,022	0,607	-0,607	0,657
hsa-miR-371-3p	7,134	0,125	6,527	0,037	0,607	-0,607	0,657
mmu-miR-147	7,191	0,054	6,575	0,042	0,616	-0,616	0,652
mmu-miR-501-3p	7,170	0,008	6,554	0,037	0,616	-0,616	0,652
mmu-miR-15b*	7,576	0,684	6,958	0,565	0,618	-0,618	0,652
miRPlus_17892	7,221	0,292	6,598	0,069	0,623	-0,623	0,649
mmu-miR-672	7,353	0,112	6,708	0,027	0,645	-0,645	0,639
mmu-miR-211	7,311	0,081	6,664	0,009	0,647	-0,647	0,638
hsa-miR-625*	7,485	0,047	6,834	0,030	0,652	-0,652	0,637
mmu-miR-302d	7,288	0,131	6,611	0,012	0,676	-0,676	0,626
hsa-miR-618	7,426	0,205	6,741	0,135	0,685	-0,685	0,622
hsa-miR-609	7,384	0,040	6,676	0,021	0,708	-0,708	0,612
mmu-miR-190b	7,367	0,103	6,646	0,027	0,721	-0,721	0,607
miRPlus_17843	7,376	0,036	6,648	0,063	0,729	-0,729	0,604
hsa-miR-99a*	7,397	0,053	6,664	0,022	0,733	-0,733	0,601
mmu-miR-465a-5p	7,402	0,052	6,661	0,019	0,741	-0,741	0,598
mmu-miR-155	7,360	0,025	6,586	0,073	0,774	-0,774	0,585
mmu-miR-683	7,419	0,076	6,641	0,027	0,778	-0,778	0,583
mmu-miR-142-3p	7,431	0,120	6,592	0,047	0,839	-0,839	0,559

8. References

- Adimoolam, S., Sirisawad, M., Chen, J., Thiemann, P., Ford, J. M., and Buggy, J. J. (2007). HDAC inhibitor PCI-24781 decreases RAD51 expression and inhibits homologous recombination. *Proc Natl Acad Sci U S A* **104**, 19482-19487.
- Alcendor, R. R., Kirshenbaum, L. A., Imai, S., Vatner, S. F., and Sadoshima, J. (2004). Silent information regulator 2alpha, a longevity factor and class III histone deacetylase, is an essential endogenous apoptosis inhibitor in cardiac myocytes. *Circ Res* **95**, 971-980.
- Ambros, V. (2004). The functions of animal microRNAs. *Nature* **431**, 350-355.
- Ambros, V., and Lee, R. C. (2004). Identification of microRNAs and other tiny noncoding RNAs by cDNA cloning. *Methods Mol Biol* **265**, 131-158.
- Axelson, H., Fredlund, E., Ovenberger, M., Landberg, G., and Pahlman, S. (2005). Hypoxia-induced dedifferentiation of tumor cells--a mechanism behind heterogeneity and aggressiveness of solid tumors. *Semin Cell Dev Biol* **16**, 554-563.
- Bals, R., Beisswenger, C., Blouquit, S., and Chinet, T. (2004). Isolation and air-liquid interface culture of human large airway and bronchiolar epithelial cells. *J Cyst Fibros* **3 Suppl 2**, 49-51.
- Bartel, D. P. (2004). MicroRNAs: genomics, biogenesis, mechanism, and function. *Cell* **116**, 281-297.
- Bartkova, J., Horejsi, Z., Koed, K., Kramer, A., Tort, F., Zieger, K., Guldberg, P., Sehested, M., Nesland, J. M., Lukas, C., et al. (2005). DNA damage response as a candidate anti-cancer barrier in early human tumorigenesis. *Nature* **434**, 864-870.
- Bartkova, J., Rezaei, N., Liontos, M., Karakaidos, P., Kletsas, D., Issaeva, N., Vassiliou, L. V., Kolettas, E., Niforou, K., Zoumpourlis, V. C., et al. (2006). Oncogene-induced senescence is part of the tumorigenesis barrier imposed by DNA damage checkpoints. *Nature* **444**, 633-637.
- Bates, S., Phillips, A. C., Clark, P. A., Stott, F., Peters, G., Ludwig, R. L., and Vousden, K. H. (1998). p14ARF links the tumour suppressors RB and p53. *Nature* **395**, 124-125.
- Beisswenger, C., Platz, J., Seifert, C., Vogelmeier, C., and Bals, R. (2004). Exposure of differentiated airway epithelial cells to volatile smoke in vitro. *Respiration* **71**, 402-409.
- Bell, L. A., and Ryan, K. M. (2004). Life and death decisions by E2F-1. *Cell Death Differ* **11**, 137-142.
- Bhaskaran, M., Wang, Y., Zhang, H., Weng, T., Baviskar, P., Guo, Y., Gou, D., and Liu, L. (2009). MicroRNA-127 modulates fetal lung development. *Physiol Genomics* **37**, 268-278.
- Bommer, G. T., Gerin, I., Feng, Y., Kaczorowski, A. J., Kuick, R., Love, R. E., Zhai, Y., Giordano, T. J., Qin, Z. S., Moore, B. B., et al. (2007). p53-mediated activation of miRNA34 candidate tumor-suppressor genes. *Curr Biol* **17**, 1298-1307.
- Braun, C. J., Zhang, X., Savelyeva, I., Wolff, S., Moll, U. M., Schepeler, T., Orntoft, T. F., Andersen, C. L., and Dobbelstein, M. (2008). p53-Responsive micrornas 192 and 215 are capable of inducing cell cycle arrest. *Cancer Res* **68**, 10094-10104.
- Brody, S. L., Yan, X. H., Wuerffel, M. K., Song, S. K., and Shapiro, S. D. (2000). Ciliogenesis and left-right axis defects in forkhead factor HFH-4-null mice. *Am J Respir Cell Mol Biol* **23**, 45-51.
- Bryant, H. E., Schultz, N., Thomas, H. D., Parker, K. M., Flower, D., Lopez, E., Kyle, S., Meuth, M., Curtin, N. J., and Helleday, T. (2005). Specific killing of BRCA2-deficient tumours with inhibitors of poly(ADP-ribose) polymerase. *Nature* **434**, 913-917.
- Budihardjo, I., Oliver, H., Lutter, M., Luo, X., and Wang, X. (1999). Biochemical pathways of caspase activation during apoptosis. *Annu Rev Cell Dev Biol* **15**, 269-290.

- Bunz, F., Dutriaux, A., Lengauer, C., Waldman, T., Zhou, S., Brown, J. P., Sedivy, J. M., Kinzler, K. W., and Vogelstein, B. (1998). Requirement for p53 and p21 to sustain G2 arrest after DNA damage. *Science* 282, 1497-1501.
- Cain, K., Bratton, S. B., and Cohen, G. M. (2002). The Apaf-1 apoptosome: a large caspase-activating complex. *Biochimie* 84, 203-214.
- Calin, G. A., and Croce, C. M. (2006). MicroRNA signatures in human cancers. *Nat Rev Cancer* 6, 857-866.
- Canman, C. E. (2001). Replication checkpoint: preventing mitotic catastrophe. *Curr Biol* 11, R121-124.
- Carew, J. S., Giles, F. J., and Nawrocki, S. T. (2008). Histone deacetylase inhibitors: mechanisms of cell death and promise in combination cancer therapy. *Cancer Lett* 269, 7-17.
- Chang, T. C., Wentzel, E. A., Kent, O. A., Ramachandran, K., Mullendore, M., Lee, K. H., Feldmann, G., Yamakuchi, M., Ferlito, M., Lowenstein, C. J., et al. (2007). Transactivation of miR-34a by p53 broadly influences gene expression and promotes apoptosis. *Mol Cell* 26, 745-752.
- Chen, J., Knowles, H. J., Hebert, J. L., and Hackett, B. P. (1998). Mutation of the mouse hepatocyte nuclear factor/forkhead homologue 4 gene results in an absence of cilia and random left-right asymmetry. *J Clin Invest* 102, 1077-1082.
- Cho, W. C. (2007). OncomiRs: the discovery and progress of microRNAs in cancers. *Mol Cancer* 6, 60.
- Chuang, P. T., and McMahon, A. P. (2003). Branching morphogenesis of the lung: new molecular insights into an old problem. *Trends Cell Biol* 13, 86-91.
- Coppola, V., De Maria, R., and Bonci, D. (2010). MicroRNAs and prostate cancer. *Endocr Relat Cancer* 17, F1-17.
- Corney, D. C., Flesken-Nikitin, A., Godwin, A. K., Wang, W., and Nikitin, A. Y. (2007). MicroRNA-34b and MicroRNA-34c are targets of p53 and cooperate in control of cell proliferation and adhesion-independent growth. *Cancer Res* 67, 8433-8438.
- Croce, C. M. (2009). Causes and consequences of microRNA dysregulation in cancer. *Nat Rev Genet* 10, 704-714.
- Dai, Y., and Grant, S. (2010). New insights into checkpoint kinase 1 in the DNA damage response signaling network. *Clin Cancer Res* 16, 376-383.
- Dannenberg, J. H., David, G., Zhong, S., van der Torre, J., Wong, W. H., and Depinho, R. A. (2005). mSin3A corepressor regulates diverse transcriptional networks governing normal and neoplastic growth and survival. *Genes Dev* 19, 1581-1595.
- DeGregori, J., and Johnson, D. G. (2006). Distinct and Overlapping Roles for E2F Family Members in Transcription, Proliferation and Apoptosis. *Curr Mol Med* 6, 739-748.
- Di Micco, R., Fumagalli, M., Cicalese, A., Piccinini, S., Gasparini, P., Luise, C., Schurra, C., Garre, M., Nuciforo, P. G., Bensimon, A., et al. (2006). Oncogene-induced senescence is a DNA damage response triggered by DNA hyper-replication. *Nature* 444, 638-642.
- Dong, J., Jiang, G., Asmann, Y. W., Tomaszek, S., Jen, J., Kislinger, T., and Wigle, D. A. (2010). MicroRNA Networks in Mouse Lung Organogenesis. *PLoS ONE* 5, e10854.
- Droge, P., and Davey, C. A. (2008). Do cells let-7 determine stemness? *Cell Stem Cell* 2, 8-9.
- Dyer, B. W., Ferrer, F. A., Klinedinst, D. K., and Rodriguez, R. (2000). A noncommercial dual luciferase enzyme assay system for reporter gene analysis. *Anal Biochem* 282, 158-161.
- Elaut, G., Rogiers, V., and Vanhaecke, T. (2007). The pharmaceutical potential of histone deacetylase inhibitors. *Curr Pharm Des* 13, 2584-2620.

- Ellis, L., Atadja, P. W., and Johnstone, R. W. (2009). Epigenetics in cancer: targeting chromatin modifications. *Mol Cancer Ther* 8, 1409-1420.
- Enders, G. H. (2008). Expanded roles for Chk1 in genome maintenance. *J Biol Chem* 283, 17749-17752.
- Espino, P. S., Drobic, B., Dunn, K. L., and Davie, J. R. (2005). Histone modifications as a platform for cancer therapy. *J Cell Biochem* 94, 1088-1102.
- Esquela-Kerscher, A., and Slack, F. J. (2006). Oncomirs - microRNAs with a role in cancer. *Nat Rev Cancer* 6, 259-269.
- Farmer, H., McCabe, N., Lord, C. J., Tutt, A. N., Johnson, D. A., Richardson, T. B., Santarosa, M., Dillon, K. J., Hickson, I., Knights, C., et al. (2005). Targeting the DNA repair defect in BRCA mutant cells as a therapeutic strategy. *Nature* 434, 917-921.
- Fearon, E. R., and Vogelstein, B. (1990). A genetic model for colorectal tumorigenesis. *Cell* 61, 759-767.
- Filipowicz, W., Bhattacharyya, S. N., and Sonenberg, N. (2008). Mechanisms of post-transcriptional regulation by microRNAs: are the answers in sight? *Nat Rev Genet* 9, 102-114.
- Fishler, T., Li, Y. Y., Wang, R. H., Kim, H. S., Sengupta, K., Vassilopoulos, A., Lahusen, T., Xu, X., Lee, M. H., Liu, Q., et al. (2010). Genetic instability and mammary tumor formation in mice carrying mammary-specific disruption of Chk1 and p53. *Oncogene*.
- Flynt, A. S., and Lai, E. C. (2008). Biological principles of microRNA-mediated regulation: shared themes amid diversity. *Nat Rev Genet* 9, 831-842.
- Fong, P. C., Boss, D. S., Yap, T. A., Tutt, A., Wu, P., Mergui-Roelvink, M., Mortimer, P., Swaisland, H., Lau, A., O'Connor, M. J., et al. (2009). Inhibition of poly(ADP-ribose) polymerase in tumors from BRCA mutation carriers. *N Engl J Med* 361, 123-134.
- Franklin, E. E., and Robertson, J. D. (2007). Requirement of Apaf-1 for mitochondrial events and the cleavage or activation of all procaspases during genotoxic stress-induced apoptosis. *Biochem J* 405, 115-122.
- Friedman, J. M., Jones, P. A., and Liang, G. (2009a). The tumor suppressor microRNA-101 becomes an epigenetic player by targeting the polycomb group protein EZH2 in cancer. *Cell Cycle* 8, 2313-2314.
- Friedman, R. C., Farh, K. K., Burge, C. B., and Bartel, D. P. (2009b). Most mammalian mRNAs are conserved targets of microRNAs. *Genome Res* 19, 92-105.
- Furukawa, Y., Nishimura, N., Satoh, M., Endo, H., Iwase, S., Yamada, H., Matsuda, M., Kano, Y., and Nakamura, M. (2002). Apaf-1 is a mediator of E2F-1-induced apoptosis. *J Biol Chem* 277, 39760-39768.
- Georges, S. A., Biery, M. C., Kim, S. Y., Schelter, J. M., Guo, J., Chang, A. N., Jackson, A. L., Carleton, M. O., Linsley, P. S., Cleary, M. A., and Chau, B. N. (2008). Coordinated regulation of cell cycle transcripts by p53-Inducible microRNAs, miR-192 and miR-215. *Cancer Res* 68, 10105-10112.
- Georges, S. A., Chau, B. N., Braun, C. J., Zhang, X., and Dobbelstein, M. (2009). Cell cycle arrest or apoptosis by p53: are microRNAs-192/215 and -34 making the decision? *Cell Cycle* 8, 680-681.
- Gialitakis, M., Kretsovali, A., Spilianakis, C., Kravariti, L., Mages, J., Hoffmann, R., Hatzopoulos, A. K., and Papamatheakis, J. (2006). Coordinated changes of histone modifications and HDAC mobilization regulate the induction of MHC class II genes by Trichostatin A. *Nucleic Acids Res* 34, 765-772.
- Griffiths-Jones, S. (2004). The microRNA Registry. *Nucleic Acids Res* 32, D109-111.
- Griffiths-Jones, S. (2006). miRBase: the microRNA sequence database. *Methods Mol Biol* 342, 129-138.

- Griffiths-Jones, S., Grocock, R. J., van Dongen, S., Bateman, A., and Enright, A. J. (2006). miRBase: microRNA sequences, targets and gene nomenclature. *Nucleic Acids Res* 34, D140-144.
- Griffiths-Jones, S., Saini, H. K., van Dongen, S., and Enright, A. J. (2008). miRBase: tools for microRNA genomics. *Nucleic Acids Res* 36, D154-158.
- Halkidou, K., Gaughan, L., Cook, S., Leung, H. Y., Neal, D. E., and Robson, C. N. (2004). Upregulation and nuclear recruitment of HDAC1 in hormone refractory prostate cancer. *Prostate* 59, 177-189.
- Hanahan, D., and Weinberg, R. A. (2000). The hallmarks of cancer. *Cell* 100, 57-70.
- Harris, K. S., Zhang, Z., McManus, M. T., Harfe, B. D., and Sun, X. (2006). Dicer function is essential for lung epithelium morphogenesis. *Proc Natl Acad Sci U S A* 103, 2208-2213.
- Haupt, Y., Maya, R., Kazaz, A., and Oren, M. (1997). Mdm2 promotes the rapid degradation of p53. *Nature* 387, 296-299.
- He, L., and Hannon, G. J. (2004). MicroRNAs: small RNAs with a big role in gene regulation. *Nat Rev Genet* 5, 522-531.
- He, L., He, X., Lim, L. P., de Stanchina, E., Xuan, Z., Liang, Y., Xue, W., Zender, L., Magnus, J., Ridzon, D., et al. (2007a). A microRNA component of the p53 tumour suppressor network. *Nature* 447, 1130-1134.
- He, L., He, X., Lowe, S. W., and Hannon, G. J. (2007b). microRNAs join the p53 network--another piece in the tumour-suppression puzzle. *Nat Rev Cancer* 7, 819-822.
- He, X., He, L., and Hannon, G. J. (2007c). The guardian's little helper: microRNAs in the p53 tumor suppressor network. *Cancer Res* 67, 11099-11101.
- Helleday, T. (2010). Homologous recombination in cancer development, treatment and development of drug resistance. *Carcinogenesis* 31, 955-960.
- Helleday, T., Bryant, H. E., and Schultz, N. (2005). Poly(ADP-ribose) polymerase (PARP-1) in homologous recombination and as a target for cancer therapy. *Cell Cycle* 4, 1176-1178.
- Helleday, T., Petermann, E., Lundin, C., Hodgson, B., and Sharma, R. A. (2008). DNA repair pathways as targets for cancer therapy. *Nat Rev Cancer* 8, 193-204.
- Hermeking, H. (2007). p53 enters the microRNA world. *Cancer Cell* 12, 414-418.
- Hermeking, H. (2009a). The miR-34 family in cancer and apoptosis. *Cell Death Differ*.
- Hermeking, H. (2009b). MiR-34a and p53. *Cell Cycle* 8, 1308.
- Hershko, T., Korotayev, K., Polager, S., and Ginsberg, D. (2006). E2F1 modulates p38 MAPK phosphorylation via transcriptional regulation of ASK1 and Wip1. *J Biol Chem* 281, 31309-31316.
- Hoesel, B., Bhujabal, Z., Przemeck, G. K., Kurz-Drexler, A., Weisenhorn, D. M., Angelis, M. H., and Beckers, J. (2010). Combination of in silico and insitu hybridisation approaches to identify potential Dll1 associated miRNAs during mouse embryogenesis. *Gene Expr Patterns*.
- Huang, X., Tran, T., Zhang, L., Hatcher, R., and Zhang, P. (2005). DNA damage-induced mitotic catastrophe is mediated by the Chk1-dependent mitotic exit DNA damage checkpoint. *Proc Natl Acad Sci U S A* 102, 1065-1070.
- Irwin, M., Marin, M. C., Phillips, A. C., Seelan, R. S., Smith, D. I., Liu, W., Flores, E. R., Tsai, K. Y., Jacks, T., Vousden, K. H., and Kaelin, W. G., Jr. (2000). Role for the p53 homologue p73 in E2F-1-induced apoptosis. *Nature* 407, 645-648.
- Jackson, S. P., and Bartek, J. (2009). The DNA-damage response in human biology and disease. *Nature* 461, 1071-1078.

- Ji, Q., Hao, X., Meng, Y., Zhang, M., Desano, J., Fan, D., and Xu, L. (2008). Restoration of tumor suppressor miR-34 inhibits human p53-mutant gastric cancer tumorspheres. *BMC Cancer* 8, 266.
- Ji, Q., Hao, X., Zhang, M., Tang, W., Yang, M., Li, L., Xiang, D., Desano, J. T., Bommer, G. T., Fan, D., et al. (2009). MicroRNA miR-34 inhibits human pancreatic cancer tumor-initiating cells. *PLoS ONE* 4, e6816.
- John, B., Enright, A. J., Aravin, A., Tuschl, T., Sander, C., and Marks, D. S. (2004). Human MicroRNA targets. *PLoS Biol* 2, e363.
- Johnson, D. G. (2000). The paradox of E2F1: oncogene and tumor suppressor gene. *Mol Carcinog* 27, 151-157.
- Johnson, D. G., Cress, W. D., Jakoi, L., and Nevins, J. R. (1994). Oncogenic capacity of the E2F1 gene. *Proc Natl Acad Sci U S A* 91, 12823-12827.
- Kalebic, T. (2003). Epigenetic changes: potential therapeutic targets. *Ann N Y Acad Sci* 983, 278-285.
- Kastan, M. B., and Bartek, J. (2004). Cell-cycle checkpoints and cancer. *Nature* 432, 316-323.
- Kim, D., Frank, C. L., Dobbin, M. M., Tsunemoto, R. K., Tu, W., Peng, P. L., Guan, J. S., Lee, B. H., Moy, L. Y., Giusti, P., et al. (2008). Dereulation of HDAC1 by p25/Cdk5 in neurotoxicity. *Neuron* 60, 803-817.
- Kim, V. N. (2005). MicroRNA biogenesis: coordinated cropping and dicing. *Nat Rev Mol Cell Biol* 6, 376-385.
- Kubbutat, M. H., Jones, S. N., and Vousden, K. H. (1997). Regulation of p53 stability by Mdm2. *Nature* 387, 299-303.
- Kumar, M. S., Lu, J., Mercer, K. L., Golub, T. R., and Jacks, T. (2007). Impaired microRNA processing enhances cellular transformation and tumorigenesis. *Nat Genet* 39, 673-677.
- Lagos-Quintana, M., Rauhut, R., Yalcin, A., Meyer, J., Lendeckel, W., and Tuschl, T. (2002). Identification of tissue-specific microRNAs from mouse. *Curr Biol* 12, 735-739.
- Landgraf, P., Rusu, M., Sheridan, R., Sewer, A., Iovino, N., Aravin, A., Pfeffer, S., Rice, A., Kamphorst, A. O., Landthaler, M., et al. (2007). A mammalian microRNA expression atlas based on small RNA library sequencing. *Cell* 129, 1401-1414.
- Langley, E., Pearson, M., Faretta, M., Bauer, U. M., Frye, R. A., Minucci, S., Pelicci, P. G., and Kouzarides, T. (2002). Human SIR2 deacetylates p53 and antagonizes PML/p53-induced cellular senescence. *Embo J* 21, 2383-2396.
- Lee, H. J., Hwang, H. I., and Jang, Y. J. (2010). Mitotic DNA damage response: Polo-like kinase-1 is dephosphorylated through ATM-Chk1 pathway. *Cell Cycle* 9.
- Lee, K. H., Chen, Y. L., Yeh, S. D., Hsiao, M., Lin, J. T., Goan, Y. G., and Lu, P. J. (2009). MicroRNA-330 acts as tumor suppressor and induces apoptosis of prostate cancer cells through E2F1-mediated suppression of Akt phosphorylation. *Oncogene* 28, 3360-3370.
- Lee, Y. S., and Dutta, A. (2007). The tumor suppressor microRNA let-7 represses the HMGA2 oncogene. *Genes Dev* 21, 1025-1030.
- Lin, T., Chao, C., Saito, S., Mazur, S. J., Murphy, M. E., Appella, E., and Xu, Y. (2005). p53 induces differentiation of mouse embryonic stem cells by suppressing Nanog expression. *Nat Cell Biol* 7, 165-171.
- Lin, T., Dong, W., Huang, J., Pan, Q., Fan, X., Zhang, C., and Huang, L. (2009). MicroRNA-143 as a tumor suppressor for bladder cancer. *J Urol* 181, 1372-1380.
- Lin, W. C., Lin, F. T., and Nevins, J. R. (2001). Selective induction of E2F1 in response to DNA damage, mediated by ATM-dependent phosphorylation. *Genes Dev* 15, 1833-1844.

- Lissy, N. A., Davis, P. K., Irwin, M., Kaelin, W. G., and Dowdy, S. F. (2000). A common E2F-1 and p73 pathway mediates cell death induced by TCR activation. *Nature* 407, 642-645.
- Lize, M., Pilarski, S., and Dobbelstein, M. (2010). E2F1-inducible microRNA 449a/b suppresses cell proliferation and promotes apoptosis. *Cell Death Differ* 17, 452-458.
- Lodygin, D., Tarasov, V., Epanchintsev, A., Berking, C., Knyazeva, T., Korner, H., Knyazev, P., Diebold, J., and Hermeking, H. (2008). Inactivation of miR-34a by aberrant CpG methylation in multiple types of cancer. *Cell Cycle* 7, 2591-2600.
- Lu, J., Getz, G., Miska, E. A., Alvarez-Saavedra, E., Lamb, J., Peck, D., Sweet-Cordero, A., Ebert, B. L., Mak, R. H., Ferrando, A. A., et al. (2005). MicroRNA expression profiles classify human cancers. *Nature* 435, 834-838.
- Lu, Y., Okubo, T., Rawlins, E., and Hogan, B. L. (2008). Epithelial progenitor cells of the embryonic lung and the role of microRNAs in their proliferation. *Proc Am Thorac Soc* 5, 300-304.
- Luo, J., Nikolaev, A. Y., Imai, S., Chen, D., Su, F., Shiloh, A., Guarante, L., and Gu, W. (2001). Negative control of p53 by Sir2alpha promotes cell survival under stress. *Cell* 107, 137-148.
- Maeda, Y., Dave, V., and Whitsett, J. A. (2007). Transcriptional control of lung morphogenesis. *Physiol Rev* 87, 219-244.
- Markey, M., and Berberich, S. J. (2008). Full-length hdmX transcripts decrease following genotoxic stress. *Oncogene* 27, 6657-6666.
- Milutinovic, S., Zhuang, Q., and Szyf, M. (2002). Proliferating cell nuclear antigen associates with histone deacetylase activity, integrating DNA replication and chromatin modification. *J Biol Chem* 277, 20974-20978.
- Moradei, O., Vaisburg, A., and Martell, R. E. (2008). Histone deacetylase inhibitors in cancer therapy: new compounds and clinical update of benzamide-type agents. *Curr Top Med Chem* 8, 841-858.
- Moroni, M. C., Hickman, E. S., Lazzerini Denchi, E., Caprara, G., Colli, E., Cecconi, F., Muller, H., and Helin, K. (2001). Apaf-1 is a transcriptional target for E2F and p53. *Nat Cell Biol* 3, 552-558.
- Naguibneva, I., Ameyar-Zazoua, M., Nonne, N., Polesskaya, A., Ait-Si-Ali, S., Groisman, R., Souidi, M., Pritchard, L. L., and Harel-Bellan, A. (2006). An LNA-based loss-of-function assay for micro-RNAs. *Biomed Pharmacother* 60, 633-638.
- Noonan, E. J., Place, R. F., Pookot, D., Basak, S., Whitson, J. M., Hirata, H., Giardina, C., and Dahiya, R. (2009). miR-449a targets HDAC-1 and induces growth arrest in prostate cancer. *Oncogene* 28, 1714-1724.
- Novotny, G. W., Sonne, S. B., Nielsen, J. E., Jonstrup, S. P., Hansen, M. A., Skakkebaek, N. E., Rajpert-De Meyts, E., Kjems, J., and Leffers, H. (2007). Translational repression of E2F1 mRNA in carcinoma in situ and normal testis correlates with expression of the miR-17-92 cluster. *Cell Death Differ* 14, 879-882.
- O'Donovan, P. J., and Livingston, D. M. (2010). BRCA1 and BRCA2: breast/ovarian cancer susceptibility gene products and participants in DNA double-strand break repair. *Carcinogenesis* 31, 961-967.
- Pan, Y., Ren, K. H., He, H. W., and Shao, R. G. (2009). Knockdown of Chk1 sensitizes human colon carcinoma HCT116 cells in a p53-dependent manner to lidamycin through abrogation of a G2/M checkpoint and induction of apoptosis. *Cancer Biol Ther* 8, 1559-1566.
- Patra, S. K., Patra, A., and Dahiya, R. (2001). Histone deacetylase and DNA methyltransferase in human prostate cancer. *Biochem Biophys Res Commun* 287, 705-713.
- Petrocca, F., Vecchione, A., and Croce, C. M. (2008a). Emerging role of miR-106b-25/miR-17-92 clusters in the control of transforming growth factor beta signaling. *Cancer Res* 68, 8191-8194.

- Petrocca, F., Visone, R., Onelli, M. R., Shah, M. H., Nicoloso, M. S., de Martino, I., Iliopoulos, D., Pilozzi, E., Liu, C. G., Negrini, M., et al. (2008b). E2F1-regulated microRNAs impair TGFbeta-dependent cell-cycle arrest and apoptosis in gastric cancer. *Cancer Cell* 13, 272-286.
- Phillips, A. C., Ernst, M. K., Bates, S., Rice, N. R., and Vousden, K. H. (1999). E2F-1 potentiates cell death by blocking antiapoptotic signaling pathways. *Mol Cell* 4, 771-781.
- Pickering, M. T., Stadler, B. M., and Kowalik, T. F. (2009). miR-17 and miR-20a temper an E2F1-induced G1 checkpoint to regulate cell cycle progression. *Oncogene* 28, 140-145.
- Polager, S., and Ginsberg, D. (2009). p53 and E2f: partners in life and death. *Nat Rev Cancer* 9, 738-748.
- Pomerantz, J., Schreiber-Agus, N., Liegeois, N. J., Silverman, A., Allard, L., Chin, L., Potes, J., Chen, K., Orlow, I., Lee, H. W., et al. (1998). The Ink4a tumor suppressor gene product, p19Arf, interacts with MDM2 and neutralizes MDM2's inhibition of p53. *Cell* 92, 713-723.
- Qin, X. Q., Livingston, D. M., Ewen, M., Sellers, W. R., Arany, Z., and Kaelin, W. G., Jr. (1995). The transcription factor E2F-1 is a downstream target of RB action. *Mol Cell Biol* 15, 742-755.
- Raver-Shapira, N., Marciano, E., Meiri, E., Spector, Y., Rosenfeld, N., Moskovits, N., Bentwich, Z., and Oren, M. (2007). Transcriptional activation of miR-34a contributes to p53-mediated apoptosis. *Mol Cell* 26, 731-743.
- Redshaw, N., Wheeler, G., Hajhosseini, M. K., and Dalmary, T. (2009). microRNA-449 is a putative regulator of choroid plexus development and function. *Brain Res* 1250, 20-26.
- Reid, G., Metivier, R., Lin, C. Y., Denger, S., Ibberson, D., Ivacevic, T., Brand, H., Benes, V., Liu, E. T., and Gannon, F. (2005). Multiple mechanisms induce transcriptional silencing of a subset of genes, including oestrogen receptor alpha, in response to deacetylase inhibition by valproic acid and trichostatin A. *Oncogene* 24, 4894-4907.
- Ren, B., Cam, H., Takahashi, Y., Volkert, T., Terragni, J., Young, R. A., and Dynlacht, B. D. (2002). E2F integrates cell cycle progression with DNA repair, replication, and G(2)/M checkpoints. *Genes Dev* 16, 245-256.
- Rodriguez, J., and Lazebnik, Y. (1999). Caspase-9 and APAF-1 form an active holoenzyme. *Genes Dev* 13, 3179-3184.
- Rogoff, H. A., and Kowalik, T. F. (2004). Life, death and E2F: linking proliferation control and DNA damage signaling via E2F1. *Cell Cycle* 3, 845-846.
- Romagnoli, S., Fasoli, E., Vaira, V., Falleni, M., Pellegrini, C., Catania, A., Roncalli, M., Marchetti, A., Santambrogio, L., Coggi, G., and Bosari, S. (2009). Identification of potential therapeutic targets in malignant mesothelioma using cell-cycle gene expression analysis. *Am J Pathol* 174, 762-770.
- Ross, A. J., Dailey, L. A., Brighton, L. E., and Devlin, R. B. (2007). Transcriptional profiling of mucociliary differentiation in human airway epithelial cells. *Am J Respir Cell Mol Biol* 37, 169-185.
- Saleh, A., Srinivasula, S. M., Acharya, S., Fishel, R., and Alnemri, E. S. (1999). Cytochrome c and dATP-mediated oligomerization of Apaf-1 is a prerequisite for procaspase-9 activation. *J Biol Chem* 274, 17941-17945.
- Schembri, F., Sridhar, S., Perdomo, C., Gustafson, A. M., Zhang, X., Ergun, A., Lu, J., Liu, G., Bowers, J., Vaziri, C., et al. (2009). MicroRNAs as modulators of smoking-induced gene expression changes in human airway epithelium. *Proc Natl Acad Sci U S A* 106, 2319-2324.
- Sell, S. (1993). Cellular origin of cancer: dedifferentiation or stem cell maturation arrest? *Environ Health Perspect Suppl* 5, 15-26.
- Shan, B., and Lee, W. H. (1994). Deregulated expression of E2F-1 induces S-phase entry and leads to apoptosis. *Mol Cell Biol* 14, 8166-8173.

- Shankar, S., and Srivastava, R. K. (2008). Histone deacetylase inhibitors: mechanisms and clinical significance in cancer: HDAC inhibitor-induced apoptosis. *Adv Exp Med Biol* 615, 261-298.
- Shenouda, S. K., and Alahari, S. K. (2009). MicroRNA function in cancer: oncogene or a tumor suppressor? *Cancer Metastasis Rev* 28, 369-378.
- Sherr, C. J., and McCormick, F. (2002). The RB and p53 pathways in cancer. *Cancer Cell* 2, 103-112.
- Sherr, C. J., and Roberts, J. M. (1999). CDK inhibitors: positive and negative regulators of G1-phase progression. *Genes Dev* 13, 1501-1512.
- Sionov, R. V., and Haupt, Y. (1999). The cellular response to p53: the decision between life and death. *Oncogene* 18, 6145-6157.
- Solomon, J. M., Pasupuleti, R., Xu, L., McDonagh, T., Curtis, R., DiStefano, P. S., and Huber, L. J. (2006). Inhibition of SIRT1 catalytic activity increases p53 acetylation but does not alter cell survival following DNA damage. *Mol Cell Biol* 26, 28-38.
- Stevens, C., Smith, L., and La Thangue, N. B. (2003). Chk2 activates E2F-1 in response to DNA damage. *Nat Cell Biol* 5, 401-409.
- Stiewe, T., and Putzer, B. M. (2000). Role of the p53-homologue p73 in E2F1-induced apoptosis. *Nat Genet* 26, 464-469.
- Stracker, T. H., Usui, T., and Petrini, J. H. (2009). Taking the time to make important decisions: the checkpoint effector kinases Chk1 and Chk2 and the DNA damage response. *DNA Repair (Amst)* 8, 1047-1054.
- Stunkel, W., Peh, B. K., Tan, Y. C., Nayagam, V. M., Wang, X., Salto-Tellez, M., Ni, B., Entzeroth, M., and Wood, J. (2007). Function of the SIRT1 protein deacetylase in cancer. *Biotechnol J* 2, 1360-1368.
- Sun, F., Fu, H., Liu, Q., Tie, Y., Zhu, J., Xing, R., Sun, Z., and Zheng, X. (2008). Downregulation of CCND1 and CDK6 by miR-34a induces cell cycle arrest. *FEBS Lett* 582, 1564-1568.
- Sun, Y., Sun, D., Li, F., Tian, L., Li, C., Li, L., Lin, R., and Wang, S. (2007). Downregulation of Sirt1 by antisense oligonucleotides induces apoptosis and enhances radiation sensitization in A549 lung cancer cells. *Lung Cancer* 58, 21-29.
- Sylvestre, Y., De Guire, V., Querido, E., Mukhopadhyay, U. K., Bourdeau, V., Major, F., Ferbeyre, G., and Chartrand, P. (2007). An E2F/miR-20a autoregulatory feedback loop. *J Biol Chem* 282, 2135-2143.
- Takahashi, K., and Yamanaka, S. (2006). Induction of pluripotent stem cells from mouse embryonic and adult fibroblast cultures by defined factors. *Cell* 126, 663-676.
- Tarasov, V., Jung, P., Verdoodt, B., Lodygin, D., Epanchintsev, A., Menssen, A., Meister, G., and Hermeking, H. (2007). Differential regulation of microRNAs by p53 revealed by massively parallel sequencing: miR-34a is a p53 target that induces apoptosis and G1-arrest. *Cell Cycle* 6, 1586-1593.
- Tazawa, H., Tsuchiya, N., Izumiya, M., and Nakagama, H. (2007). Tumor-suppressive miR-34a induces senescence-like growth arrest through modulation of the E2F pathway in human colon cancer cells. *Proc Natl Acad Sci U S A* 104, 15472-15477.
- Tominaga, Y., Wang, A., Wang, R. H., Wang, X., Cao, L., and Deng, C. X. (2007). Genistein inhibits Brca1 mutant tumor growth through activation of DNA damage checkpoints, cell cycle arrest, and mitotic catastrophe. *Cell Death Differ* 14, 472-479.
- Trosko, J. E. (2009). Review paper: cancer stem cells and cancer nonstem cells: from adult stem cells or from reprogramming of differentiated somatic cells. *Vet Pathol* 46, 176-193.

- Tsai, K. Y., Hu, Y., Macleod, K. F., Crowley, D., Yamasaki, L., and Jacks, T. (1998). Mutation of E2f-1 suppresses apoptosis and inappropriate S phase entry and extends survival of Rb-deficient mouse embryos. *Mol Cell* 2, 293-304.
- Uhl, M., Csernok, A., Aydin, S., Kreienberg, R., Wiesmuller, L., and Gatz, S. A. (2010). Role of SIRT1 in homologous recombination. *DNA Repair (Amst)* 9, 383-393.
- Vassilev, L. T., Vu, B. T., Graves, B., Carvajal, D., Podlaski, F., Filipovic, Z., Kong, N., Kammlott, U., Lukacs, C., Klein, C., et al. (2004). In vivo activation of the p53 pathway by small-molecule antagonists of MDM2. *Science* 303, 844-848.
- Vaziri, H., Dessain, S. K., Ng Eaton, E., Imai, S. I., Frye, R. A., Pandita, T. K., Guarente, L., and Weinberg, R. A. (2001). hSIR2(SIRT1) functions as an NAD-dependent p53 deacetylase. *Cell* 107, 149-159.
- Verlinden, L., Vanden Bempt, I., Eelen, G., Drijkoningen, M., Verlinden, I., Marchal, K., De Wolf-Peeters, C., Christiaens, M. R., Michiels, L., Bouillon, R., and Verstuyf, A. (2007). The E2F-regulated gene Chk1 is highly expressed in triple-negative estrogen receptor /progesterone receptor /HER-2 breast carcinomas. *Cancer Res* 67, 6574-6581.
- Vert, J. P., Foveau, N., Lajaunie, C., and Vandenbrouck, Y. (2006). An accurate and interpretable model for siRNA efficacy prediction. *BMC Bioinformatics* 7, 520.
- Vogelstein, B., and Kinzler, K. W. (1993). The multistep nature of cancer. *Trends Genet* 9, 138-141.
- Volinia, S., Calin, G. A., Liu, C. G., Ambs, S., Cimmino, A., Petrocca, F., Visone, R., Iorio, M., Roldo, C., Ferracin, M., et al. (2006). A microRNA expression signature of human solid tumors defines cancer gene targets. *Proc Natl Acad Sci U S A* 103, 2257-2261.
- Voorhoeve, P. M., le Sage, C., Schrier, M., Gillis, A. J., Stoop, H., Nagel, R., Liu, Y. P., van Duijse, J., Drost, J., Griekspoor, A., et al. (2006). A genetic screen implicates miRNA-372 and miRNA-373 as oncogenes in testicular germ cell tumors. *Cell* 124, 1169-1181.
- Wang, R. H., Sengupta, K., Li, C., Kim, H. S., Cao, L., Xiao, C., Kim, S., Xu, X., Zheng, Y., Chilton, B., et al. (2008). Impaired DNA damage response, genome instability, and tumorigenesis in SIRT1 mutant mice. *Cancer Cell* 14, 312-323.
- Wang, Y., Brahmakshatriya, V., Zhu, H., Lupiani, B., Reddy, S. M., Yoon, B. J., Gunaratne, P. H., Kim, J. H., Chen, R., Wang, J., and Zhou, H. (2009). Identification of differentially expressed miRNAs in chicken lung and trachea with avian influenza virus infection by a deep sequencing approach. *BMC Genomics* 10, 512.
- Wang, Y., Decker, S. J., and Sebolt-Leopold, J. (2004). Knockdown of Chk1, Wee1 and Myt1 by RNA interference abrogates G2 checkpoint and induces apoptosis. *Cancer Biol Ther* 3, 305-313.
- Wang, Y., Weng, T., Gou, D., Chen, Z., Chintagari, N. R., and Liu, L. (2007). Identification of rat lung-specific microRNAs by microRNA microarray: valuable discoveries for the facilitation of lung research. *BMC Genomics* 8, 29.
- Weichert, W. (2009). HDAC expression and clinical prognosis in human malignancies. *Cancer Lett* 280, 168-176.
- Weichert, W., Denkert, C., Noske, A., Darb-Esfahani, S., Dietel, M., Kalloger, S. E., Huntsman, D. G., and Kobel, M. (2008a). Expression of class I histone deacetylases indicates poor prognosis in endometrioid subtypes of ovarian and endometrial carcinomas. *Neoplasia* 10, 1021-1027.
- Weichert, W., Roske, A., Gekeler, V., Beckers, T., Stephan, C., Jung, K., Fritzsche, F. R., Niesporek, S., Denkert, C., Dietel, M., and Kristiansen, G. (2008b). Histone deacetylases 1, 2 and 3 are highly expressed in prostate cancer and HDAC2 expression is associated with shorter PSA relapse time after radical prostatectomy. *Br J Cancer* 98, 604-610.
- Welch, C., Chen, Y., and Stallings, R. L. (2007). MicroRNA-34a functions as a potential tumor suppressor by inducing apoptosis in neuroblastoma cells. *Oncogene* 26, 5017-5022.

- Williams, A. E., Moschos, S. A., Perry, M. M., Barnes, P. J., and Lindsay, M. A. (2007). Maternally imprinted microRNAs are differentially expressed during mouse and human lung development. *Dev Dyn* 236, 572-580.
- Wilson, A. J., Byun, D. S., Popova, N., Murray, L. B., L'Italien, K., Sowa, Y., Arango, D., Velcich, A., Augenlicht, L. H., and Mariadason, J. M. (2006). Histone deacetylase 3 (HDAC3) and other class I HDACs regulate colon cell maturation and p21 expression and are deregulated in human colon cancer. *J Biol Chem* 281, 13548-13558.
- Wong, S., and Weber, J. D. (2007). Deacetylation of the retinoblastoma tumour suppressor protein by SIRT1. *Biochem J* 407, 451-460.
- Woods, K., Thomson, J. M., and Hammond, S. M. (2007). Direct regulation of an oncogenic micro-RNA cluster by E2F transcription factors. *J Biol Chem* 282, 2130-2134.
- Wu, X., and Levine, A. J. (1994). p53 and E2F-1 cooperate to mediate apoptosis. *Proc Natl Acad Sci U S A* 91, 3602-3606.
- Xiao, Z., Xue, J., Sowin, T. J., Rosenberg, S. H., and Zhang, H. (2005). A novel mechanism of checkpoint abrogation conferred by Chk1 downregulation. *Oncogene* 24, 1403-1411.
- Yamakuchi, M., Ferlito, M., and Lowenstein, C. J. (2008). miR-34a repression of SIRT1 regulates apoptosis. *Proc Natl Acad Sci U S A* 105, 13421-13426.
- Yamakuchi, M., and Lowenstein, C. J. (2009). MiR-34, SIRT1 and p53: the feedback loop. *Cell Cycle* 8, 712-715.
- Yamasaki, L., Jacks, T., Bronson, R., Goillot, E., Harlow, E., and Dyson, N. J. (1996). Tumor induction and tissue atrophy in mice lacking E2F-1. *Cell* 85, 537-548.
- Yan, H. L., Xue, G., Mei, Q., Wang, Y. Z., Ding, F. X., Liu, M. F., Lu, M. H., Tang, Y., Yu, H. Y., and Sun, S. H. (2009). Repression of the miR-17-92 cluster by p53 has an important function in hypoxia-induced apoptosis. *Embo J* 28, 2719-2732.
- Yang, A., and McKeon, F. (2000). P63 and P73: P53 mimics, menaces and more. *Nat Rev Mol Cell Biol* 1, 199-207.
- Yang, X., Feng, M., Jiang, X., Wu, Z., Li, Z., Aau, M., and Yu, Q. (2009). miR-449a and miR-449b are direct transcriptional targets of E2F1 and negatively regulate pRb-E2F1 activity through a feedback loop by targeting CDK6 and CDC25A. *Genes Dev* 23, 2388-2393.
- Yarden, R. I., and Brody, L. C. (1999). BRCA1 interacts with components of the histone deacetylase complex. *Proc Natl Acad Sci U S A* 96, 4983-4988.
- Yarden, R. I., Pardo-Reoyo, S., Sgagias, M., Cowan, K. H., and Brody, L. C. (2002). BRCA1 regulates the G2/M checkpoint by activating Chk1 kinase upon DNA damage. *Nat Genet* 30, 285-289.
- Yu, H. (2007). Cdc20: a WD40 activator for a cell cycle degradation machine. *Mol Cell* 27, 3-16.
- Zhang, H., Mishra, A., Chintagari, N. R., Gou, D., and Liu, L. (2010). Micro-RNA-375 inhibits lung surfactant secretion by altering cytoskeleton reorganization. *IUBMB Life* 62, 78-83.
- Zhang, Y., Xiong, Y., and Yarbrough, W. G. (1998). ARF promotes MDM2 degradation and stabilizes p53: ARF-INK4a locus deletion impairs both the Rb and p53 tumor suppression pathways. *Cell* 92, 725-734.
- Zhang, Z., Yamashita, H., Toyama, T., Sugiura, H., Ando, Y., Mita, K., Hamaguchi, M., Hara, Y., Kobayashi, S., and Iwase, H. (2005). Quantitation of HDAC1 mRNA expression in invasive carcinoma of the breast*. *Breast Cancer Res Treat* 94, 11-16.
- Zhao, T., and Xu, Y. (2010). p53 and stem cells: new developments and new concerns. *Trends Cell Biol* 20, 170-175.
- Zou, H., Henzel, W. J., Liu, X., Lutschg, A., and Wang, X. (1997). Apaf-1, a human protein homologous to *C. elegans* CED-4, participates in cytochrome c-dependent activation of caspase-3. *Cell* 90, 405-413.

9. Acknowledgements

First of all, I would like to thank my supervisor Matthias Dobbelstein for giving me the opportunity to work in his group, and for his support and scientific guidance throughout my PhD time. Our weekly meetings and vivid discussions helped me in many aspects, especially for the development of a critical scientific approach.

I thank my PhD committee members Tomas Pieler and Ralf Ficner for their time and support, and for the interesting and helpful discussions and suggestions.

Furthermore, I want to thank Magda Morawska-Onyszczuk, Konstantina Marinoglou, Xin Zhang, Ines Rudolf and Steven Johnsen for the incredibly helpful proof reading and the nice scientific discussions. I would also like to thank Frederik Köpper, Miriam Weiss and Ines Rudolf for their productive lab rotations and co-work on this project.

I thank all the lab members of the Molecular Oncology department for being such friendly and helpful colleagues, and for creating a wonderful atmosphere in the lab. Thank to you it is a nice place to be, even during stressful times. My thanks go especially to Cathrin Hippel, Antje Dickmanns and Claudia Buabe for their excellent technical assistance.

I am very grateful to my wonderful external collaborators Alex Klimke, Sven Pilarski, Christian Herr, Robert Bals and Michael Kessel. It is a pleasure to work with such dedicated scientists.

I also thank Karen Vousden for the Saos2 cells with tet-inducible E2F1, Reuven Agami for the miR-Vec library and the transcriptome analysis unit at our University for help with the array hybridization.

10. Curriculum Vitae

Name: **Muriel Lize**
Date of birth: 29.01.1981 in Pontoise, France
Nationality: French

Education

From March 2007

Dissertation at the Department of Molecular Oncology, University of Goettingen, Germany. Topic: E2F1 and microRNAs in DNA damage and apoptosis.

February 2006 – Jan. 2007

Diploma thesis „Manipulation of the Mdm2-oncoprotein: pharmacological activation of p53-responsive genes“, overall grade 1.3 “very good”, Department of Molecular Oncology, University of Goettingen, Germany

January 2006

Diploma in Biology (master) final examination in Biochemistry (Major), Pharmacology und Human Genetics, overall grade 1.3 “very good”, University of Goettingen, Germany

June 1999

High school diploma “Diplôme du Baccalauréat général scientifique avec mention”, Major Natural Sciences, overall grade 1.8, France

Work Experience

From March 2007

Research assistant at the Department of Molecular Oncology, University of Goettingen, Germany

April 2006 – Jan. 2007

Student assistant at the Department of Molecular Oncology, University of Goettingen, Germany

Sept. 2005 – March 2007

Student assistant at the Department of Bioinformatics, Project EndoNet, University of Goettingen, Germany

Okt. 2005 – Dec. 2005

Student assistant, supervision of the module Biochemistry for Medical Students, University of Goettingen, Germany

Volunteering

From December 2007

Member of the registered non-profit association “Initiative Frieden e.V.”, Initiative Peace, voluntary service in Germany and Tansania.

From May 2007- September 2008

Voluntary service for registered non-profit cultural institution „Rockbüro e.V.“, Goettingen, Germany

February 2007 – December 2007

Voluntary service in the registered non-profit making youth welfare organisation „Blechtrommel“, Goettingen, Germany

Practical training

Aug. 2005 – Sept. 2005

Non-curricular internship, Department of Molecular Structural Biology, University of Goettingen, Germany

June 2005 – July 2005

Laboratory practical training, Department of Plant Biochemistry, University of Goettingen, Germany

April 2005 – May 2005

Laboratory practical training, Department of Cytogenetics, University of Goettingen, Germany

Jan. 2005 – Feb. 2005

Laboratory practical training for Biochemistry, University of Goettingen, Germany

July 2004 – Aug. 2004

Laboratory practical training in Pharmacology and Toxicology, University of Goettingen, Germany

Language skills

Fluent in French (native speaker) and German (DSH certificate), very good English (Cambridge Advanced Certificate grade A June 2009), elementary Suaheli and Italian.

Poster presentations at conferences

Genes & Cancer 2009, 26th Meeting December 2009, University of Warwick, United Kingdom

15th International AEK Cancer Congress, Deutsche Krebsgesellschaft e. V., March 2009, Berlin, Germany

5th International PhD student Symposium Horizons in Molecular Biology, September 2008, Goettingen, Germany

International Advanced ICAS/ApopTrain Training Course on Advances in Cell Death Research, July 2008, Gunzburg, Germany

Talk at conference

21st Meeting of the European Association for Cancer Research EACR-21, June 2010, Oslo, Norway.

The Mattyasovsky-Meziani Bursary Award Talk at the Presidential Session I.

Publications

Manuscript in review (June 2010):

MicroRNA-449a levels increase by several orders of magnitude during mucociliary differentiation of airway epithelia.

M. Lizé, C. Herr, A. Klimke, R. Bals, and M. Dobbelstein

Department of Molecular Oncology, Ernst Caspari Haus, University of Goettingen

E2F1-inducible microRNA 449a/b suppresses cell proliferation and promotes apoptosis.

M. Lizé, S. Pilarski and M. Dobbelstein.

Cell Death and Differentiation, 2010 Mar; 17(3):452-8.

Department of Molecular Oncology, Ernst Caspari Haus, University of Goettingen

EndoNet: an information resource about regulatory networks of cell-to-cell communication.

Dönitz J, Goemann B, Lizé M, Michael H, Sasse N, Wingender E, Potapov AP.

Nucleic Acids Res. 2008 Jan.

Department of Bioinformatics, University of Goettingen/Medical School.

<http://endonet.bioinf.med.uni-goettingen.de/>